1980

Analysis and testing to improve the flow from the plenum of a subsonic cascade wind tunnel.

Moebius, Richard Carl

Monterey, California. Naval Postgraduate School

ANALYSIS AND TESTING TO IMPROVE THE FLOW FROM THE PLENUM OF A SUBSONIC CASCADE WIND TUNNEL

Richard Carl Moebius

NAVAL POSTGRADUATE SCHOOL
Monterey, California

THESIS

ANALYSIS AND TESTING TO IMPROVE
THE FLOW FROM THE PLENUM OF A
SUBSONIC CASCADE WIND TUNNEL

by

Richard Carl Moebius

March 1980

Thesis Advisor: Raymond P. Shreeve

Approved for public release; distribution unlimited

UNCLASSIFIED

SECURITY CLASSIFICATION OF THIS PAGE (When Data Entered)

REPORT DOCUMENTATION PAGE		READ INSTRUCTIONS BEFORE COMPLETING FORM
1. REPORT NUMBER	2. GOVT ACCESSION NO.	3. RECIPIENT'S CATALOG NUMBER
4. TITLE (and Subtitle) Analysis and Testing to Improve the Flow from the Plenum of a Subsonic Cascade Wind Tunnel		5. TYPE OF REPORT & PERIOD COVERED Master's Thesis; March 1980 6. PERFORMING ORG. REPORT NUMBER
7. AUTHOR(s) Richard Carl Moebius		8. CONTRACT OR GRANT NUMBER(s)
9. PERFORMING ORGANIZATION NAME AND ADDRESS Naval Postgraduate School Monterey, California 93940		10. PROGRAM ELEMENT, PROJECT, TASK AREA & WORK UNIT NUMBERS
11. CONTROLLING OFFICE NAME AND ADDRESS Naval Postgraduate School Monterey, California 93940		12. REPORT DATE March 1980 13. NUMBER OF PAGES 132
14. MONITORING AGENCY NAME & ADDRESS(if different from Controlling Office) Naval Postgraduate School Monterey, California 93940		15. SECURITY CLASS. (of this report) Unclassified 15a. DECLASSIFICATION/DOWNGRADING SCHEDULE

16. DISTRIBUTION STATEMENT (of this Report)

Approved for public release; distribution unlimited.

17. DISTRIBUTION STATEMENT (of the abstract entered in Block 20, if different from Report)

18. SUPPLEMENTARY NOTES

19. KEY WORDS (Continue on reverse side if necessary and identify by block number)

Subsonic Cascade

Flow Improvement

Finite Element Flow Analysis

20. ABSTRACT (Continue on reverse side if necessary and identify by block number)

The original design of the plenum and bellmouth contraction arrangement of a subsonic cascade test facility did not produce sufficiently uniform flow conditions at the bellmouth exit plane. Pneumatic measurements revealed sizeable blade-to-blade variations in velocity and flow angle. A finite element numerical analysis of the inviscid flow field was carried out which both confirmed

DD FORM 1 JAN 73 1473 EDITION OF 1 NOV 68 IS OBSOLETE
S/N 0102-014-6601
(Page 1)

UNCLASSIFIED

SECURITY CLASSIFICATION OF THIS PAGE (When Data Entered)

the need for and guided the design of a modification to the bellmouth contraction from the plenum. Following the modification, in which the original contraction was changed to two two-dimensional contractions in series, and a program of development tests, acceptably small variations in velocity and flow angle were measured at the bellmouth exit plane.

Approved for public release; distribution unlimited.

Analysis and Testing to Improve the Flow from the Plenum of a Subsonic Cascade Wind Tunnel

by

Richard Carl Moebius
Lieutenant, United States Navy
B.S., Pennsylvania State University, 1973

Submitted in partial fulfillment of the
requirements for the degree of

MASTER OF SCIENCE IN AERONAUTICAL ENGINEERING

from the

NAVAL POSTGRADUATE SCHOOL
March 1980

ABSTRACT

The original design of the plenum and bellmouth contraction arrangement of a subsonic cascade test facility did not produce sufficiently uniform flow conditions at the bellmouth exit plane. Pneumatic measurements revealed sizeable blade-to-blade variations in velocity and flow angle. A finite element numerical analysis of the inviscid flow field was carried out which both confirmed the need for and guided the design of a modification to the bellmouth contraction from the plenum. Following the modification, in which the original contraction was changed to two two-dimensional contractions in series, and a program of development tests, acceptably small variations in velocity and flow angle were measured at the bellmouth exit plane.

TABLE OF CONTENTS

LIST OF TABLES

LIST OF FIGURES

ACKNOWLEDGEMENTS

The author wishes to express his sincere gratitude to Professor Ray Shreeve, Lab Manager Jim Hammer, and Technician John Morris for their willing assistance in every facet of this study. Their efforts have assisted in making this a most worthwhile and rewarding engineering experience.

I. INTRODUCTION

In 1963 construction was completed on the Naval Postgraduate School's subsonic cascade test facility. Its primary function was to be used to provide information applicable to compressor and turbine blade design. As described in Ref. 1, several unique features were incorporated in the design of the cascade to ensure a two-dimensional, periodic flow at the test blading. Previously the lack of good two-dimensionality in other facilities had plagued efforts to correlate air turning angles and blade surface pressure distribution data [Ref. 2].

Initial evaluations of the facility were carried out and reported in references 1 and 3. The test section entrance flow was examined and initially found to be unacceptably non-uniform. Several measures were taken at that time to correct the deficiency, but an examination of subsequent data revealed that only partial success was obtained. In particular, an investigation was performed using NACA 65 series blades as inlet guide vanes [Ref. 4]. Difficulty in obtaining two-dimensionality was reported and a strong recommendation was made that the test section inlet flow conditions be improved.

In preparing for tests of new compressor blade designs, the goal of the present study was to take whatever steps were necessary to first obtain a two-dimensional and periodic flow at the entrance to the cascade test section.

For purposes of this report, a two-dimensional and periodic flow will be considered to exist when the dynamic pressure variations are less than $\pm$ 1%, total pressure variations are less than $\pm$ .5%, and flow angles are within $\pm$ 1.5 degrees of their centerline value.

Preliminary pneumatic measurements indicated that the flow from the plenum itself was not uniform. A numerical analysis of the flow field through the plenum chamber and contraction bellmouth was therefore performed using the finite element method, (FEM). Based on the results of the preliminary measurements and the FEM analysis, plenum redesign and development test programs were carried through. The final pneumatic survey results showed acceptable levels of dynamic pressure, total pressure, and flow angle variations.

This report documents the experimental and analytical steps taken to obtain a suitable plenum geometry for the cascade facility. Following a description of the cascade and measurement techniques given in Section II, the steps taken in the development of a successful plenum arrangement are first outlined in Section III and then described in the following three sections. In order to present a clear account of the development, details of each section of the work have been confined to appendices. First, the FEM program is given in detail in Appendix A. Data from the original plenum configuration are given in Appendix B and the plenum development test results in Appendix C. Finally, detailed drawings of

the construction of the modification to the plenum and bellmouth are given in Appendix D.

II. FACILITY AND MEASUREMENT APPROACH

A. CASCADE AND INSTRUMENTATION

A description of the Naval Postgraduate School's Rectilinear Cascade as it was originally designed is given in reference 1. The layout of the complete facility is shown in Figure 1. The addition of two fine mesh screens at the bellmouth entrance to improve flow stability is the only modification to the plenum which is reported in reference 1. A follow-on study into the cascade performance was conducted by Bartocci and is reported in reference 3. Plenum turning vanes were installed by Bartocci to direct plenum inlet air towards the bellmouth entrance and to decrease the total pressure fluctuations. Multiple views of the plenum chamber and the bellmouth contraction arrangement as it was at the inception of the present work are shown in Figure 2.

All testing in the present study was conducted with the cascade test section walls vertical, with all inlet guide vanes (Fig. 1) and test blading removed. The effects of changes in plenum geometry were evaluated primarily by conducting pneumatic probe surveys at the exit of the bellmouth, hereafter referred to as the test plane. Additional information was obtained using tufts for surface flow visualization in the plenum and from static pressure distributions displayed on water columns. A Datametrics Series 100 VT Air Velocity Meter was also used to measure velocities in the plenum.

B. PNEUMATIC PROBE SURVEYS

1. Probe and Installation

The installation for probe surveys at the test plane is shown in Figure 3. A wooden two-by-four was used to traverse the probe in the blade-to-blade direction. The coordinate system adopted is shown in Figure 4. The X-wise displacement of the probe was manually set by sliding the bar. The displacement in the Y direction and rotation of the probe were adjusted using the traversing probe mount shown in Figure 5, which was attached to the two-by-four and incorporates potentiometers for the measurement of the immersion (Y) and yaw (β) displacements.

The five hole United Sensor D-125 probe shown in Figure 6 was used to determine total and static pressure, and yaw and pitch angle. A U-tube water manometer connected to the P_2 and P_3 ports was used to indicate when the probe was correctly aligned with respect to yaw angle. An approximate value for the static pressure was obtained by pneumatically averaging P_2 and P_3. An exact calibration of the probe was not carried out since only relative measurements (showing the degree of uniformity across the test plane) were required.

2. Data Acquisition and Reduction

Probe and other reference pressures were multiplexed via a Scanivalve to a single transducer referenced to atmospheric pressure. The transducer and Scanivalve were connected to a B and F scanning data system. Signal conditioning

circuits in the data system were adjusted so that pressures were recorded in units of 10^{-1} inches of water. Data was printed and also output on punched paper tape.

A Hewlett-Packard Model 9830A Programmable Calculator System with a two Megabyte mass memory disc unit and X-Y plotter were used to process the probe survey data from the paper tape.

The measured quantities and uncertainty intervals are given in Table I. The uncertainties in the pneumatic quantities were calculated from the 2σ intervals of 25 consecutive readings at the test plane center. The position and yaw angle uncertainties were determined by the accuracy to which the appropriate scales could be read.

Since test plane Mach number did not exceed .25, compressibility effects were ignored. Test plane Reynolds number was 1.5×10^6 per foot scale, with variations of $\pm$ 5%. In addition to the measured yaw angles, the following (relative) dimensionless flow properties were evaluated from the measurements in Table I, and their distributions across the test plane were examined:

Dynamic Pressure ($\bar{Q}$)

$$\bar{Q} = \frac{Q(X,Y)}{Q_{REF}}, \quad \text{uncertainty} = \pm .01,$$

where $Q(X,Y) = P_T(X,Y) - P_S(X,Y)$

$$Q_{REF} = P_T(30, 5) - P_S(30, 5) = Q(30, 5)$$

and the uncertainty in Q is $\pm$ .008.

Total Pressure ($\overline{\Delta P}_T$)

$$\overline{\Delta P}_T = \frac{\Delta P_T(X,Y)}{Q_{REF}} , \quad \text{uncertainty} = \pm .05,$$

where $\Delta P_T(X,Y) = P_{PL} - P_T(X,Y)$,

and the uncertainty is $\pm$ .049.

Static Pressure ($\overline{\Delta P}_S$)

$$\overline{\Delta P}_S = \frac{\Delta P_S(X,Y)}{Q_{REF}} , \quad \text{uncertainty} = \pm .015,$$

where $\Delta P_S(X,Y) = P_S(X,Y) - P_W$, uncertainty = $\pm$ .01.

Note that the uncertainties in $\overline{\Delta P}_T$ and $\overline{\Delta P}_S$ are rather high since these quantities are derived from small differences between two larger quantities. Note also that the values of Q_{REF} changed over the period of a test run due to variations in the plenum pressure. The value of Q_{REF} at each (X,Y) was therefore derived from the plenum pressure reading taken at the time of the Q(X,Y) measurement. This technique assumed a linear relationship between Q(30, 5) and P_{PL}.

C. OTHER TECHNIQUES

Qualitative information which was simple to obtain, greatly accelerated the development of the final plenum configuration.

1. Tufts

Tufts were attached to the plenum walls and were observed and photographed using a Polaroid camera during testing.

(Average velocities of less than 10 ft/sec allowed the presence of an observer in the plenum.) A tufted probe was also used extensively.

2. Static Pressure Distribution

The uniformity, but particularly the steadiness, of the cascade sidewall static pressures displayed on water manometer columns were monitored as changes in configurations were made.

3. Velocity Meter

Velocities from the sound baffles in the plenum were measured using a Datametrics Series 100 VT Air Velocity Meter.

III. PROGRAM OUTLINE

The goal was to obtain a plenum and contraction arrangement which would give at the test plane (outside the boundary layers) maximum peak-to-peak variations of $\pm$ 1% in dynamic pressure, $\pm$ .5% in the total pressure, and $\pm$ 1.5 degrees in the flow yaw angle.

The program was carried out in three steps. First, tests were made to determine the performance of the existing plenum configuration. Second, a finite element analysis was carried out which confirmed that the existing bellmouth could not generate a sufficiently uniform flow at the test plane. The analysis also guided the design of a suitable modification to the plenum. Third, an experimental program was carried out during which a major modification was made in the plenum geometry and a plenum and contraction configuration which gave satisfactory flow was subsequently developed.

These three steps in the program are documented in the following three sections of this report.

A summary of the configurations tested during the program is given in Table II. Effects of configuration changes were evaluated at the test plane by conducting blade-to-blade probe surveys (first at 50% span) and spanwise surveys at selected locations. The other measurement techniques listed in Section III.C. often were used first to determine whether a particular configuration should be measured in detail.

IV. PRELIMINARY TEST RESULTS

Blade-to-blade probe surveys were obtained with the original plenum arrangement (Configuration Ø) at 10, 30, 50, and 90% span. The results at 50% span are shown in Figures 7a, 7c, and 7e. (The remaining data are given in Appendix B.) The results showed unacceptable variations in total and dynamic pressure in both the blade-to-blade and spanwise directions. Spanwise variation of the various parameters can be seen by comparing values at given blade-to-blade locations in the results at 10, 30, 50, and 90% spans. The yaw angles were also outside the required bounds.

The source of the total pressure variation was traced to the screens at the bellmouth inlet. Clearly, the normal flow into the bellmouth would generate a velocity which would vary in magnitude and direction over the face of the screen, thereby generating a corresponding variation in the total pressure drop.

The screens were removed (Configuration 1) and the measurements repeated. Blade-to-blade survey results are shown in Figures 7b, 7d, and 7f. A spanwise survey was conducted at X = 30 inches and is shown in Figure 8. The total pressure variation ($\overline{\Delta P}_T$) across the test plane was seen to have decreased to $\pm$ .5%. The variation in $\overline{Q}$ was within tolerance in the spanwise direction; however, an unacceptable gradient still existed in the blade-to-blade direction

at all spanwise stations surveyed. The yaw angles in Figures 7e and 7f suggested that the flow was still converging through the center 50% of the test plane. In addition, observed spanwise variations in flow angle near the ends in the blade-to-blade direction suggested the presence of large scale vorticity. This was verified using a small string tuft attached to the end of the pneumatic probe.

The question then was, - was the measured velocity field simply the result of the geometry of the bellmouth contraction, or could something be done in the plenum itself to correct the profile? An analysis of the flow from the plenum was required to answer this question.

V. FINITE ELEMENT FLOW MODEL PREDICTIONS

A two-dimensional finite element analysis was used to analyze the potential flow field through the plenum and bellmouth contraction. Two questions were of specific interest. First, what was the velocity profile created by the bellmouth contraction at its exit plane, and secondly, what distance downstream was required to attain an acceptable uniform velocity profile? The details of the analysis and the Fortran programs developed for the IBM 360 to answer these questions are given in Appendix A.

The plenum, bellmouth, and exit passage were modeled in two ways as shown in Figure 9. Model 1 was the most simplified representation, and was used to obtain a first estimate of the velocity profile developed by the bellmouth contraction. Due to the vertical axis of symmetry in Model 1, only half of the model needed to be included in the calculations. A more realistic model was that shown in Figure 9 as Model 2. In Model 2 the flow entered the plenum from one side as in the actual plenum.

The computer analysis of each model was performed in a similar manner. Namely, the exit boundary condition, which specified flow to be parallel to the exit walls, was applied at boundary planes located at progressively increasing distances downstream of the bellmouth exit plane (Fig. 9). For each boundary plane, the computed velocity profiles across

the bellmouth exit plane and the boundary plane were compared with the results from the previous run. The following similarities were noted in the results of the two models:

1) The exit boundary plane velocity profiles were always more nearly uniform than the bellmouth exit plane velocity profiles.

2) As the exit boundary planes were moved farther downstream, the exit plane velocity profile became more nearly uniform. The bellmouth exit plane velocity profiles changed during this process.

3) As the exit plane velocity profile approached a uniform condition, the still non-uniform bellmouth exit plane velocity profile did not change as the exit boundary was moved even farther downstream.

The results of Model 1, shown in Figure 10, indicated that at exit plane (GH), 41.5 inches downstream of bellmouth exit plane (CL), the velocity profile had relaxed to give a maximum variation of 0.3%. The velocity profile at plane (CL) had a variation then of 14% between peak velocity at the contour wall and minimum velocity at the axis of symmetry. Similarly, the results of Model 2, shown in Figure 11, indicated that at exit plane (LM), 50 inches downstream of the bellmouth exit plane (FS), there existed only a 1.3% velocity variation. This velocity profile was not, however, symmetrical due to the asymmetry of the flow model. Higher velocities existed on the inlet side of the exit plane. The velocity profile at plane (FS) also exhibited the asymmetry and a

15% variation between maximum and minimum velocities. Figure 12 shows a comparison between the measured profile of $\overline{Q}$ for Configuration 1 at 50% span, and that calculated from the velocity profile of Figure 11.

While the magnitudes are different, the trends in the computed and measured distributions of $\overline{Q}$ are clearly similar. Since the analysis is a two-dimensional one, the magnitudes should not be expected to fully agree. While a three-dimensional inviscid analysis could be expected to be more representative, the inclusion of viscosity would be necessary to closely approximate the actual flow.

There is sufficient documentation in the literature to presume significant amounts of vorticity exist in this flow. The rectangular duct shape in itself can create sizeable corner vorticity [Ref. 5 and Ref. 6]. Velocity gradients in the boundary layer, under the influence of transverse pressure gradients, can produce sizeable amounts of vorticity also [Ref. 7]. As was stated by C. Truesdell [1954], "Even in nearly irrotational flows the relatively small amount of vorticity present may be of central importance in determining the major flow characteristics."

An analysis of the flow in the orthogonal plane (i.e., in the spanwise direction), was not performed. However, an approximate analytical solution for a similar but simpler model sheds light on the probable trends in the velocity distribution. For this analysis, the flow field is created by a circular cylinder immersed in the flow between two

parallel walls. This is illustrated in Figure 13. The velocity distribution across the stream at the plane of maximum contraction is given in Ref. 8 as the following:

$$V_X = U \left[1 - \frac{\sinh^2(\pi b/H) \cos(2\pi Y/H)}{\cosh^2(\pi X/H) - \cos^2(\pi Y/H)} + \right.$$

$$\left. + \frac{1/2 \sinh^2(\pi b/H) \sin^2(2\pi Y/H)}{[\cosh^2(\pi X/H) - \cos^2(\pi Y/H)]^2} \right]$$

The important result to note is that as the ratio b/H increases, the magnitude of the velocity variation decreases. Using a similar argument for the cascade bellmouth contraction, one would expect a difference in the maximum velocity variations, between the blade-to-blade and spanwise directions, of almost an order of magnitude. This was consistent with experimental observation.

VI. PLENUM DESIGN MODIFICATION AND TEST RESULTS

The measurements reported in Section IV and the analysis reported in Section V suggested that the bellmouth contraction, as designed, could produce an acceptably uniform velocity profile in the spanwise direction, but not in the blade-to-blade direction. Several perturbations were subsequently made in the original plenum geometry, and the test results supported this conclusion. A complete account of the tests leading to, and subsequently verifying, the design of a modification to the plenum is given in Appendix C.

The basic idea in the modification was to arrange two two-dimensional contractions in series, each with sufficient length to allow relaxation to uniform velocity of the accelerated flow. The spanwise contraction of the original bellmouth contour was retained, and a new contraction section in the blade-to-blade plane was built down into the original plenum. The contours and construction of the new section are given in Appendix D. The final configuration (Configuration 7) of the plenum, including features which were determined to be necessary as a result of subsequent development testing (Appendix C), is shown in Figure 14 and Figure 15. Referring to these figures, the baffles were installed to dampen flow oscillations observed in earlier tests. The flow diverter fastened to the west end ceiling was installed to deflect

high velocity air from along the ceiling, downward through the baffles toward the plenum center. The velocity and yaw angle distributions (Configuration 7 at 50% span) are shown in Figure 16. Measurements from Configuration 1 are shown for comparison. The results of a spanwise traverse at X = 50 for Configuration 7 are shown in Figure 17. The variations in both dynamic pressure and yaw angle were seen to have been brought to within the prescribed limits of $\pm$ 1% and $\pm$ 1.5 degrees respectively.

VII. CONCLUSIONS

The original design of the plenum and bellmouth contraction arrangement did not produce sufficiently uniform flow conditions at the bellmouth exit plane. While the large area contraction ratio (40:1) ensured uniformity in the total pressure when no screens were introduced, the original bellmouth contraction contours in the blade-to-blade plane gave unacceptable variations in velocity and flow angle at the inlet guide vane station. The inlet guide vanes would normally be adjusted to control air-inlet angle to the test cascade.

Following the design and installation of a modification to the plenum, in which the original contraction was changed to two two-dimensional contractions in series, and a program of development tests, acceptably small variations in velocity and flow angle were measured at the inlet guide vane station.

Future tests will involve installation of the inlet guide vanes and an evaluation of the flow downstream at the cascade test blading location.

TABLE I

MEASURED QUANTITIES

Item	Description	Method	Uncertainty
X	Blade-to-Blade dimension X = 0 in. East end X = 60 in. West end	Tape measure	± .1 in.
Y	Spanwise dimension Y = 0 in. South wall Y = 10 in. North wall	Immersion Potentiometer on probe mount	± .01 in.
β	Flow yaw angle	Yaw angle Potentiometer on probe mount	± .25 deg.
$P_T(X,Y)$	Total pressure at the test plane	Pressure P_1 on Pitot probe	± .1 in. H_2O
P_{PL}	Plenum total pressure	Static tap in plenum chamber V ≃ 0	± .1 in. H_2O
$P_S(X,Y)$	Static pressure at the test plane	Pneumatic average of P_2 and P_3 on Pitot probe	± .15 in. H_2O
P_W	Static pressure at X = 30 in., Y = 0 in.	Static tap on south wall	± .1 in H_2O
P_{ATM}	Atmospheric pressure	Mercury barometer	± .01 in. H_2O
P_{TARE}	Tare reading across pressure transducer	$P_{ATM} - P_{ATM}$	± .01 in. H_2O

Note: All pressures are gauge pressure.

TABLE II

PLENUM/BELLMOUTH TEST CONFIGURATIONS

Configuration Number	Description	Figure Number
Ø	Original design	1 and 2
1	Removed screens from bellmouth entrance	1 and 2 minus screens
2	Simulated "relaxation" concept Added plywood vertical wall	C-1
3	Added eastern and western lower contractions	C-4 minus fillets
4	Same as above, but moved turning vanes 3 ft. to the east	As above
5	Inserted cardboard fillets between upper and lower contraction	C-4
6	Removed plenum turning vanes	C-4 minus turning vanes
7	Installed baffles and flow diverter	14 and 15

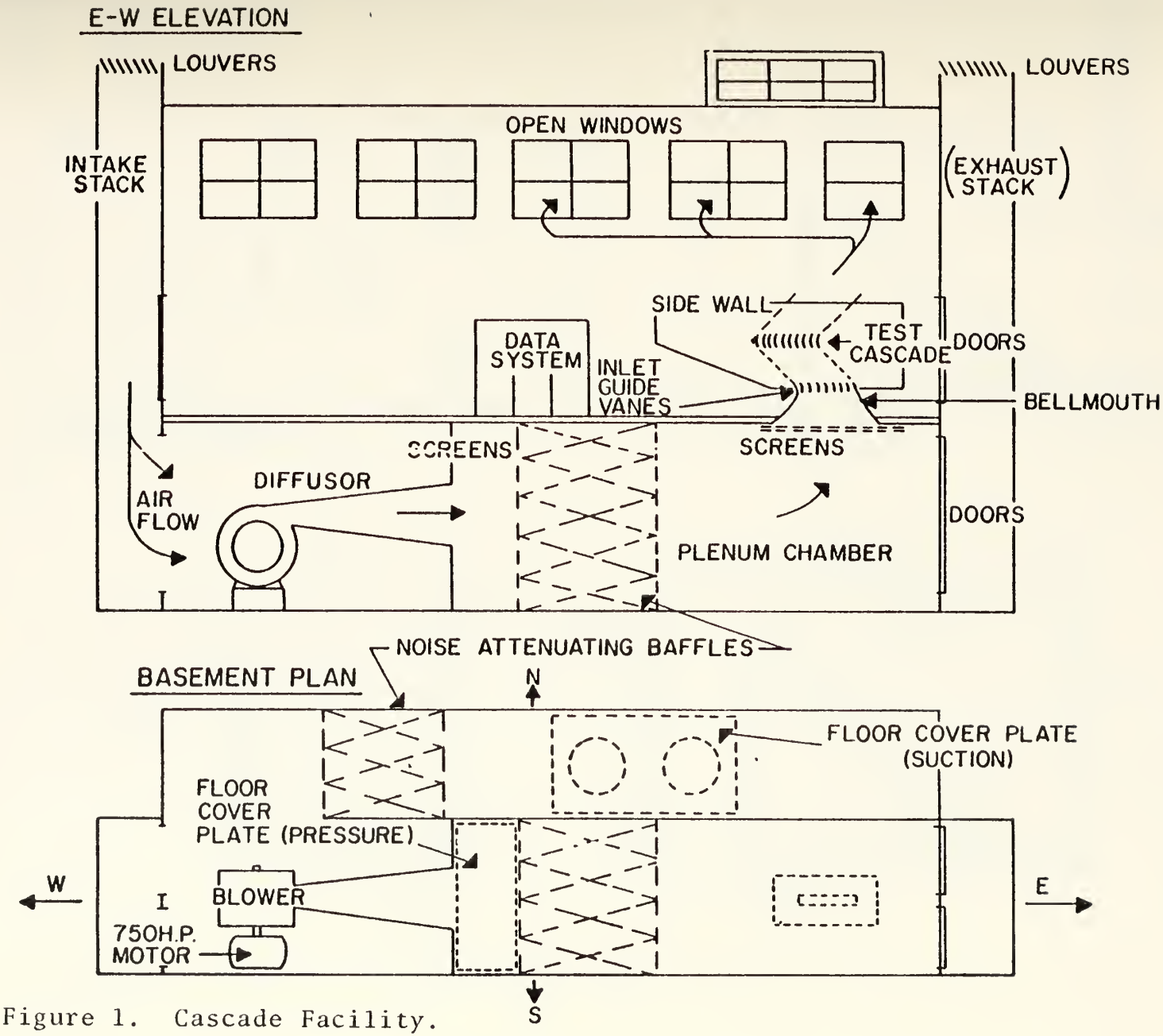

Figure 1. Cascade Facility.

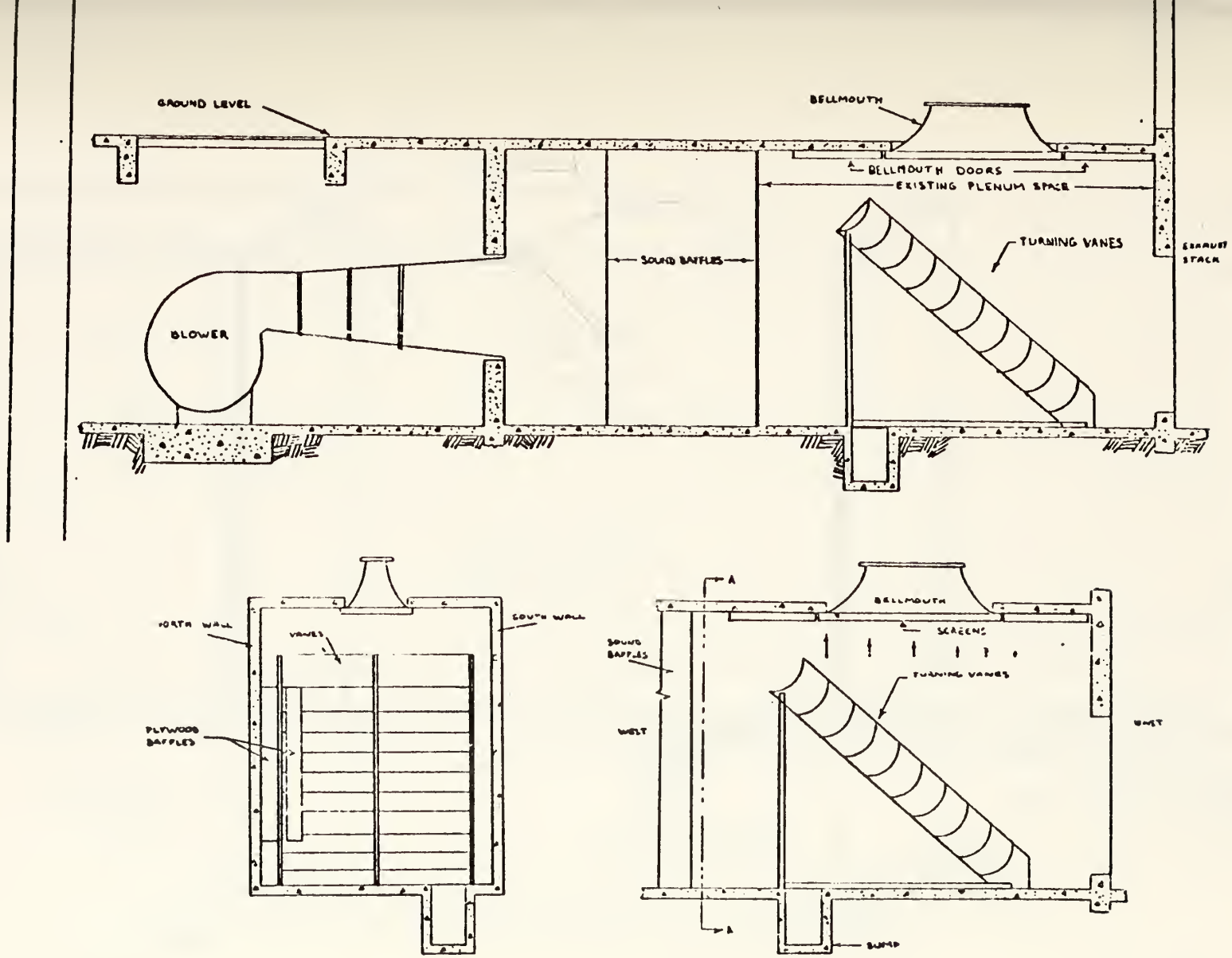

Figure 2. Plenum - Configuration #Ø

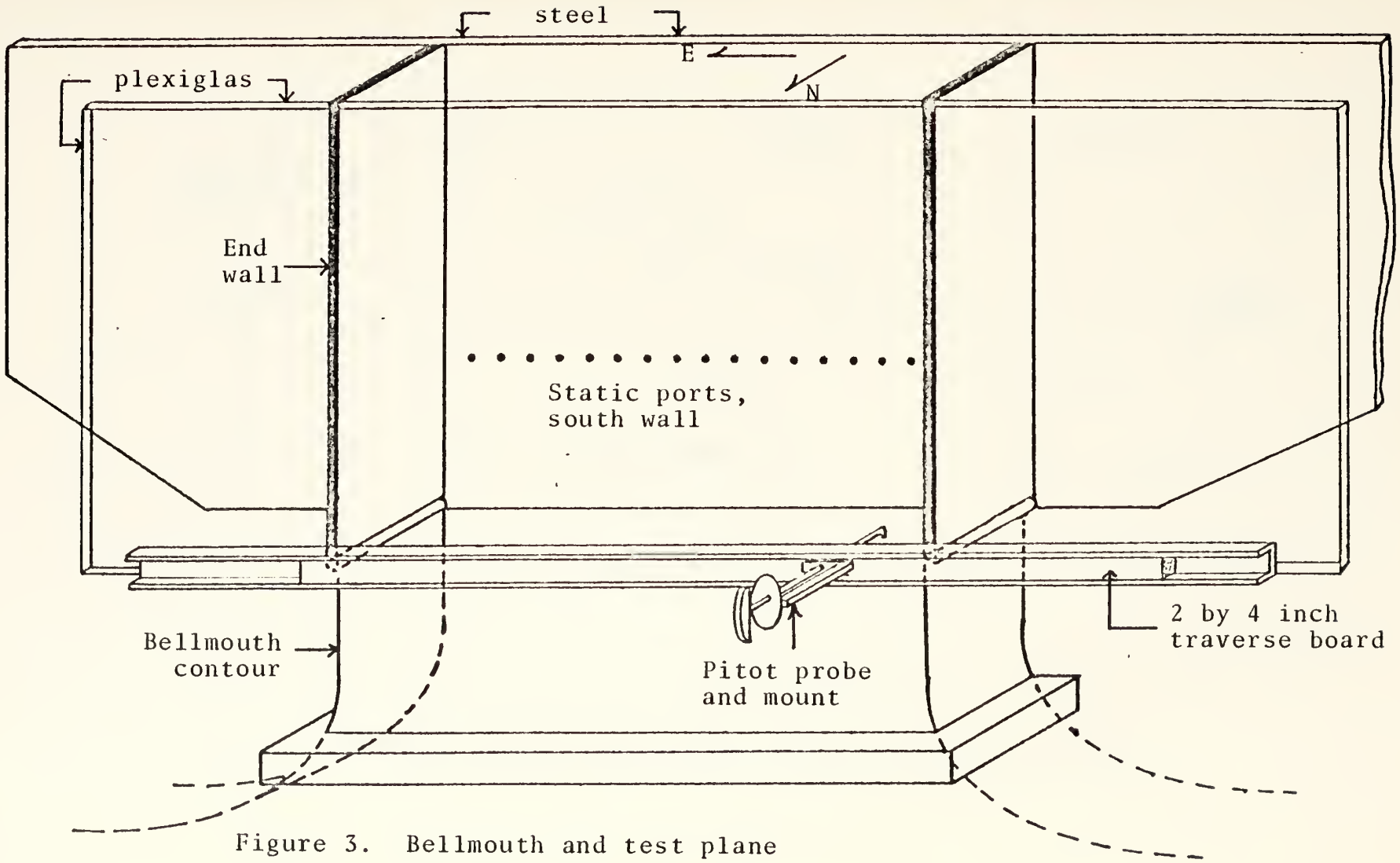

Figure 3. Bellmouth and test plane

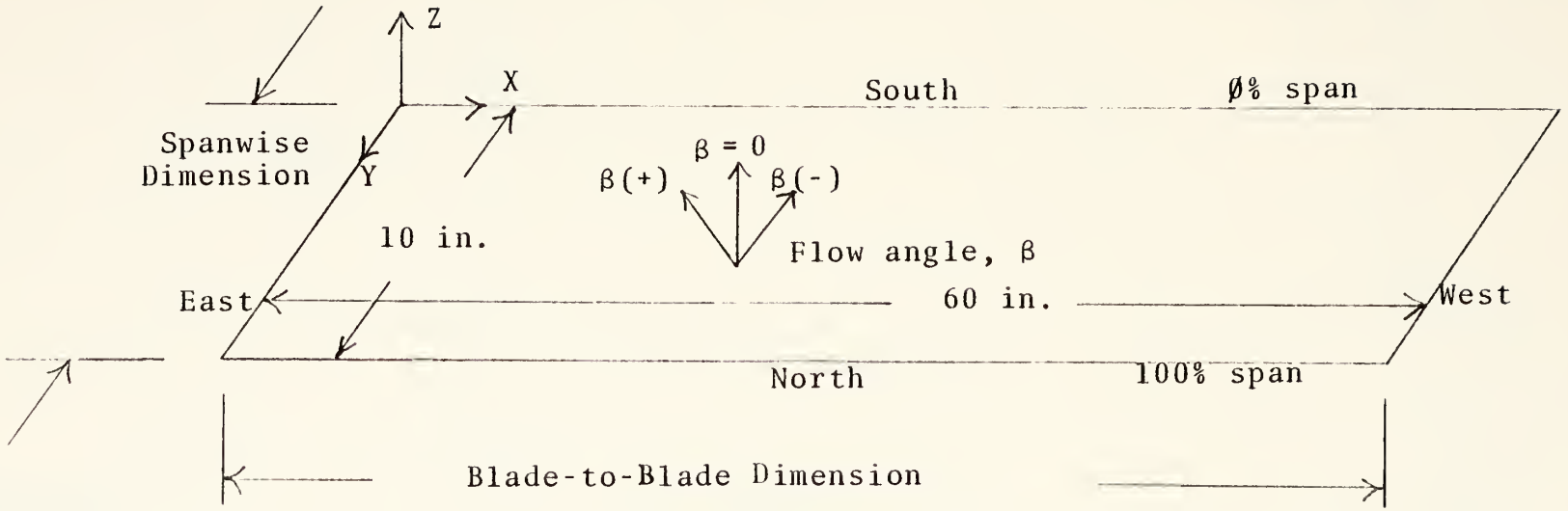

Figure 4. Cascade Nomenclature (Test Plane at Bellmouth Exit)

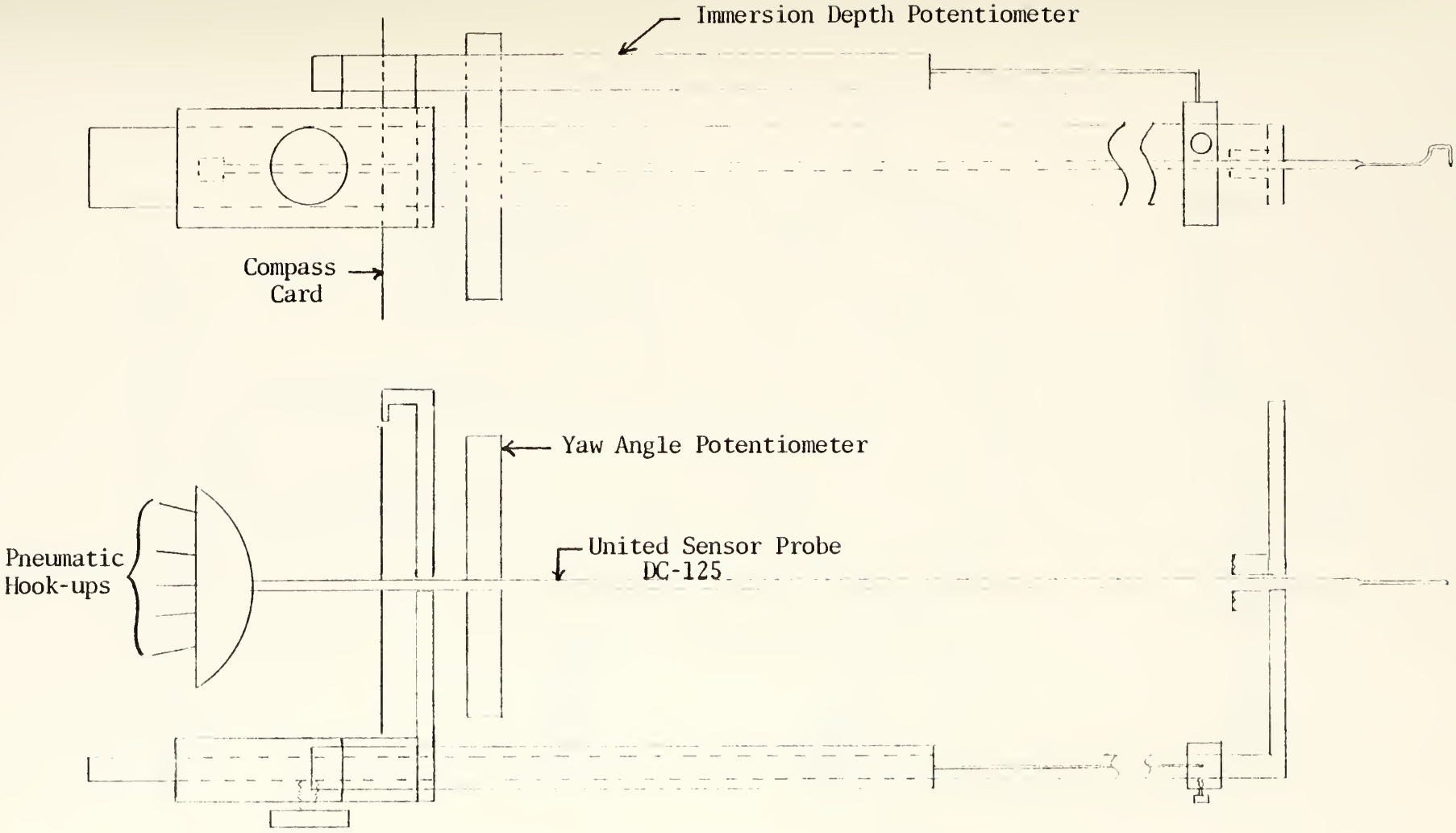

Figure 5. Pneumatic Probe and Traversing Probe Mount

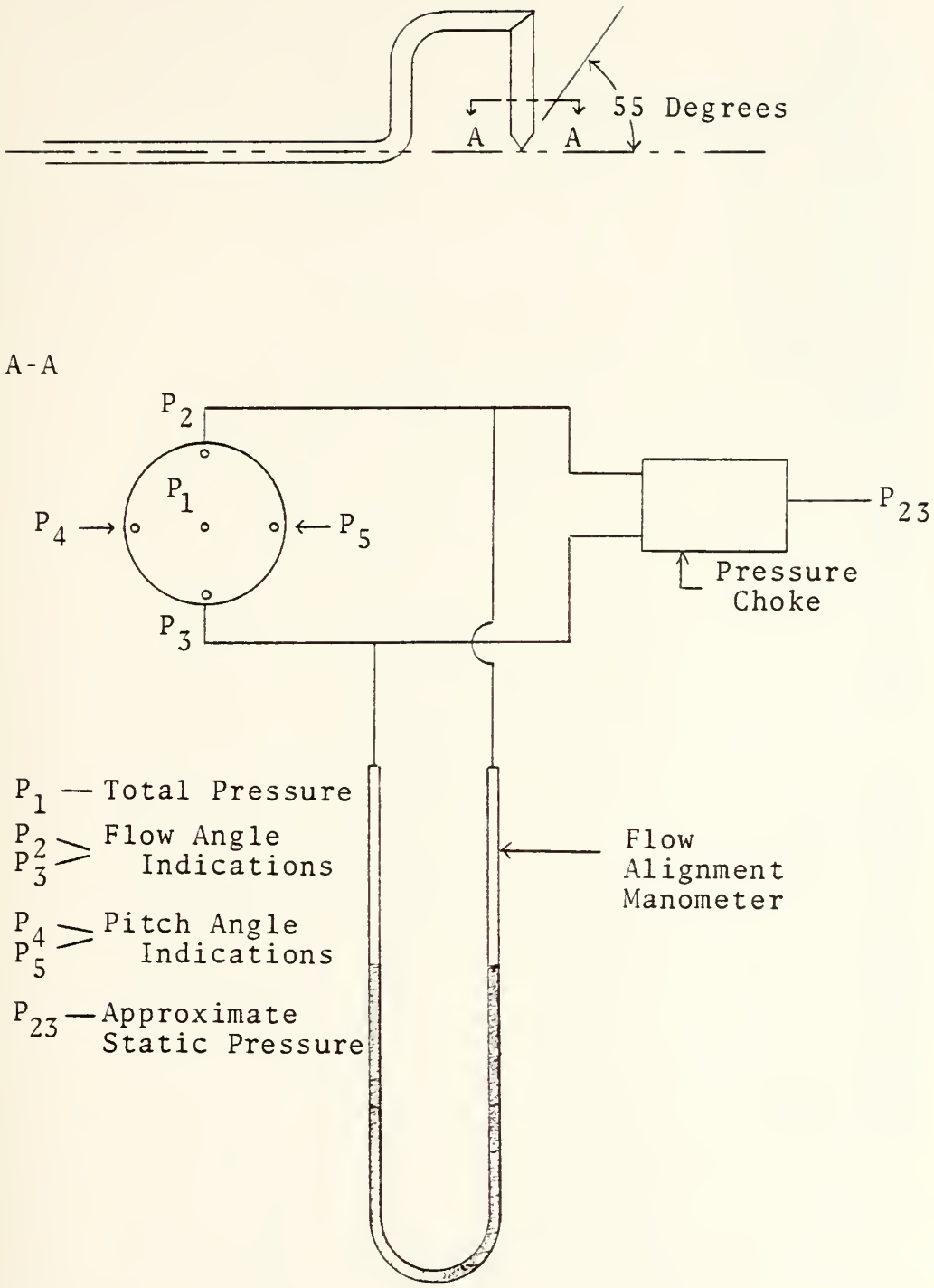

Figure 6. United Sensor DC-125 5-Hole Pneumatic Probe

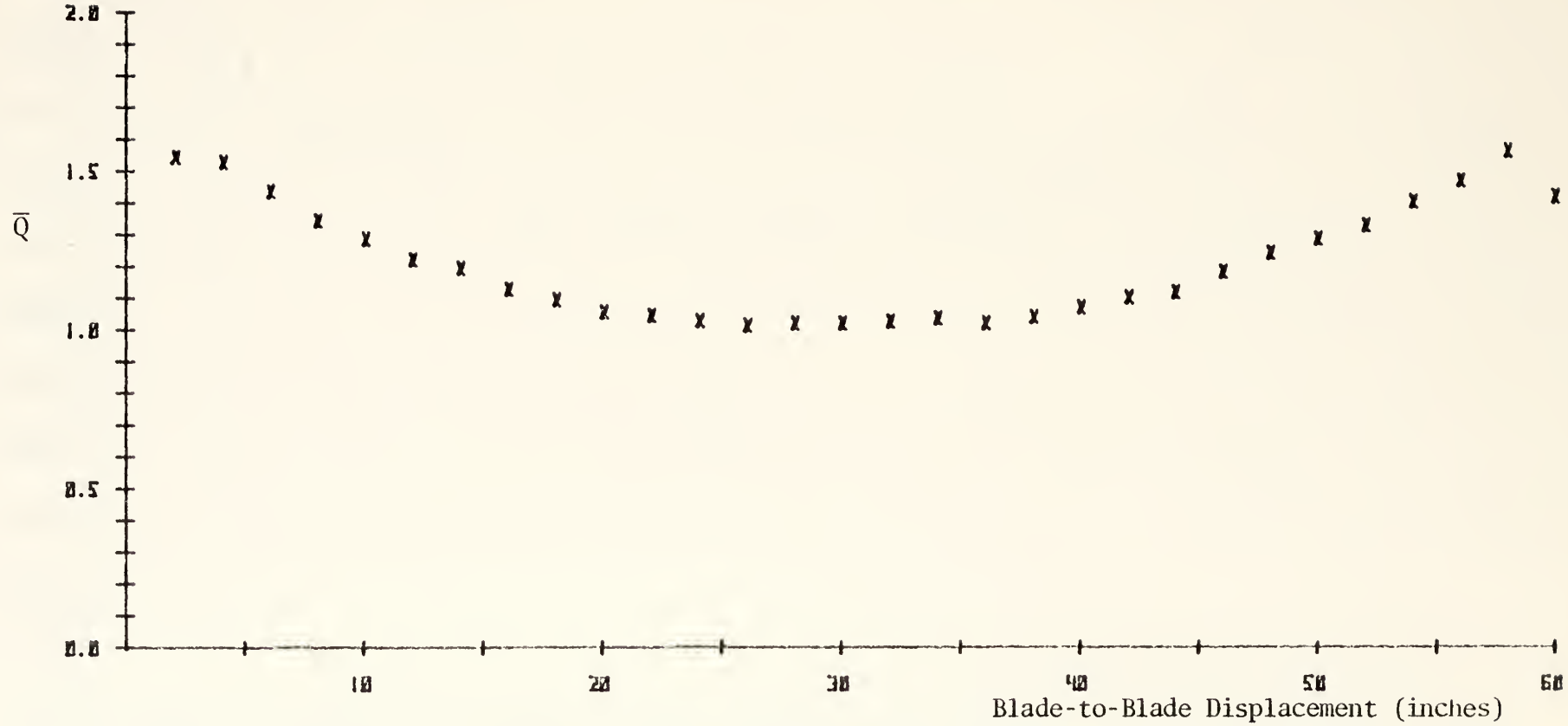

Figure 7a. Blade-to-Blade Dynamic Pressure Distribution at the Test Plane (at 50% Span, Velocity = 230 ft/sec) - Configuration #Ø

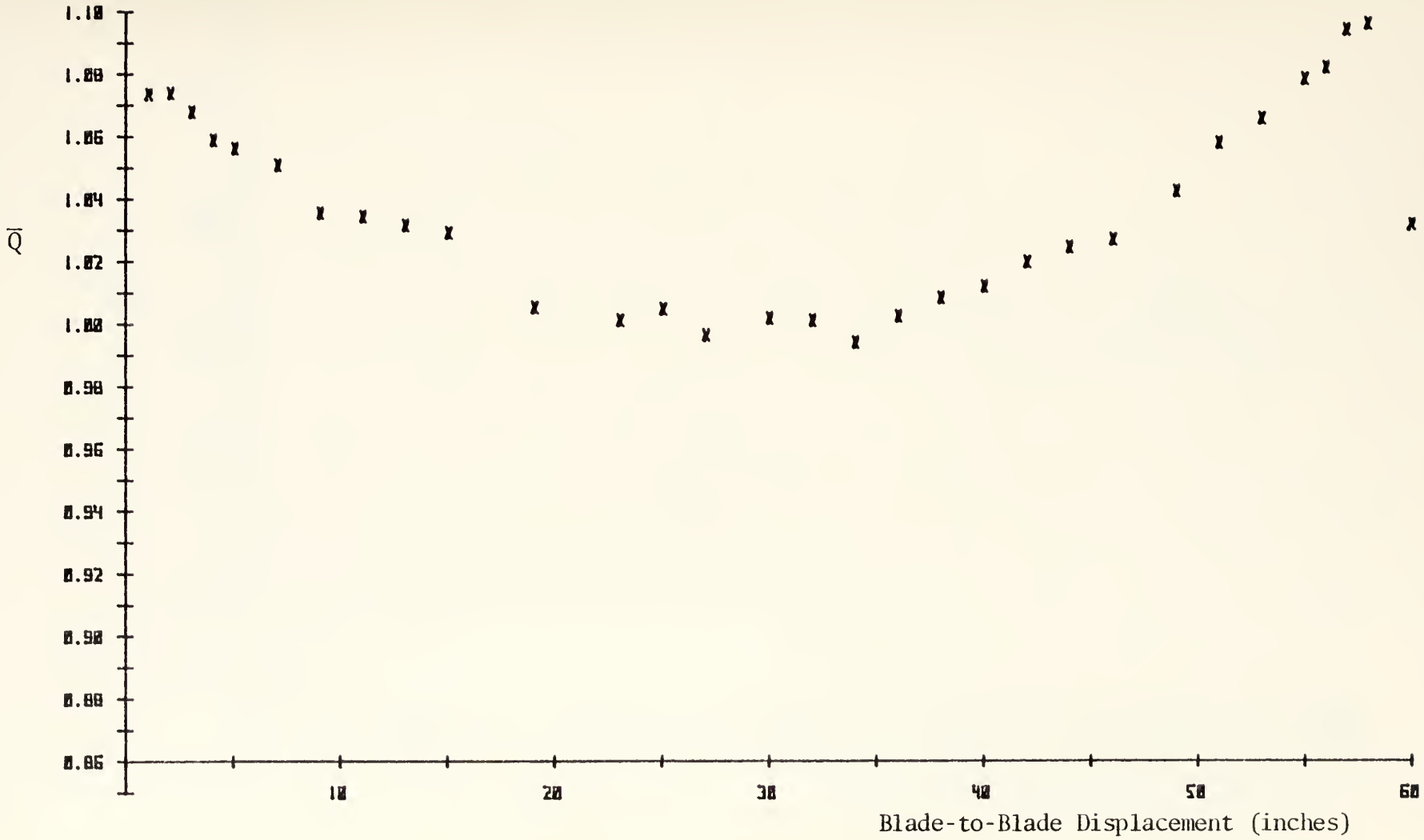

Figure 7b. Blade-to-Blade Dynamic Pressure Distribution at the Test Plane (at 50% Span, Velocity = 270 ft/sec) - Configuration #1

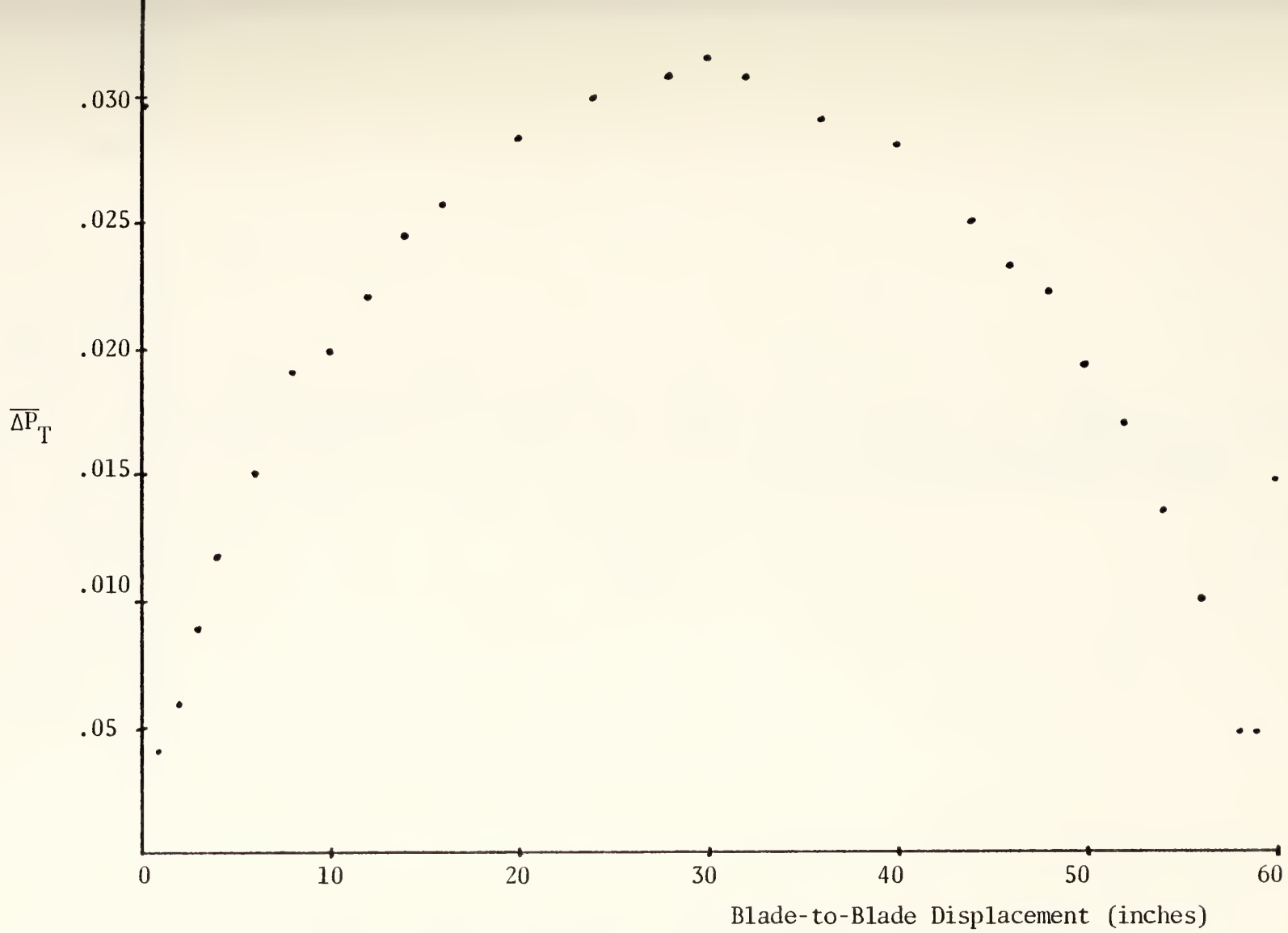

Figure 7c. Blade-to-Blade Total Pressure Distribution at the Test Plane (at 50% Span, Velocity = 230 ft/sec) - Configuration #Ø

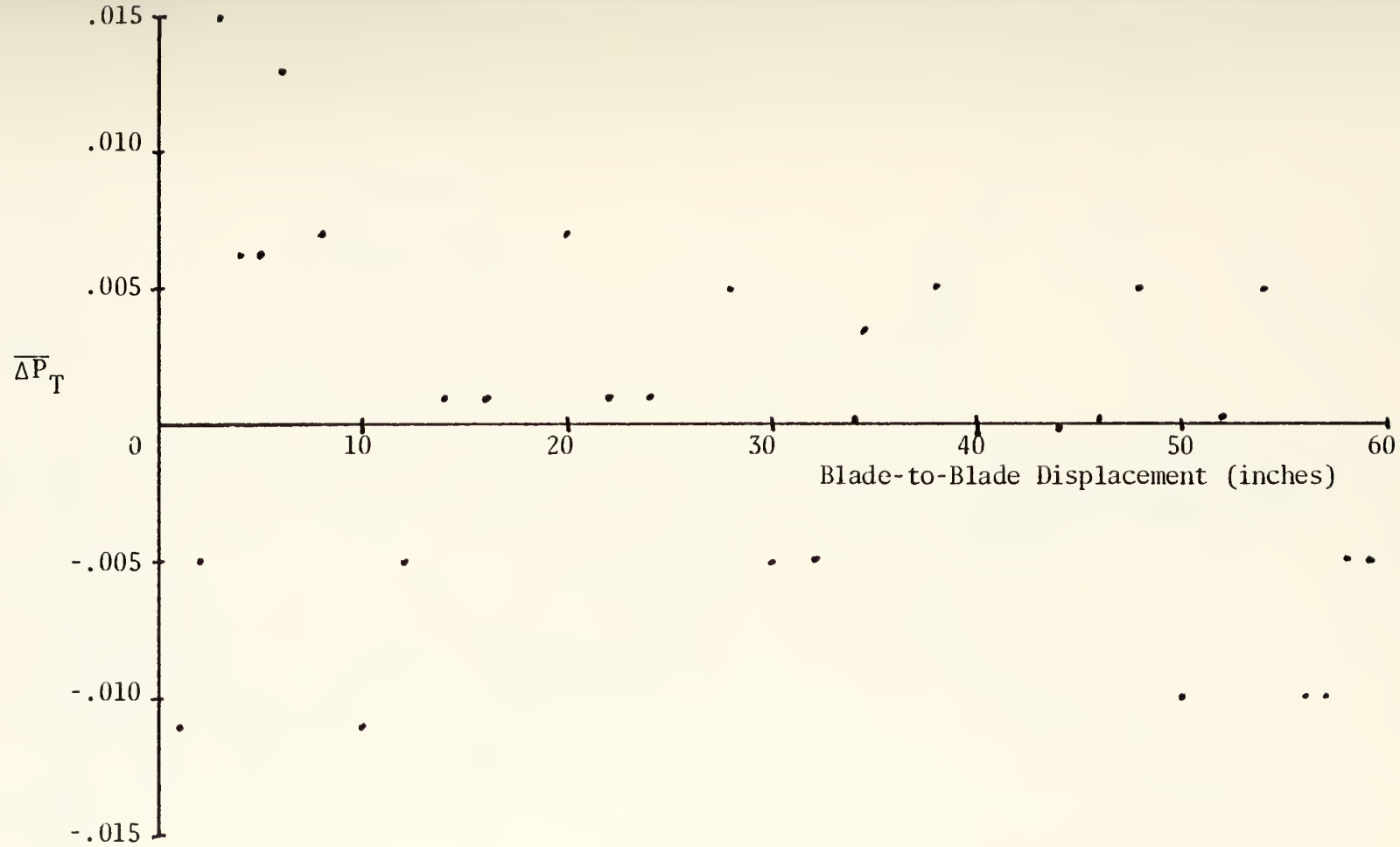

Figure 7d. Blade-to-Blade Total Pressure Distribution at the Test Plane (at 50% Span, Velocity = 280 ft/sec) - Configuration #1

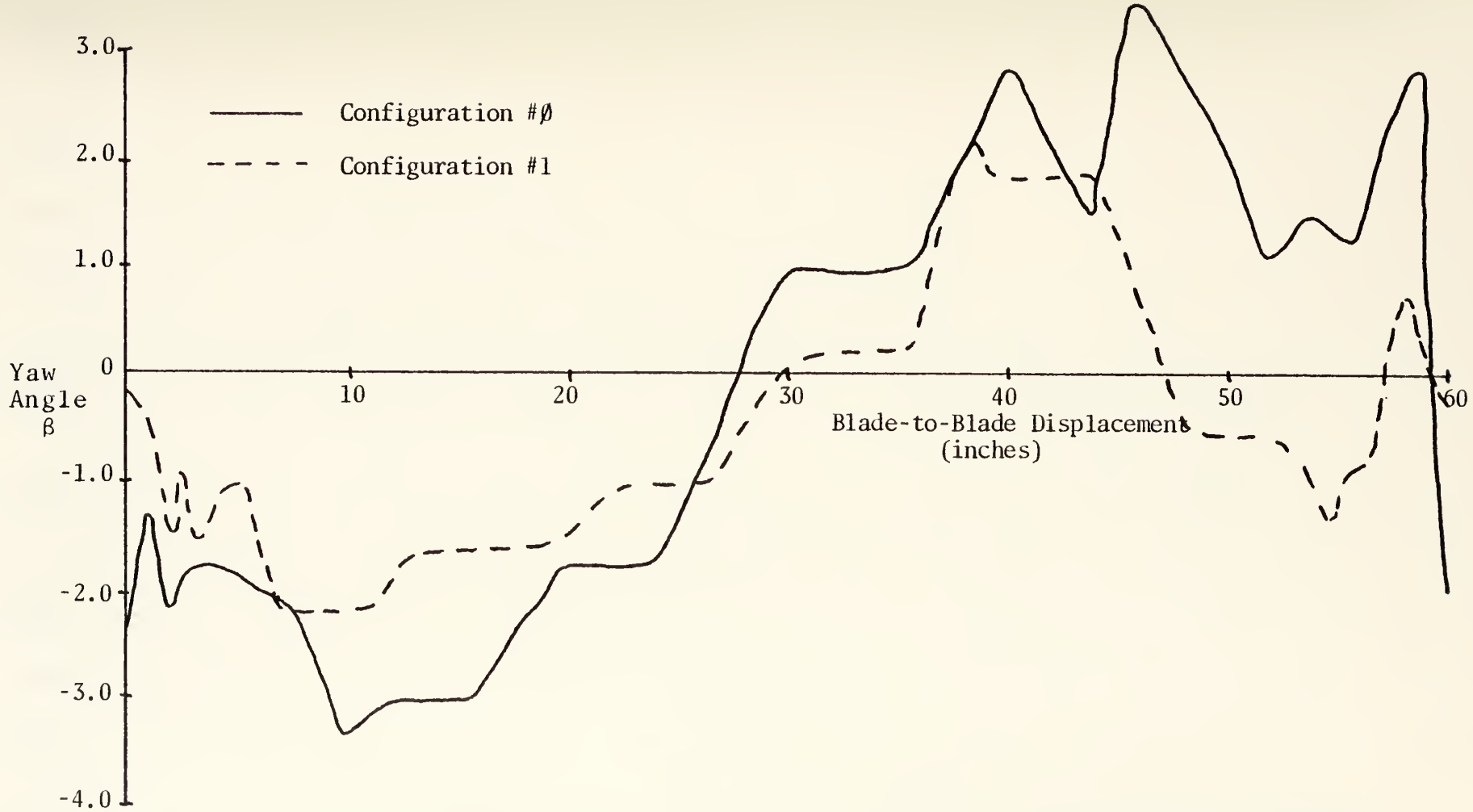

Figure 7e. Blade-to-Blade Yaw Angle Distribution at the Test Plane (at 50% Span, Velocity = 230, 280 ft/sec) - Configuration #Ø and #1

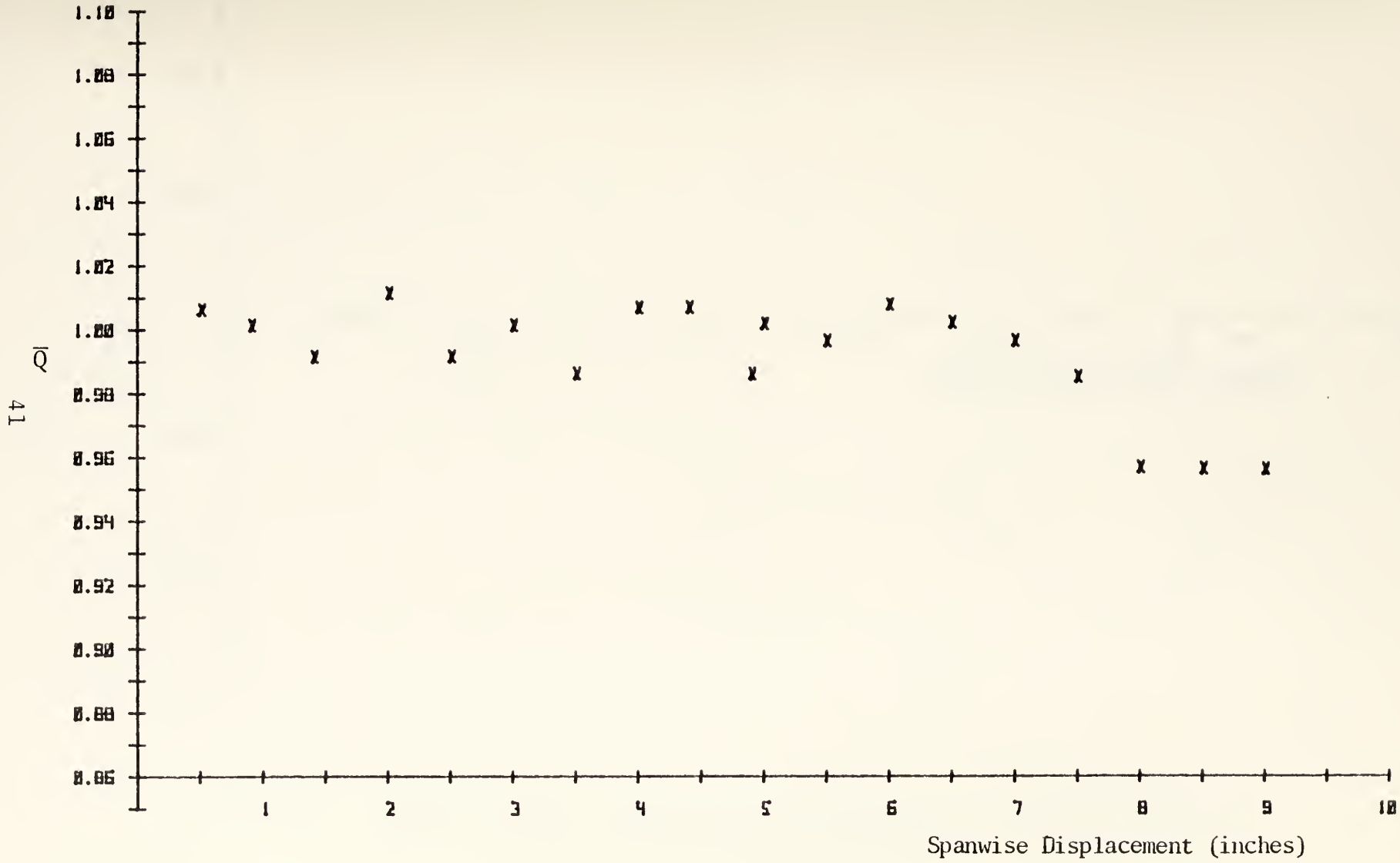

Figure 8a. Spanwise Dynamic Pressure Distribution at the Test Plane (at X = 30 in., Velocity = 280 ft/sec) - Configuration #1

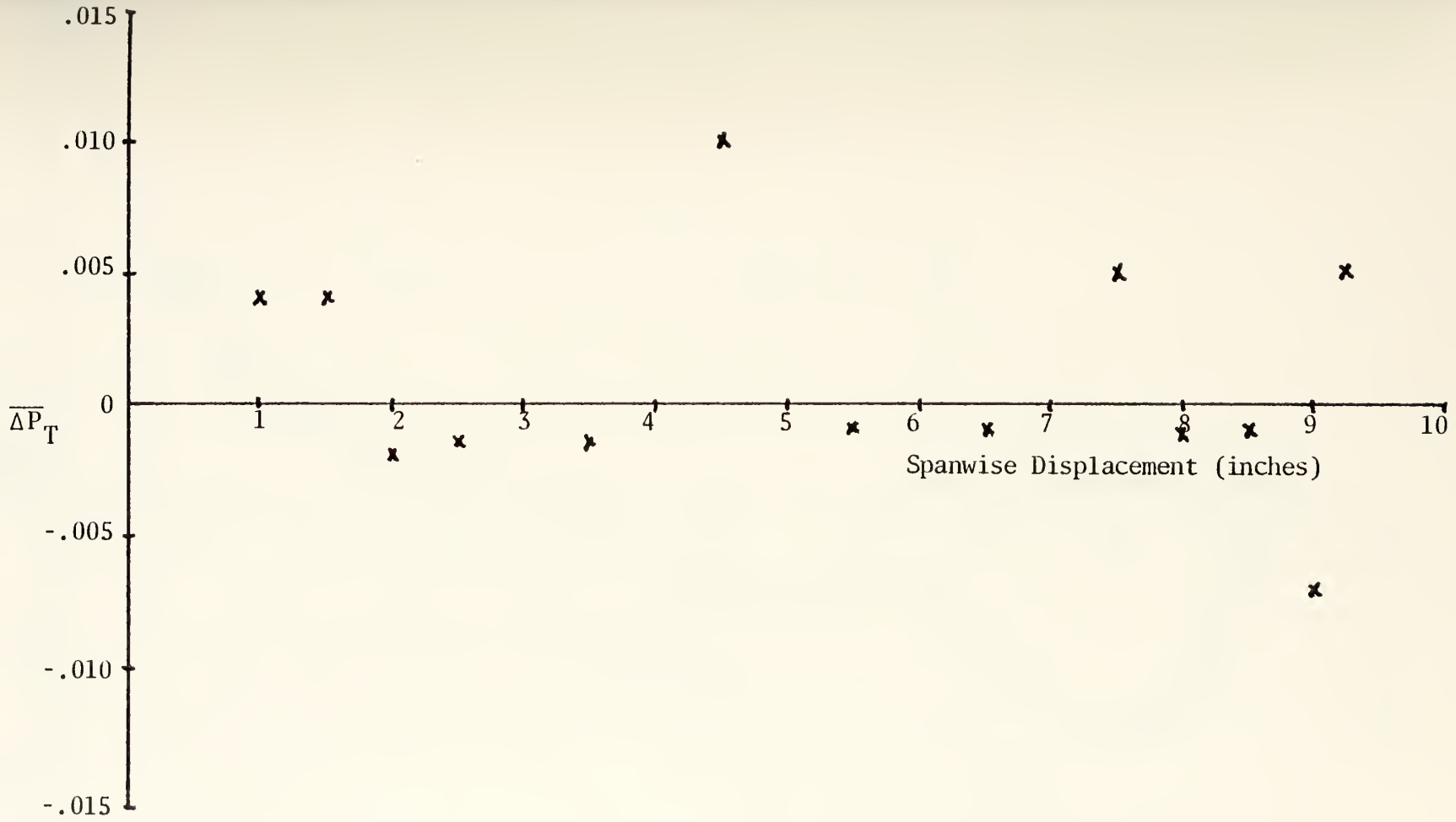

Figure 8b. Spanwise Total Pressure Distribution at the Test Plane (at X = 30 in., Velocity = 280 ft/sec) - Configuration #1

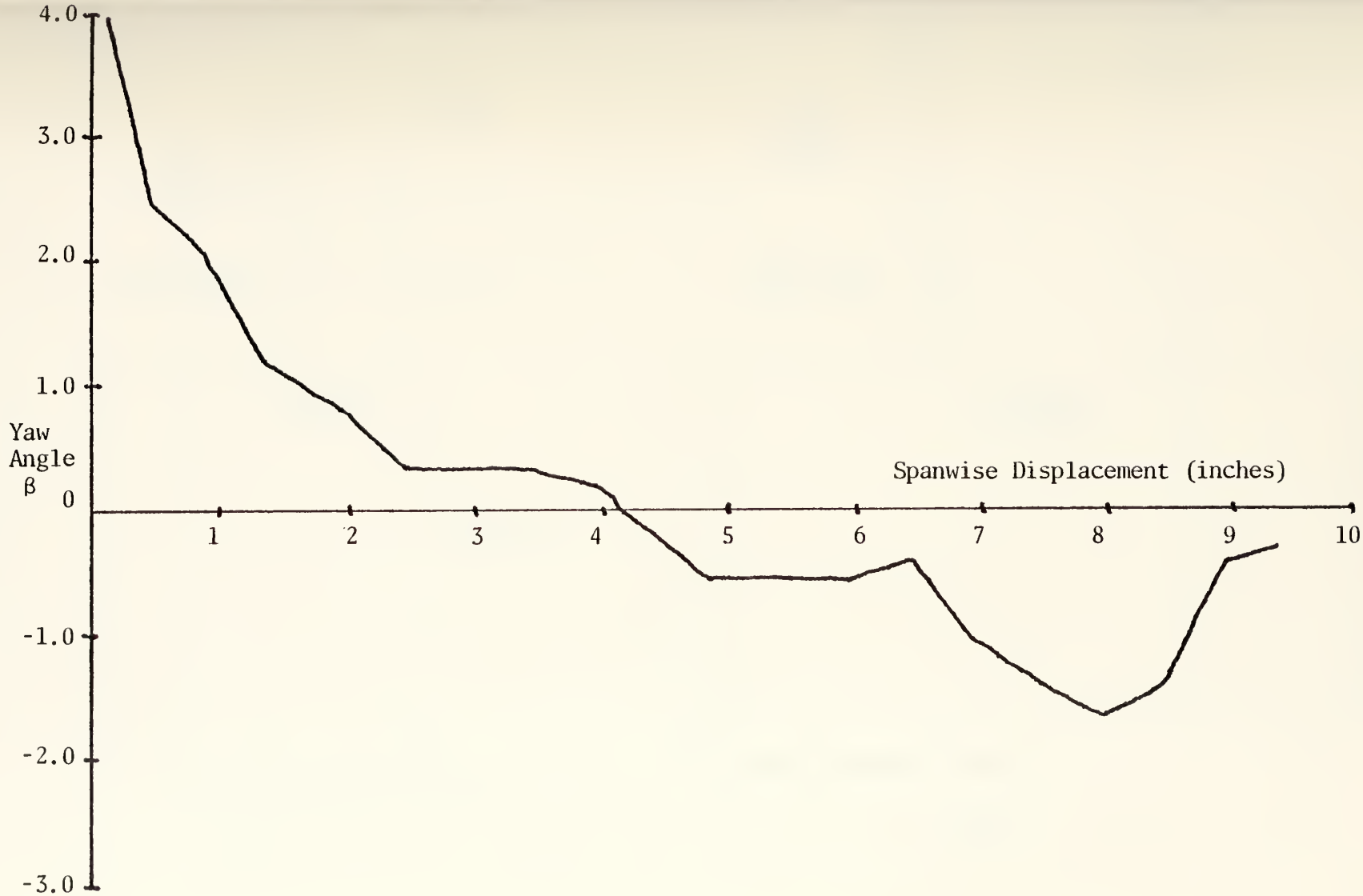

Figure 8c. Spanwise Yaw Angle Distribution at the Test Plane (at X = 30 in., Velocity = 280 ft/sec) - Configuration #1

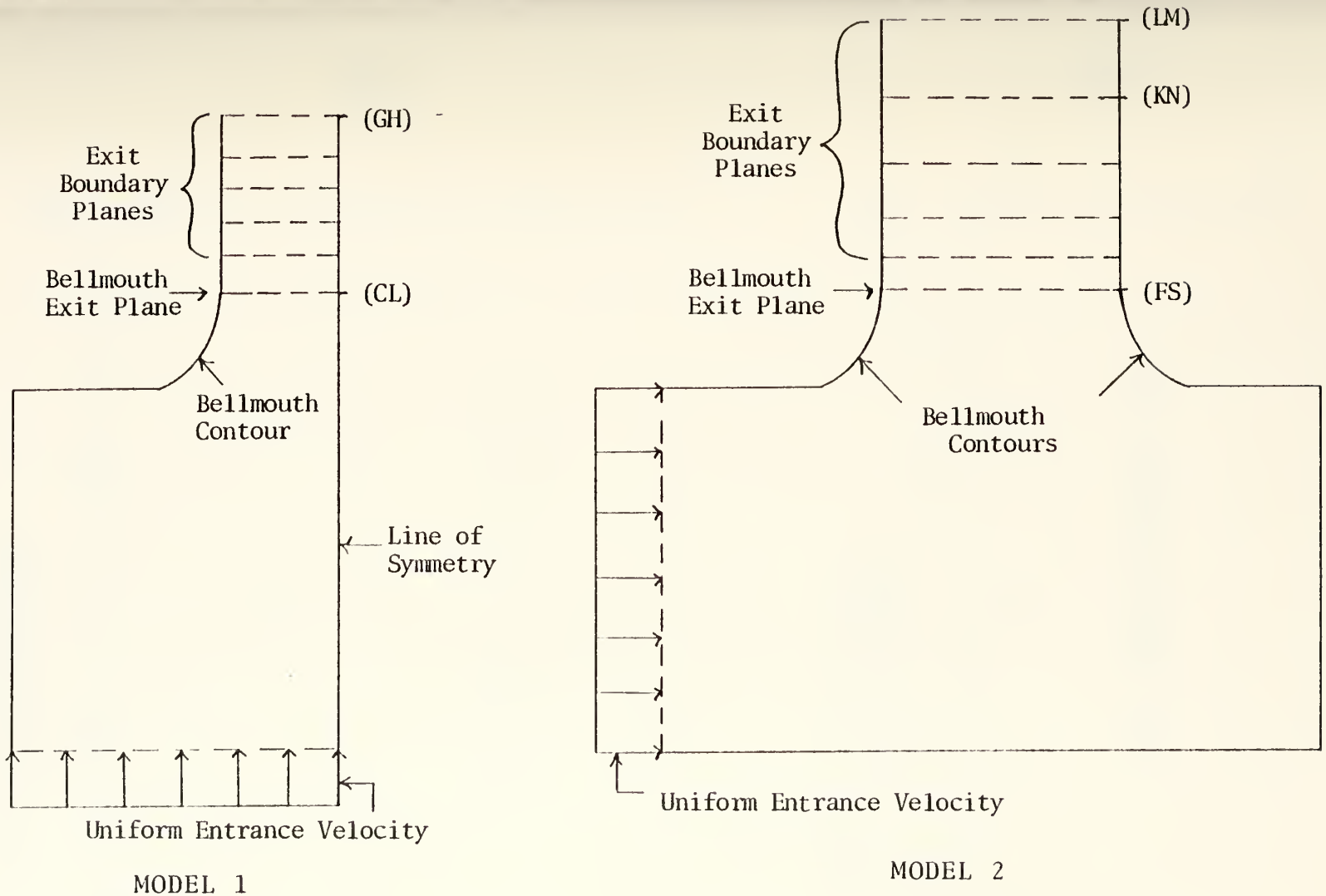

Figure 9. Plenum and Bellmouth Finite Element Flow Analysis Models

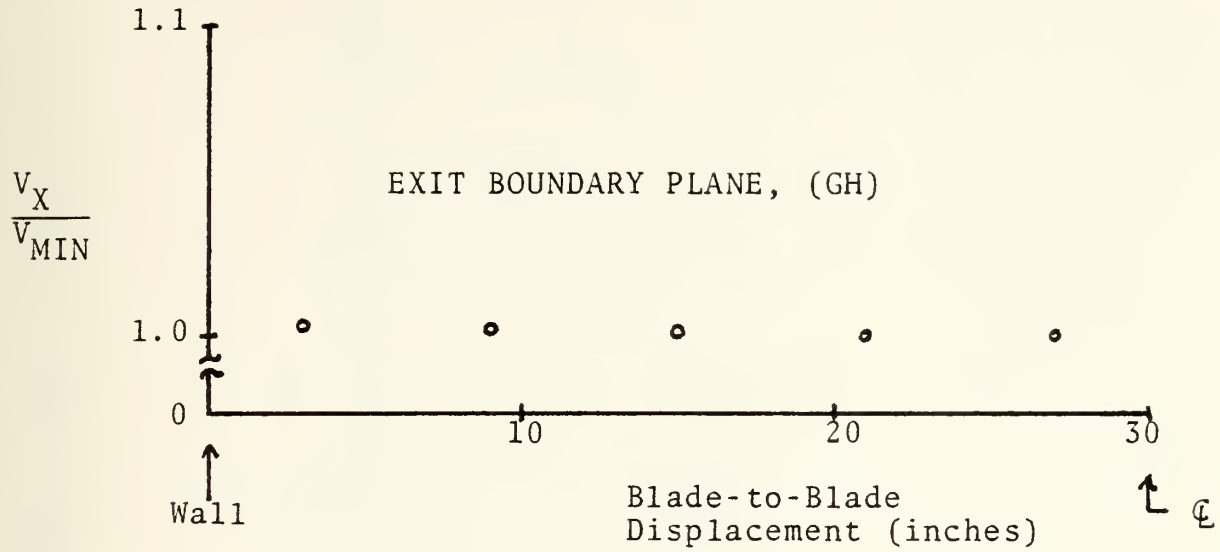

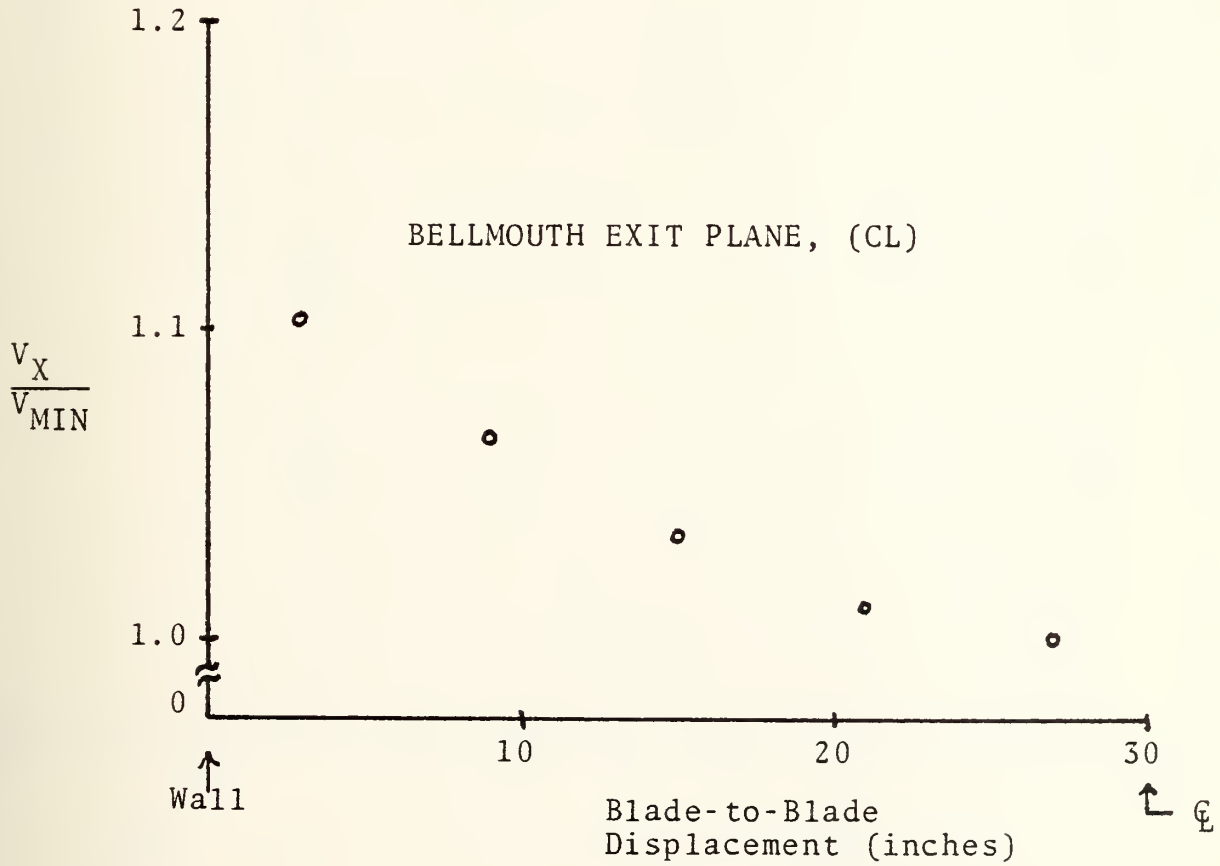

Figure 10. Finite Element Analysis, Velocity Distributions Using Model 1

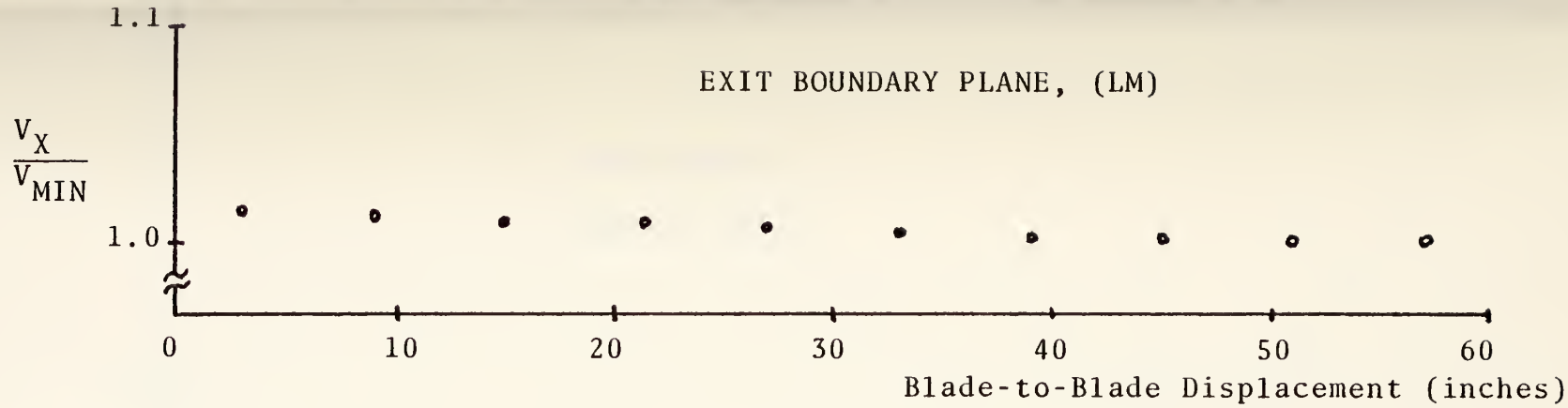

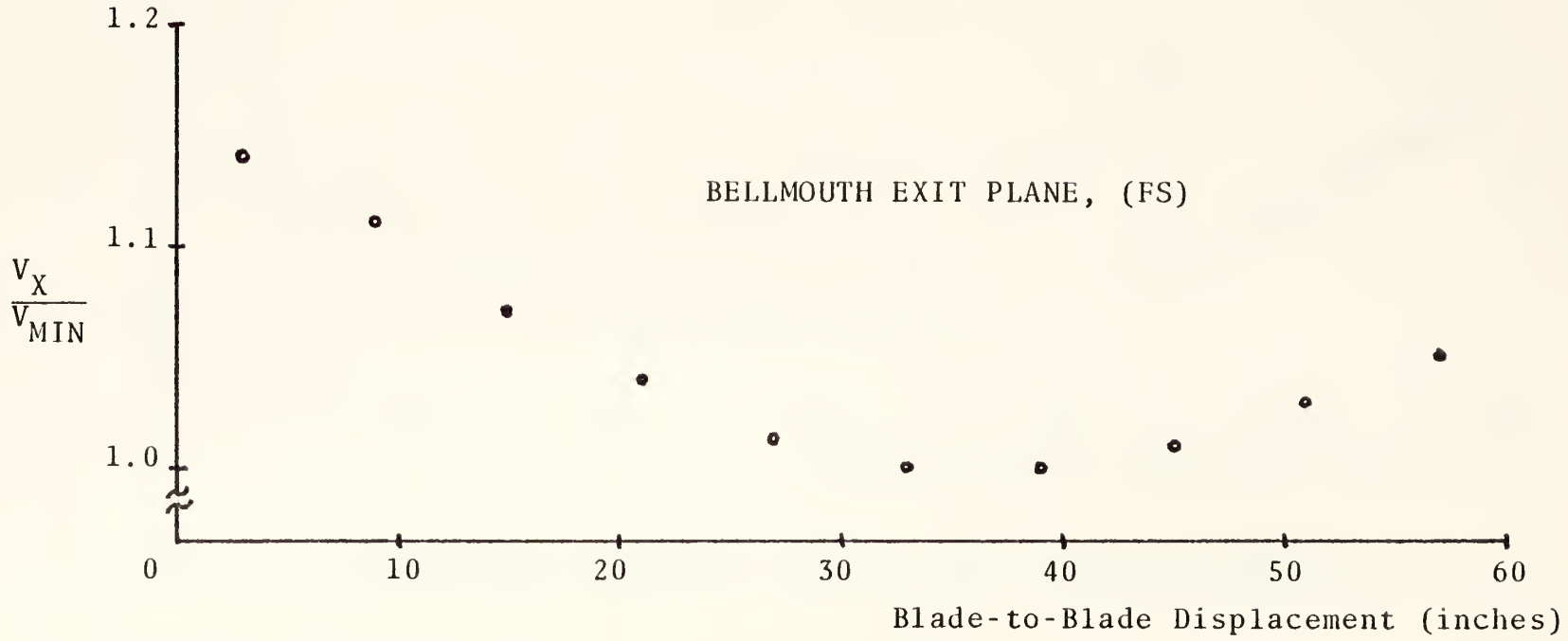

Figure 11. Finite Element Analysis, Velocity Distributions Using Model 2

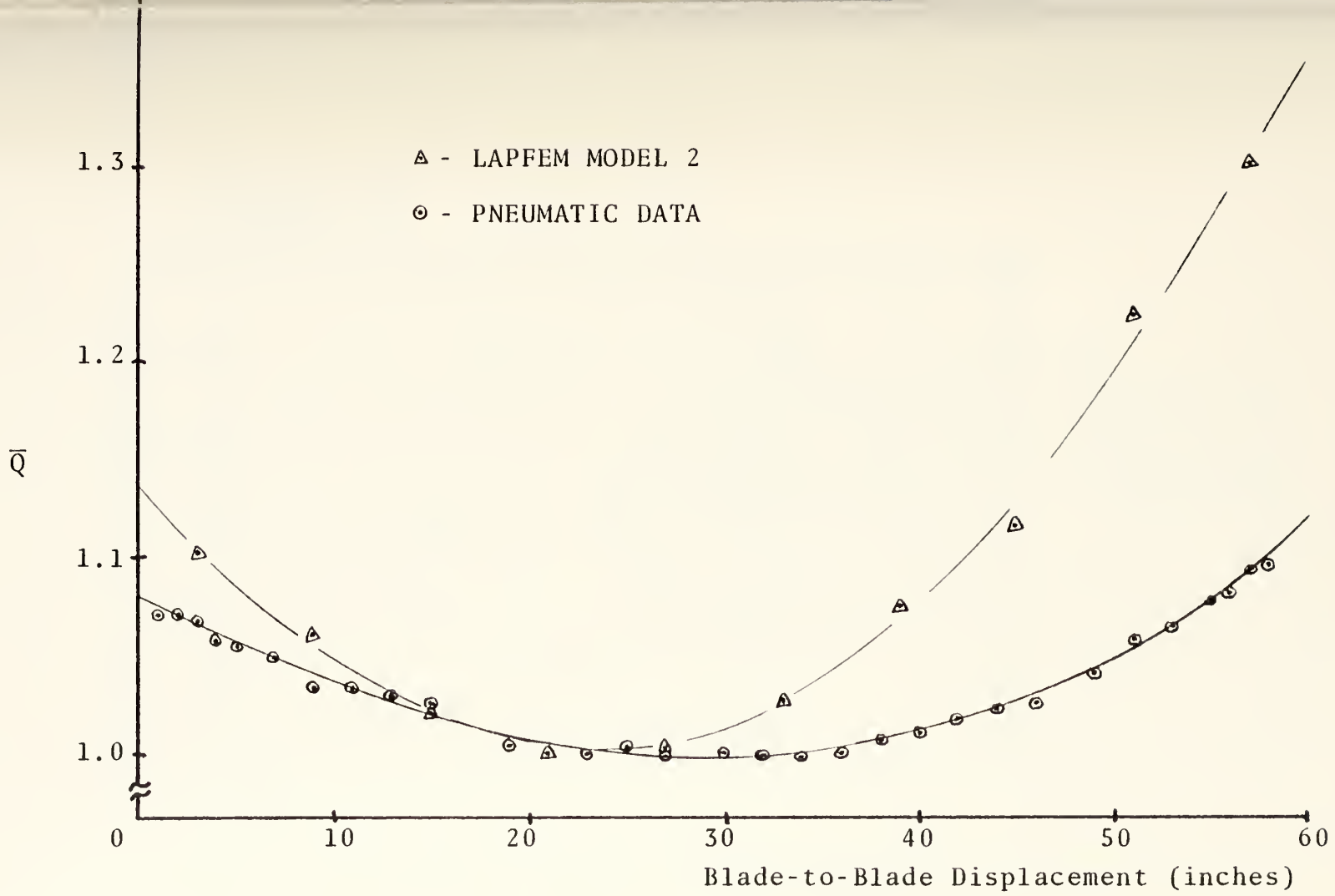

Figure 12. Comparison of Dynamic Pressure Distributions (Pneumatic Data at 50% Span, Velocity = 270 ft/sec) - Configuration #1

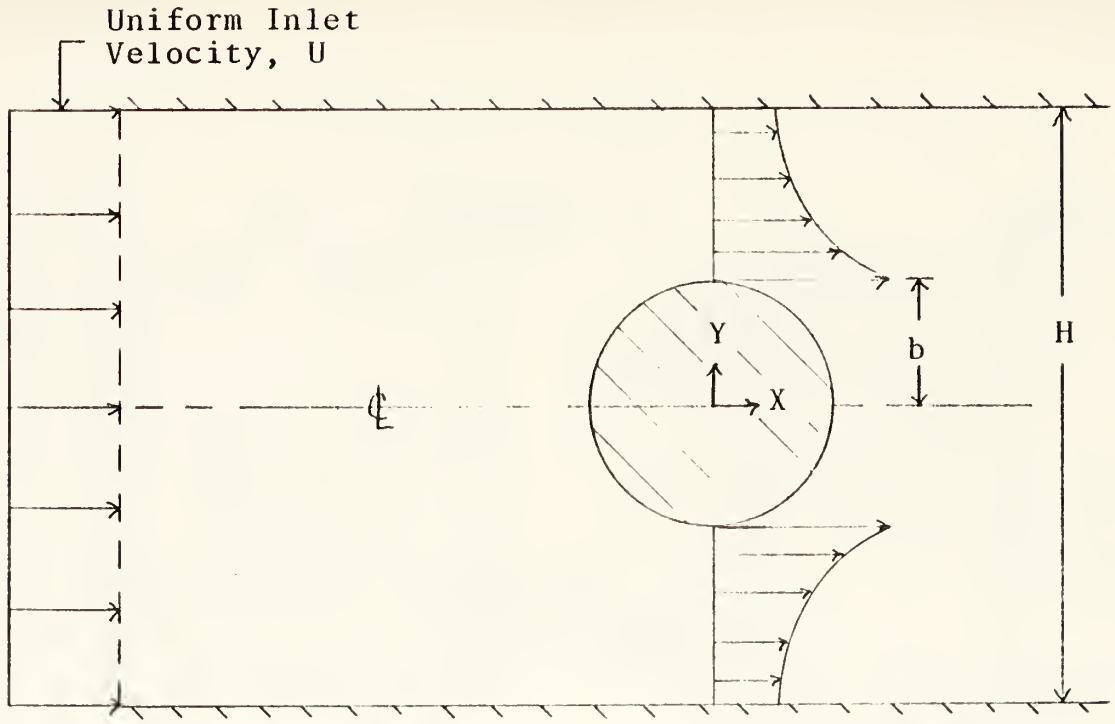

Figure 13. Flow Model Analyzed in Reference 8

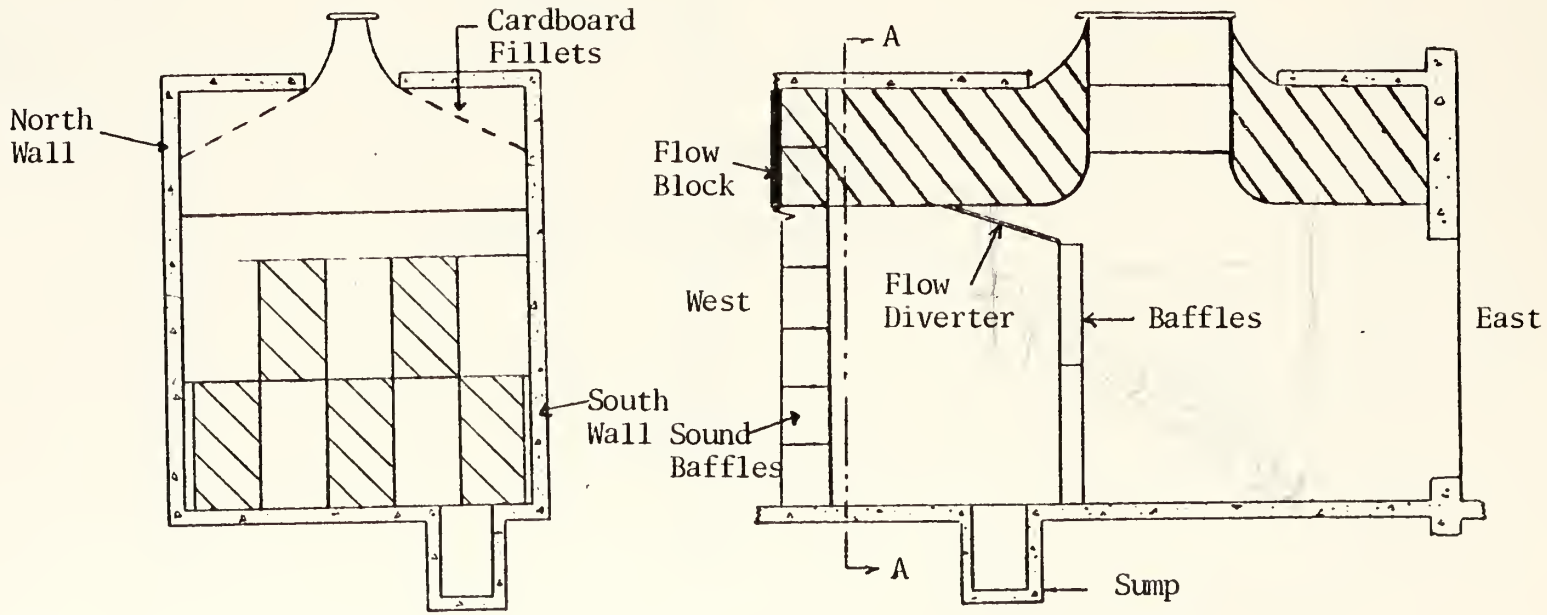

Figure 14. Plenum - Configuration #7 (Side Views)

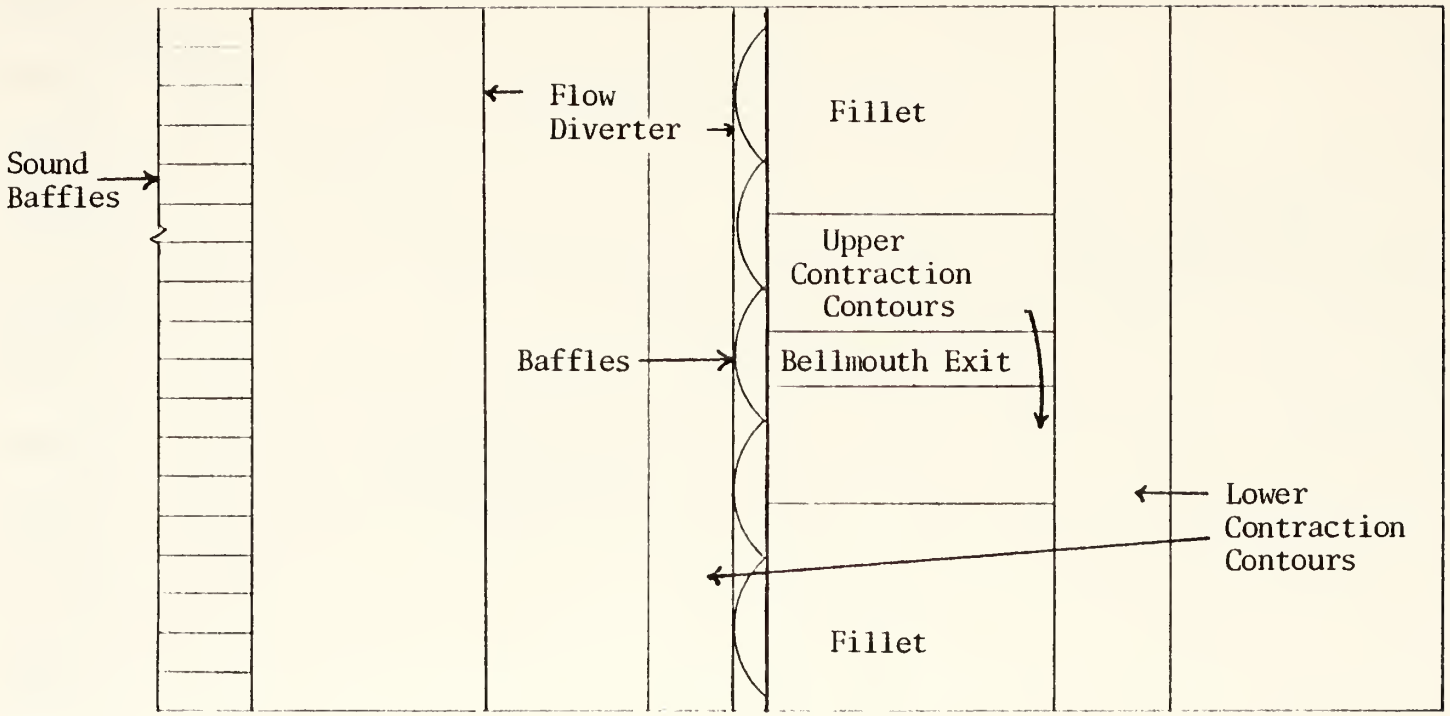

Figure 15. Plenum - Configuration #7 (Plan View)

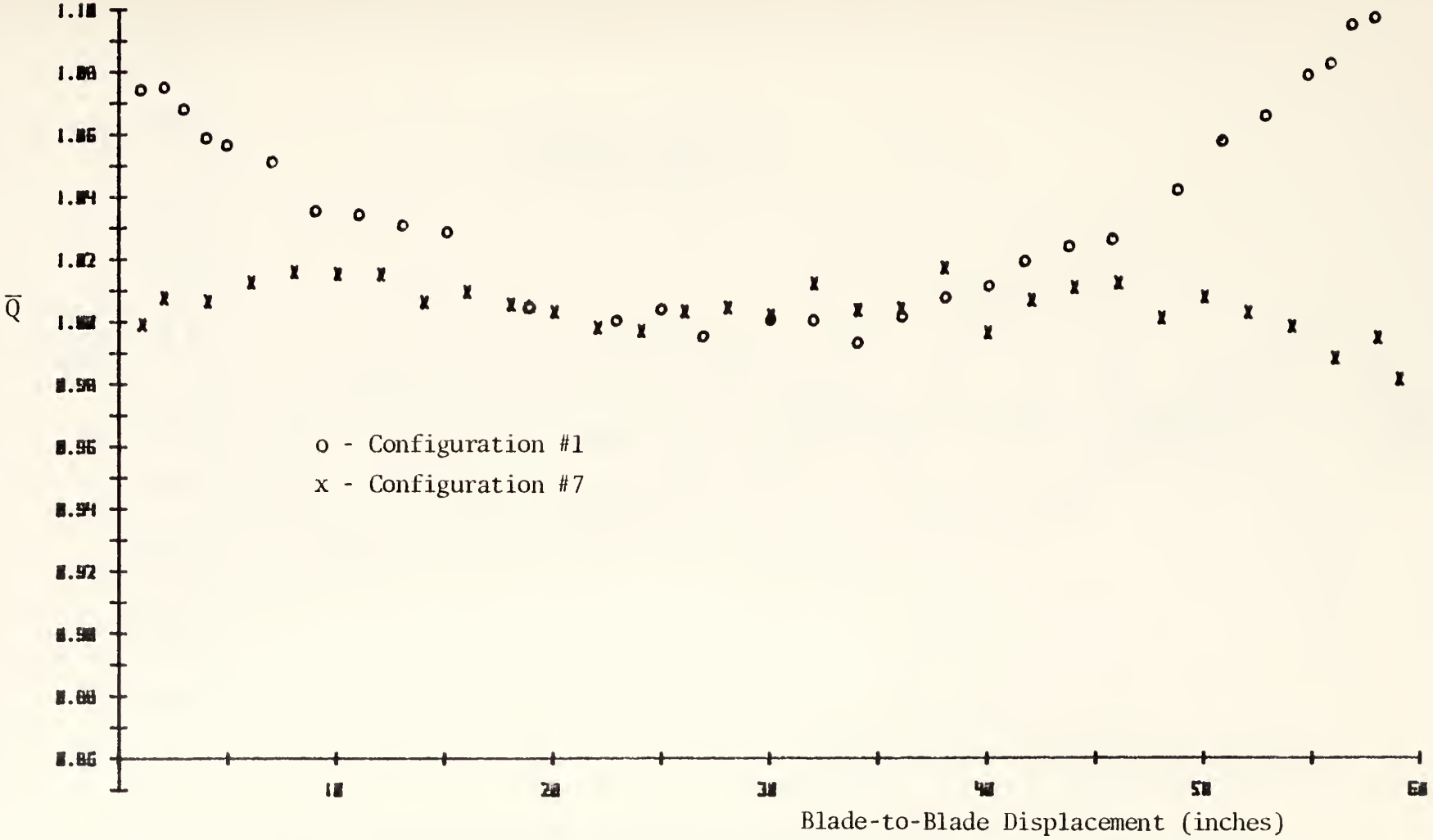

Figure 16a. Blade-to-Blade Dynamic Pressure Distribution at the Test Plane (at 50% Span, Velocity = 270 ft/sec) - Configurations #1 and #7.

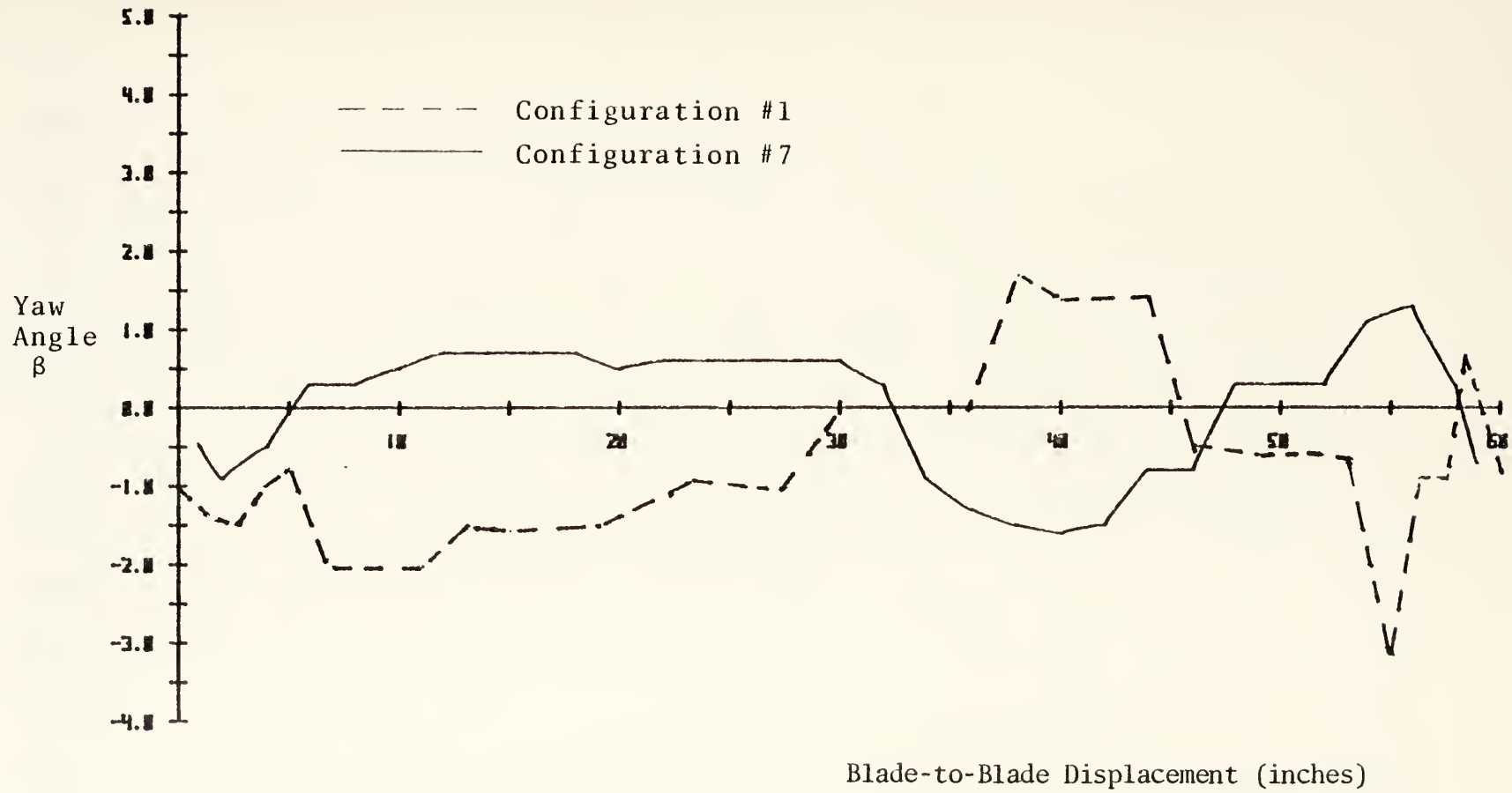

Figure 16b. Blade-to-Blade Yaw Angle Distribution at the Test Plane (at 50% Span, Velocity = 270 ft/sec) - Configurations #1 and #7

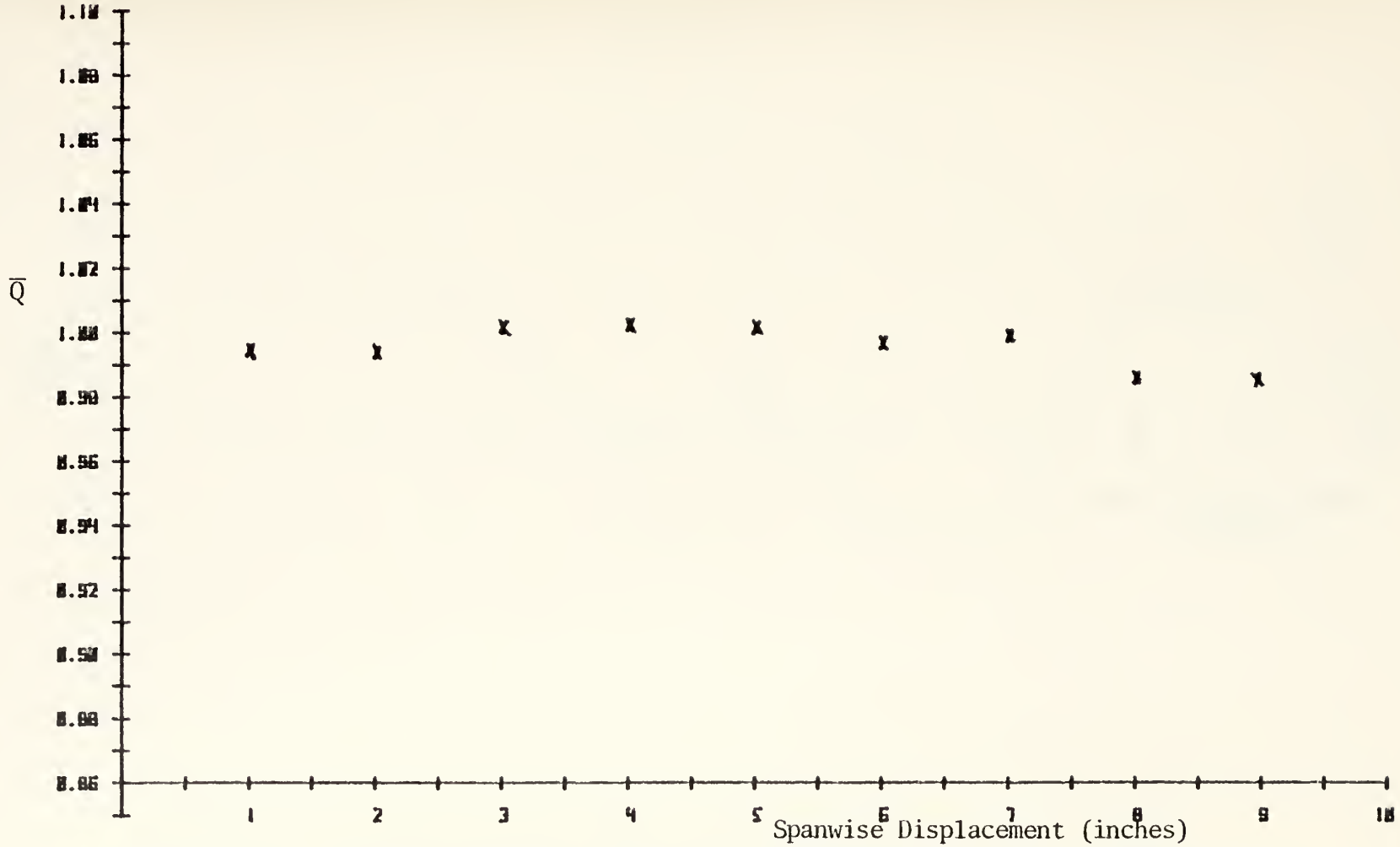

Figure 17a. Spanwise Dynamic Pressure Distribution at the Test Plane (at X = 50 in., Velocity = 270 ft/sec) - Configuration #7

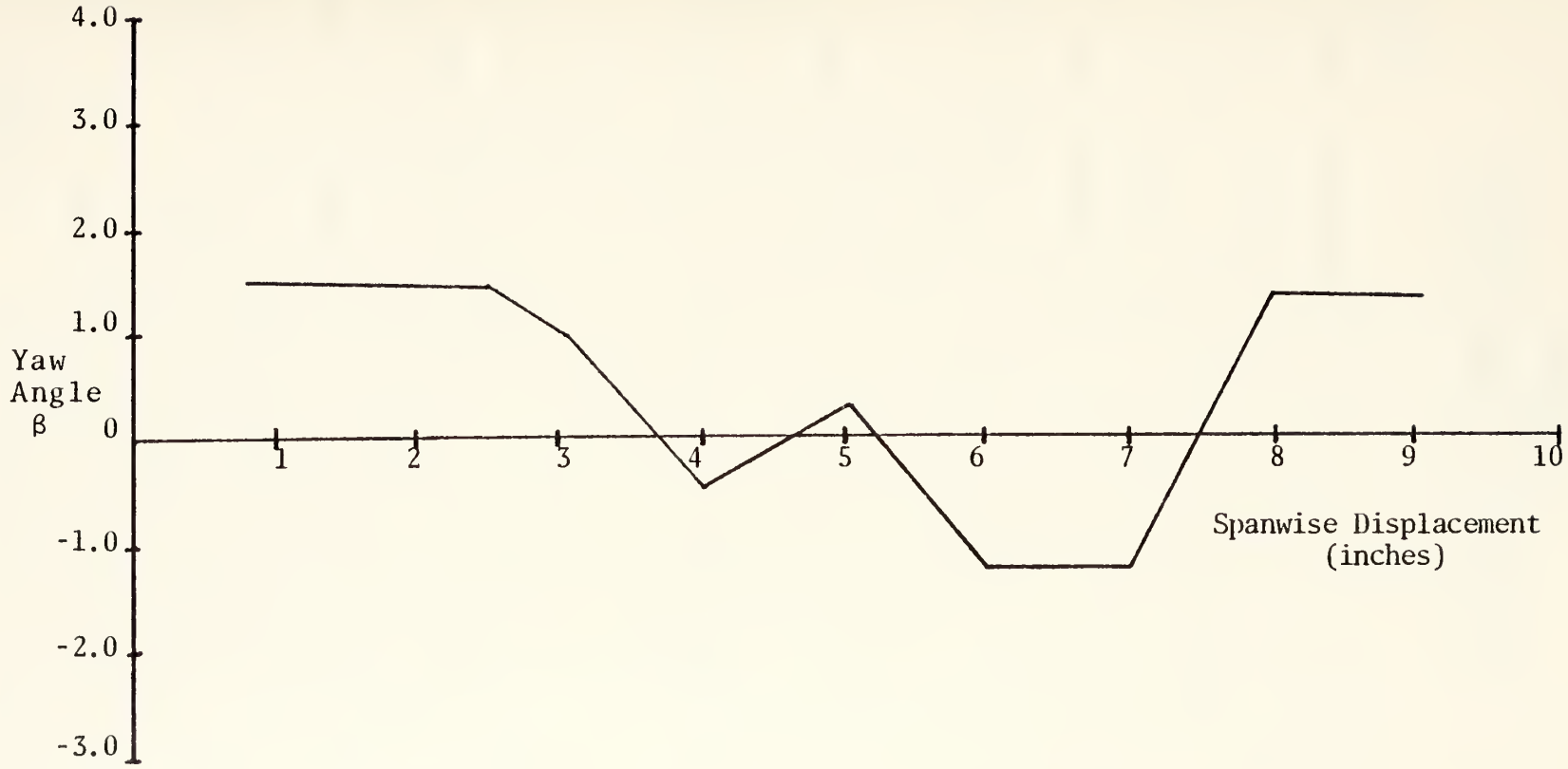

Figure 17b. Spanwise Yaw Angle Distribution at the Test Plane (at X = 50 in., Velocity = 270 ft/sec) - Configuration #7

APPENDIX A

FINITE ELEMENT FLOW ANALYSIS

A.1 Method

A computer program was developed to solve LaPlace's Equation (two-dimensional potential flow) in terms of the stream function, ψ. The purpose of the analysis was to substantiate the premise that the measured velocity distributions in the blade-to-blade directions were a result of the inlet contraction design. The finite element method analysis, FEM, was used to solve this continuum problem. The detailed procedures for an FEM analysis are presented in Ref. 9, with numerous specific fluid flow applications in Ref. 8.

An FEM analysis results in a piecewise approximation of the field variable in the governing flow equation. In the present case, the flow is governed by LaPlace's Equation, $\nabla^2 \psi = 0$, where ψ is the field variable. The solution was sought for the flow through a two-dimensional contraction with the same physical shape as the bellmouth of the NPS Rectilinear Cascade. Two different models were used to represent the incoming flow and plenum boundaries.

The first step in applying the FEM was to divide the continuum into a discrete number of elements. Model 1 is shown in Fig. A-1 with the appropriate boundary conditions specified. Only one-half of the contraction required analysis due to symmetry. The discretization of the area ABGH

was carried out with a framework of graphically estimated lines of constant velocity potential, ϕ = constant, and streamlines of constant ψ. This method was both accurate and efficient since it gave smaller elements where velocity gradients were high (or boundary geometry changes occurred, as in the contraction contour), and larger elements where gradients were small.

The next step was to assign nodes to the element vertices and to select an interpolation function to represent the variation in ψ over the element [Ref. 9, Chap. 5]. A linear two-dimensional interpolation polynomial was chosen.

The third step was to determine the matrix equations expressing the properties of a single element. Galerkin's method of weighted residuals was chosen to accomplish this task [Ref. 9, Chap. 4].

The fourth step required an assembly of the sets of matrix equations for each element into a large system matrix. The system matrix was modified at this point to introduce the specified boundary conditions [Ref. 9, Chap. 3]. The boundary conditions were specified in terms of node values of the field variable of its first derivative.

Fifth, the combined set of system equations were solved simultaneously for the nodal values of the field variable. In the present case, a computer library subroutine called "LEQTIF" was used. However, any equivalent linear equation solver could be used here.

Once the values of ψ at each of the nodes were determined, the final step was to obtain a value for the average velocity between any two adjacent nodes. Since ψ was assumed to vary linearly between nodes, and the velocity was given by, for example,

$$U = \frac{\partial \psi}{\partial Y} ,$$

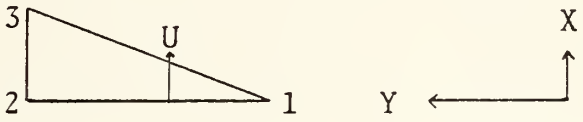

the average velocity was calculated using

$$U = \frac{\psi_2 - \psi_1}{Y_2 - Y_1} .$$

A.2 Computer Program

A listing of the Fortran IV FEM program "LAPFEM," written for the NPS IBM 360, is given in Table A-I. Table A-II is a listing of terms not defined in the program comments. The data required for input is given in each "READ" statement. The data used for Model 1 with (GH) as the exit plane (see Fig. 9) are given in Table A-III.

Referring to Fig. A-1, and using for example the element number 1, the correspondence between element and system coordinates was as follows:

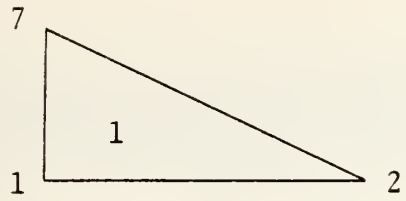

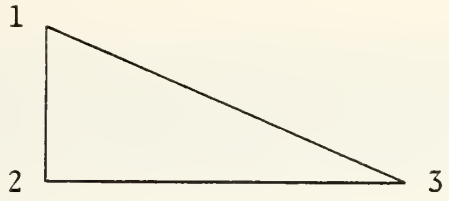

System Element

General Element

ICOR (1,1) = 7

ICOR (1,2) = 1

ICOR (1,3) = 2

In general, the rules are as follows:

1) Correspond all elements in either a clockwise or an anti-clockwise manner.

2) If an element has 1 side on a boundary, then ICOR (I,1) and ICOR (I,2) will be the two nodes of that side.

3) If an element has two sides on boundaries, as does element #1, then the correspondance proceeds anti-clockwise along the bounded sides first, as shown above.

The finite element construction for Model 2 is shown in Fig. A-2. The data used when the exit plane was at (LM) are presented in Table A-IV. The results are shown in Fig. 11. As one can see, a larger number of system elements are required when there is no axis of symmetry.

The values output from "LAPFEM" are as follows:

1) Values of ψ at each node point.

2) Velocities between specified nodes.

TABLE A-I. "LAPFEM" PROGRAM LISTING

```
C****     THIS PROGRAM SOLVES LAPLACES EQUATION                                  LAP00010
C****     BY THE FINITE ELEMENT METHOD USING LINEAR TRIANGULAR ELEMENTS          LAP00020
C    ITYPE=0 FOR A)INTERIOR ELEMENTS, B)ELEMENTS W. A SINGLE POINT ON THE       LAP00030
C              C)DIRICHLET B.C.'S ON ALL BDRY EDGES, D)ELEMENTS WITH            LAP00040
C               NEUMANN BOUNDARY VALUE = ZERO.                                  LAP00050
C    ITYPE=1,2 FOR ELEMENTS W. CAUCHY B.C.'S A)ON EDGE 1-2 ONLY B) ON EDG       LAP00060
C              AND 2-3                                                         LAP00070
C    ITYPE=3,4 FOR ELEMENTS W. NEUMANN B.C.'S A)ON EDGE1-2,B)ON EDGES 1-3      LAP00080
C                              |                                               LAP00090
C                           NON-ZERO                                           LAP00100
C   **********************                                                     LAP00110
      COMMON/MAFO/SYSA(215,215),SYSF(215),X(215),Y(215),ICOR(365,3),           LAP00120
     1ITYPE(365),NEL,NSNP,CVC(365),CVN(365)                                    LAP00130
      DIMENSION WKAREA(500),INBC(125),BCVC(125),BCVN(125),BCVD(125)            LAP00140
     X,ICBC(125),IDBC(125),INVN(20),INVNE(20),VEL(20),IIEL(365),VELE(20)       LAP00150
C****       I. MODEL DESCRIPTION                                               LAP00160
C                                                                              LAP00170
C  ******************                                                          LAP00180
C   NNBC IS THE NO. OF NODES WITH NEUMANN B.C.                                 LAP00190
C   BCVN IS THE VALUE OF THE NEUMANN B.C.(AVG VALUE)                           LAP00200
C   NCBC IS THE NO. OF NODES WITH CAUCHY B.C.                                  LAP00210
C   BCVC IS THE VALUE OF THE CAUCHY B.C. (AVG VALUE)                           LAP00220
C   NDBC IS THE NO. OF NODES WITH DIRICHLET B.C.                               LAP00230
C   BCVD IS THE VALUE OF THE DIRICHLET B.C.                                    LAP00240
C   ZOMEGA IS THE VALUE OF OMEGA IN THE CAUCHY B.C.                            LAP00250
C   NVN IS THE NO. OF NODES THAT I WANT VELOCITIES BETWEEN.                    LAP00260
C  ***************************                                               LAP00270
      READ(5,10) NEL,NSNP,NCBC,NNBC,NDBC,NVN                                   LAP00280
 10   FORMAT(6I5)                                                              LAP00290
      DO 77 I=1,125                                                            LAP00300
      BCVC(I)=0.0                                                              LAP00310
      BCVN(I)=0.0                                                              LAP00320
      BCVD(I)=0.0                                                              LAP00330
      ICBC(I)=0                                                                LAP00340
      INBC(I)=0                                                                LAP00350
      IDBC(I)=0                                                                LAP00360
 77   CONTINUE                                                                 LAP00370
      WRITE(6,11) NEL,NSNP,NCBC,NNBC,NDBC                                      LAP00380
 11   FORMAT(/2X,'NO. OF ELEMENTS = ',I5,//2X,'NO. OF SYSTEM NODES = '         LAP00390
     X,I5,//2X,'NO. OF CAUCHY B.C. = ',I5,//2X,'NO. OF NEUMANN B.C. = '       LAP00400
     X,I5,//2X,'NO. OF DIRICHLET B.C. = ',I5)                                  LAP00410
C   ****************                                                           LAP00420
C   ICBC IS THE IDENTITY OF THE CAUCHY B.C. NODE   } i.e. NODE NUMBER          LAP00430
C   INBC IS THE IDENTITY OF THE NEUMANN B.C. NODE  }                           LAP00440
C   IDBC IS THE IDENTITY OF THE DIRICHLET B.C. NODE }                          LAP00450
C   INVN IS THE IDENTITY OF THE NODES THAT I WANT VEL. BETWEEN.                LAP00460
C  ***************                                                           LAP00470
 12   FORMAT(14I5)                                                             LAP00480
```

```
 13     FORMAT(6F10.3)                                                          LAP00490
        IF(NCBC.EQ.0) GO TO 1000                                                LAP00500
        READ(5,12) (ICBC(I), I=1,NCBC)                                          LAP00510
        READ(5,13) (BCVC(I),I=1,NCBC)                                           LAP00520
        WRITE(6,14) (ICBC(I),BCVC(I),I=1,NCBC)                                  LAP00530
 14     FORMAT(/2X,'NODE NO. 1 ',I5,5X,'CAUCHY BOUNDARY VALUE = ',F10.2)        LAP00540
 10CC   IF(NNBC.EQ.0) GO TO 2000                                                LAP00550
        READ(5,12) (INBC(I), I=1,NNBC)                                          LAP00560
        READ(5,13) (BCVN(I),I=1,NNBC)                                           LAP00570
        WRITE(6,15) (INBC(I),BCVN(I),I=1,NNBC)                                  LAP00580
 15     FORMAT(/2X,'NODE NO. = ',I5,5X,'NEUMANN BOUNDARY VALUE = ',F10.2)       LAP00590
 20CC   IF(NDBC.EQ.0) GO TO 3000                                                LAP00600
        READ(5,12) (IDBC(I), I=1,NDBC)                                          LAP00610
        READ(5,13) (BCVD(I),I=1,NDBC)                                           LAP00620
        WRITE(6,16) (IDBC(I),BCVD(I),I=1,NDBC)                                  LAP00630
 16     FORMAT(/2X,'NODE NO. = ',I5,5X,'DIRICHLET B.V. = ',8X,F10.2)            LAP00640
        READ(5,27) (INVN(I),I=1,NVN)                                            LAP00650
        READ(5,27) (INVNE(I),I=1,NVN)                                           LAP00660
 27     FORMAT(14I5)                                                            LAP00670
        WRITE(6,28) (INVN(I),I=1,NVN)                                           LAP00680
 28     FORMAT(/2X,'VELOCITIES ARE WANTED BETWEEN NODES ',14I5)                 LAP00690
        WRITE(6,74) (INVNE(I),I=1,NVN)                                          LAP00700
 74      FORMAT(/2X,'EXIT VELOCITIES ARE WANTED BETWEEN NODES ',                LAP00710
     X14I5)                                                                     LAP00720
 30CC   READ(5,17) ZOMEGA                                                       LAP00730
 17     FORMAT(F10.2)                                                           LAP00740
        WRITE(6,18) ZOMEGA                                                      LAP00750
 18     FORMAT(/2X,' THE VALUE OF ZOMEGA IS  ',F6.2)                            LAP00760
C         LOCATION OF SYSTEM NODAL POINTS                                       LAP00770
       READ(5,20) (X(I),Y(I),I=1,NSNP)                                          LAP00780
    20 FORMAT(2G10.5)                                                           LAP00790
       WRITE(6,25)                                                              LAP00800
    25 FORMAT(/15X,'NP',15X,'X LOCATION',15X,'Y LOCATION')                      LAP00810
       WRITE(6,30) (I,X(I),Y(I),I=1,3)                                          LAP00820
    30 FORMAT(12X,I5,18X,G12.5,12X,G12.5)                                       LAP00830
C  **********                                                                   LAP00840
C     CORRESPONDENCE TABLE                                                      LAP00850
C  **********                                                                   LAP00860
       READ(5,35) (IIEL(IEL),ICOR(IEL,1),ICOR(IEL,2),ICOR(IEL,3)               LAP00870
     X,ITYPE(IEL),IEL=1,NEL)                                                    LAP00880
    35 FORMAT(5I5)                                                              LAP00890
       WRITE(6,40)                                                              LAP00900
    40 FORMAT(/2X,'ELEMENT',6X,'NP 1',9X,'NP 2',9X,'NP 3',9X,'ITYPE')           LAP00910
       WRITE(6,45) (IIEL(IEL),(ICOR(IEL,I),I=1,3),ITYPE(IEL),IEL=1,3)           LAP00920
    45 FORMAT(I5,8X,I5,8X,I5,8X,I5,8X,I5)                                       LAP00930
       DO 205 I=1,365                                                           LAP00940
       CVC(I)=0.0                                                               LAP00950
 205   CVN(I)=0.0                                                               LAP00960
```

```
      IF(NCBC.EQ.0) GO TO 700                                          LAP00970
      DO 48  I=1,NCBC                                                  LAP00980
      J=ICBC(I)                                                        LAP00990
 48   CVC(J)=BCVC(I)                                                   LAP01000
 700  IF(NNBC.EQ.0) GO TO 800                                          LAP01010
      DO 49  I=1,NNBC                                                  LAP01020
      J=INBC(I)                                                        LAP01030
 49   CVN(J)=BCVN(I)                                                   LAP01040
C************                                                         LAP01050
C*****      II. FORMATION OF AU=F                                      LAP01060
C***********                                                          LAP01070
 800  CALL FORMAF                                                      LAP01080
C                                                                     LAP01090
C  *****************                                                  LAP01100
C    A AND F MATRIX MANIPULATED FOR DIRICHLET B.C.                    LAP01110
C  *****************                                                  LAP01120
      DO 501 I=1,NDBC                                                  LAP01130
      J=IDBC(I)                                                        LAP01140
      DO 502  K=1,NSNP                                                 LAP01150
      IF(K.EQ.J) GO TO 94                                              LAP01160
      FI= SYSA(K,J)* BCVD(I)                                           LAP01170
      SYSF(K)= SYSF(K) -FI                                             LAP01180
 94   SYSA(K,J) = 0.0                                                  LAP01190
 502  SYSA(J,K)= 0.0                                                   LAP01200
      SYSA(J,J)= 1.0                                                   LAP01210
 501  SYSF(J)=   BCVD(I)                                               LAP01220
      WRITE(6,95) ((SYSA(I,J),J=1,NSNP),I=1,1)                         LAP01230
 95   FORMAT('0',10G10.2)                                              LAP01240
      WRITE(6,95) (SYSF(I),I=1,NSNP)                                   LAP01250
C************                                                         LAP01260
C*****      III. SOLUTION OF AU=F                                      LAP01270
C  **************                                                     LAP01280
      CALL LEQT1F(SYSA,1,NSNP,215,SYSF,0,WKAREA,IER)                   LAP01290
C  *************                                                      LAP01300
C        THE U(I) VALUES                                              LAP01310
C  *************                                                      LAP01320
     WRITE(6,50)                                                       LAP01330
  50 FORMAT(2X,'THE SOLUTION')                                         LAP01340
      WRITE(6,55) (I,SYSF(I),I=1,NSNP)                                 LAP01350
 55   FORMAT(' ',I5,5X,G12.5)                                          LAP01360
      N=NVN-1                                                          LAP01370
      DO 52 I=1,N                                                      LAP01380
      J=INVN(I)                                                        LAP01390
      K=INVN(I+1)                                                      LAP01400
      L=INVNE(I)                                                       LAP01410
      M=INVNE(I+1)                                                     LAP01420
      VELE(I)=(SYSF(M)-SYSF(L))/(Y(L)-Y(M))                            LAP01430
      WRITE(6,54) M,L,VELE(I)                                          LAP01440
```

```
 54      FORMAT(/2X,'EXIT VELOCITY BETWEEN NODES ',I3,' AND ', I3,          LAP01450
     X' IS',F10.3)                                                          LAP01460
        VEL(I) = (SYSF(K)-SYSF(J))/(Y(J)-Y(K))                              LAP01470
        WRITE(6,53) K,J,VEL(I)                                              LAP01480
 53     FORMAT(/2X,'VELOCITY BETWEEN NODES ',I3,' AND ',I3,' IS',F10.3)     LAP01490
 52     CONTINUE                                                            LAP01500
        END                                                                 LAP01510
C **********                                                               LAP01520
C*****     II. FORMATION OF AU=F                                           LAP01530
C **************                                                           LAP01540
      SUBROUTINE FORMAF                                                     LAP01550
      COMMON/MAFO/SYSA(215,215),SYSF(215),X(215),Y(215),ICOR(365,3),        LAP01560
     1ITYPE(365),NEL,NSNP,CVC(365),CVN(365)                                 LAP01570
C****          INITIALIZE A AND F                                          LAP01580
      DO 100 I=1,NSNP                                                       LAP01590
      SYSF(I)=0.0                                                           LAP01600
      DO 90 J=1,NSNP                                                        LAP01610
      SYSA(I,J)=0.0                                                         LAP01620
   90 CONTINUE                                                              LAP01630
  100 CONTINUE                                                              LAP01640
C****          CALCULATE ELEMENT A AND F COEFFICIENTS                      LAP01650
C                                                                           LAP01660
      WRITE(6,10)                                                           LAP01670
   10 FORMAT(2X,'ELEM',6X,'B1',13X,'B2',13X,'B3',13X,'C1',13X,'C2',13X      LAP01680
     1,'C3',13X,'AREA')                                                     LAP01690
      DO 500 IEL=1,NEL                                                      LAP01700
C****          ESTABLISH SYSTEM-ELEMENT CORRESPONDENCE                     LAP01710
      II=ICOR(IEL,1)                                                        LAP01720
      JJ=ICOR(IEL,2)                                                        LAP01730
      KK=ICOR(IEL,3)                                                        LAP01740
C****          CALCULATE ELEMENT GEOMETRY                                  LAP01750
      B1=Y(JJ)-Y(KK)                                                        LAP01760
      B2=Y(KK)-Y(II)                                                        LAP01770
      B3=Y(II)-Y(JJ)                                                        LAP01780
      C1=X(KK)-X(JJ)                                                        LAP01790
      C2=X(II)-X(KK)                                                        LAP01800
      C3=X(JJ)-X(II)                                                        LAP01810
      DEL=ABS(C2*B1-C1*B2)                                                  LAP01820
       AREA= DEL/2.                                                         LAP01830
C****          CALCULATE ELEMENT A AND F COEFFICIENTS (ELA,ELF)            LAP01840
       AR=1/(2.*DEL)                                                        LAP01850
      ELA11=((ABS(B1)**2.)+(ABS(C1)**2.))*AR                                LAP01860
      ELA12=(B1*B2+C1*C2)*AR                                                LAP01870
      ELA21=ELA12                                                           LAP01880
      ELA13=(B1*B3+C1*C3)*AR                                                LAP01890
      ELA31=ELA13                                                           LAP01900
      ELA22=((ABS(B2)**2.)+(ABS(C2)**2.))*AR                                LAP01910
      ELA23=(B2*B3+C2*C3)*AR                                                LAP01920
```

```
      ELA32=ELA23                                                       LAP01930
      ELA33=((ABS(B3)**2.)+(ABS(C3)**2.))*AR                            LAP01940
       ELF1=0.0                                                         LAP01950
       ELF2=0.0                                                         LAP01960
       ELF3=0.0                                                         LAP01970
C  ***********                                                          LAP01980
C          MODIFY ELEMENT MATRICES FOR CAUCHY  BOUNDARY CONDITIC        LAP01990
C     ZOMEGA IS ASSUMED CONSTANT BETWEEN NODES                          LAP02000
C  ***************                                                      LAP02010
C                                                                       LAP02020
      IF(ITYPE(IEL).EQ.0) GO TO 150                                     LAP02030
       IF(ITYPE(IEL).GE.3) GO TO 145                                    LAP02040
      EL12=SQRT(((ABS(X(II)-X(JJ)))**2.)+((ABS(Y(II)-Y(JJ)))**2.))      LAP02050
      AM=EL12*ZOMEGA/6.                                                 LAP02060
      ELA11=ELA11+2.*AM                                                 LAP02070
      ELA12=ELA12+AM                                                    LAP02080
      ELA21=ELA12                                                       LAP02090
      ELA22=ELA11                                                       LAP02100
      IF(ITYPE(IEL).EQ.1) GO TO 140                                     LAP02110
      EL23=SQRT(((ABS(X(JJ)-X(KK)))**2.)+((ABS(Y(JJ)-Y(KK)))**2.))      LAP02120
      AN=EL23*ZOMEGA/6.                                                 LAP02130
      ELA23=ELA23+AN                                                    LAP02140
      ELA32=ELA23                                                       LAP02150
      ELA22=ELA22+2.*AN                                                 LAP02160
      ELA33=ELA33+2.*AN                                                 LAP02170
C  ******************                                                   LAP02180
C    THE GENERAL FORM FOR THE BOUNDARY CONDITIONS IS AS FOLLOWS         LAP02190
C                                                                       LAP02200
C       DPHI/DN + ZOMEGA*PHI = BCVC  OR BCVN.                           LAP02210
C       ZOMEGA IS EQUAL TO 0 FOR A NEUMANN B.C.                         LAP02220
C                                                                       LAP02230
C  ****************                                                     LAP02240
C          MODIFY ELEMENT FORCE VECTORS FOR CAUCHY BOUNDARY CONDITIONS  LAP02250
C          AND NEUMANN BOUNDARY CONDITIONS                              LAP02260
C     THE VALUES OF BCVC AND BCVN ARE ASSUMED CONSTANT BETWEEN NODES    LAP02270
C  **************                                                       LAP02280
C                                                                       LAP02290
 140   ELF1=EL12*(-CVC(II)/2.)                                          LAP02300
       ELF2=EL12*(-CVC(JJ)/2.)                                          LAP02310
       IF(ITYPE(IEL).EQ.1) GO TO 150                                    LAP02320
       ELF3=EL23*(-CVC(KK)/2.)                                          LAP02330
       GO TO 150                                                        LAP02340
 145   EL12=SQRT(((ABS(X(II)-X(JJ)))**2.)+((ABS(Y(II)-Y(JJ)))**2.))     LAP02350
       EL23=SQRT(((ABS(X(JJ)-X(KK)))**2.)+((ABS(Y(JJ)-Y(KK)))**2.))     LAP02360
       ELF1=EL12*(-CVN(II)/2.)                                          LAP02370
       ELF2=EL12*(-CVN(JJ)/2.)                                          LAP02380
       IF(ITYPE(IEL).EQ.3) GO TO 150                                    LAP02390
       ELF3=EL23*(-CVN(KK)/2.)                                          LAP02400
```

```
C  ************                                                        LAP02410
C          DISTRIBUTE ELEMENTS COEFFICIENTS INTO SYSTEM A AND F        LAP02420
C  ************                                                        LAP02430
  150   SYSA(II,II)=SYSA(II,II)+ELA11                                  LAP02440
        SYSA(II,JJ)=SYSA(II,JJ)+ELA12                                  LAP02450
        SYSA(II,KK)=SYSA(II,KK)+ELA13                                  LAP02460
        SYSA(JJ,JJ)=SYSA(JJ,JJ)+ELA22                                  LAP02470
        SYSA(JJ,II)=SYSA(II,JJ)                                        LAP02480
        SYSA(JJ,KK)=SYSA(JJ,KK)+ELA23                                  LAP02490
        SYSA(KK,II)=SYSA(II,KK)                                        LAP02500
        SYSA(KK,JJ)=SYSA(JJ,KK)                                        LAP02510
        SYSA(KK,KK)=SYSA(KK,KK)+ELA33                                  LAP02520
        SYSF(II)=SYSF(II)+ELF1                                         LAP02530
        SYSF(JJ)=SYSF(JJ)+ELF2                                         LAP02540
        SYSF(KK)=SYSF(KK)+ELF3                                         LAP02550
  500   CONTINUE                                                       LAP02560
        RETURN                                                         LAP02570
        END                                                            LAP02580
```

TABLE A-II

DEFINITION OF TERMS NOT DEFINED IN THE "LAPFEM" PROGRAM COMMENTS

ITYPE	Specifies type of boundary condition
NEL	Total number of system elements
NSNP	Total number of system nodal points
IIEL	Number of element
ICOR	A term to correspond single element node numbers (1,2,3), with system node numbers (1,2,3,4,5,..., NEL)
A	System matrix of coefficients of ψ
U	Column vector of unknown values of ψ $(\psi_1, \psi_2, \ldots, \psi_{NSNP})$
F	Column vector of external node values
SYSA(I,II)	System A matrix
SYSF(I,II)	System F matrix
ELA I II	Elemental A matrix
ELF II	Elemental F matrix
AREA	Element area
I,II	Matrix row and column respectively
X,Y	X and Y locations of each node

TABLE A-III. DATA FOR MODEL 1 ANALYSIS

05/27/79 17.40.49

FILE: LAPDAT FTOSF001 P1 NAVAL POSTGRADUATE SCHOOL

```
  141   91    0    0   35    6
    1    2    3    4    5    6    7   12   13   18   19   24   25   26
   31   32   37   38   43   44   49   50   55   56   61   62   67   68
   73   74   79   80   85   86   91
80.          64.          48.          32.          16.          0.0
80.          0.0          80.          0.0          80.          0.0
80.          80.          0.0          80.          0.0          80.
0.0          80.          0.0          80.          0.0          80.
0.0          80.          0.0          80.          0.0          80.
0.0          80.0         0.0          80.0         0.0
   91   90   89   88   87   86
   91   90   89   88   87   86
 0.0
0.0         160.0
0.0       128.
0.0       96.
0.0       64.
0.0       32.
0.0       0.0
27.5      160.
28.       127.5
28.5      96.
29.       63.5
29.5      31.5
30.       0.0
58.       160.
58.       127.
58.       95.
57.5      62.5
56.5      30.5
55.5      0.0
100.      160.
95.       125.5
85.5      92.
79.       62.
76.       30.
75.       0.0
140.      160.
152.5     120.
129.      104.
110.      81.
99.       55.
94.       26.
93.5      0.0
160.      90.
145.      81.
131.      66.5
117.5     47.5
109.5     23.
107.5     0.0
166.5     76.5
155.      68.
144.      56.
134.      38.5
128.      18.5
125.5     0.0
173.      67.5
164.      59.5
155.5     47.
149.      32.
144.      16.
143.5     0.0
179.0     61.5
172.      52.
166.      40.5
162.      28.
159.5     14.
158.      0.0
185.      57.
179.      47.
```

```
178.        36.
175.5       25.
170.5       13.0
170.        0.0
190.        54.
180.        44.
185.        33.
184.        23.0
183.        12.
183.        0.0
195.        52.0
193.5       42.5
193.        32.
192.5       22.
192.5       11.5
192.5       0.0
201.        51.
200.5       41.5
200.5       32.
200.5       22.
200.5       11.5
200.5       0.0
208.          50.25
208.        41.25
208.          31.5
208.          22.0
208.          11.0
208.          0.0
217.          50.0
217.          41.25
217.          31.5
217.          21.5
217.          11.0
217.          0.0
    1     7     1     2     0
    2     7     2     8     0
    3     2     3     8     0
    4     8     3     9     0
    5     3     4     9     0
    6     9     4    10     0
    7     4     5    10     0
    8    10     5    11     0
    9     5     6    11     0
   10     6    12    11     0
   11    13     7     8     0
   12    13     8    14     0
   13    14     8     9     0
   14    14     9    15     0
   15    15     9    10     0
   16    15    10    16     0
   17    16    10    11     0
   18    16    11    17     0
   19    17    11    12     0
   20    12    18    17     0
   21    19    13    14     0
   22    19    14    20     0
   23    20    14    15     0
   24    20    15    21     0
   25    21    15    16     0
   26    21    16    22     0
   27    22    16    17     0
   28    22    17    23     0
   29    23    17    18     0
   30    18    24    23     0
   31    25    19    20     0
   32    25    20    27     0
   33    27    20    21     0
   34    27    21    28     0
   35    28    21    22     0
   36    28    22    29     0
```

37	29	22	23	0
38	29	23	30	0
39	30	23	24	0
40	24	31	30	0
41	26	25	27	0
42	32	26	27	0
43	32	27	33	0
44	33	27	28	0
45	33	28	34	0
46	34	28	29	0
47	34	29	35	0
48	35	29	30	0
49	35	30	36	0
50	36	30	31	0
51	31	37	36	0
52	38	32	33	0
53	38	33	39	0
54	39	33	34	0
55	39	34	40	0
56	40	34	35	0
57	40	35	41	0
58	41	35	36	0
59	41	36	42	0
60	42	36	37	0
61	37	43	42	0
62	44	38	39	0
63	44	39	45	0
64	45	39	40	0
65	45	40	46	0
66	46	40	41	0
67	46	41	47	0
68	47	41	42	0
69	47	42	48	0
70	48	42	43	0
71	43	49	48	0
72	50	44	45	0
73	50	45	51	0
74	51	45	46	0
75	51	46	52	0
76	52	46	47	0
77	52	47	53	0
78	53	47	48	0
79	53	48	54	0
80	54	48	49	0
81	54	49	55	0
82	56	50	51	0
83	56	51	57	0
84	57	51	52	0
85	57	52	58	0
86	58	52	53	0
87	58	53	59	0
88	59	53	54	0
89	59	54	60	0
90	60	54	55	0
91	55	61	60	0
92	62	56	57	0
93	62	57	63	0
94	63	57	58	0
95	63	58	64	0
96	64	58	59	0
97	64	59	65	0
98	65	59	60	0
99	65	60	66	0
100	66	60	61	0
101	61	67	66	0
102	68	62	63	0
103	68	63	69	0
104	69	63	64	0
105	69	64	70	0
106	70	64	65	0

107	70	65	71	0
108	71	65	66	0
109	71	66	72	0
110	72	66	67	0
111	67	73	72	0
112	74	68	69	0
113	75	74	69	0
114	75	69	70	0
115	76	75	70	0
116	76	70	71	0
117	77	76	71	0
118	77	71	72	0
119	78	77	72	0
120	78	72	73	0
121	73	79	78	0
122	80	74	75	0
123	81	80	75	0
124	81	75	76	0
125	82	81	76	0
126	82	76	77	0
127	83	82	77	0
128	83	77	78	0
129	84	83	78	0
130	84	78	79	0
131	79	85	84	0
132	86	80	81	0
133	87	86	81	0
134	87	81	82	0
135	88	87	82	0
136	88	82	83	0
137	89	88	83	0
138	89	83	84	0
139	90	89	84	0
140	90	84	85	0
141	85	91	90	0
142	92	86	87	0
143	93	92	87	0
144	93	87	88	0
145	94	93	88	0
146	94	88	89	0
147	95	94	89	0
148	95	89	90	0
149	96	95	90	0
150	96	90	91	0
151	91	97	96	0
152	98	92	93	0
153	99	98	93	0
154	99	93	94	0
155	100	99	94	0
156	100	94	95	0
157	101	100	95	0
158	101	95	96	0
159	102	101	96	0
160	102	96	97	0
161	97	103	102	0
162	104	98	99	0
163	105	104	99	0
164	105	99	100	0
165	106	105	100	0
166	106	100	101	0
167	107	106	101	0
168	107	101	102	0
169	108	107	102	0
170	108	102	103	0
171	103	109	108	0
172	110	104	105	0
173	111	110	105	0
174	111	105	106	0
175	112	111	106	0
176	112	106	107	0

177	113	112	107	0
178	113	107	108	0
179	114	113	108	0
180	114	108	109	0
181	109	115	114	0

TABLE A-IV. DATA FOR MODEL 2 ANALYSIS

```
  365   215     0     0    54    11
    1     2     3     4     5     6     7     8     9    10    11    21    31    60
   76    91   102   101   105   116   127   138   149   160    12    22    32    39
   45    53    61    66    77    92    93    94    95    96   103   106   117   128
  139   150   161   171   172   182   183   193   194   204   205   215
0.0         0.0         0.0         0.0         0.0         0.0
0.0         0.0         0.0         0.0         0.0         0.0
0.0         0.0         0.0         0.0         0.0         0.0
0.0         0.0         0.0         0.0         0.0         0.0
16.         32.         48.         64.         80.         96.
112.        128.        144.        160.        160.        160.
160.        160.        160.        160.        160.        160.
160.        160.        160.        0.0         160.        0.0
160.        0.0         160.        0.0         160.        0.0
  215   214   213   212   211   210   209   208   207   206   205
  160   159   158   157   156   155   154   153   152   151   150
0.0
0.0         0.0
0.0         35.
0.0         75.
0.0         110.
0.0         155.
0.0         195.
0.0         250.
0.0         290.
0.0         330.
0.0         380.
0.0         420.
23.         0.0
23.         35.
23.         75.
22.         110.
23.         155.
24.         195.
25.         250.
45.         320.
50.         380.
50.         420.
46.         0.0
46.         35.
46.         75.
49.         108.
48.         155.
50.         195.
56.         250.
80.         295.
105.        366.
100.        420.
```

69.	0.0
69.	35.
69.	75.
70.	107.
70.	153.
74.	190.
90.	237.
92.	0.0
92.	35.
92.	75.
92.	108.
96.	150.
104.	182.
115.	0.0
115.	35.
115.	75.
117.	107.
125.	145.
120.	215.
125.	275.
125.	318.
138.	0.0
138.	35.
138.	75.
140.	108.
144.	188.
160.	313.
150.	365.
140.	420.
161.	0.0
161.	35.
161.	75.
163.	109.
154.	151.
184.	0.0
184.	35.
184.	75.
185.	110.
174.	141.
180.	190.
172.	219.
172.	251.
182.	280.
183.	342.
185.	420.
207.	0.0
207.	35.
207.	75.

208.	107.
204.	157.
192.	170.
211.	188.
205.	207.
199.	228.
200.	250.
207.	271.
194.	297.
210.	310.
210.	355.
230.	420.
230.	0.0
230.	35.
230.	75.
230.	108.
230.	140.
218.	146.
219.	173.
215.	285.
224.	296.
230.	320.
230.	365.
236.	153.
228.	163.
236.	307.
246.	166.
241.	174.
236.	185.
232.	199.
230.	213.
229.	230.
230.	244.
232.	260.
236.	274.
240.	284.
246.	294.
257.	175.
254.	184.
252.	193.
250.	204.
249.	217.
247.	230.
248.	242.
249.	254.
252.	266.
255.	276.
258.	285.

179.
188.
197.
207.
218.
230.
242.
253.
263.
272.
281.
180.
189.
198.
208.
219.
230.
241.
252.
262.
271.
280.
180.
189.
198.5
208.5
219.
230.
241.5
251.5
261.
271.
280.
180.
189.
199.5
208.5
219.
230.
241.5
251.5
261.
271.
280.
180.
189.
199.5
208.5
219.
230.
241.5
251.5
261.
271.
280.
180.
190.
200.
210.

270.
269.
268.
267.
266.
265.
266.
267.
268.
269.
270.
282.
282.
281.
281.
281.
280.
281.
281.
282.
282.
290.
290.
290.
290.
290.
290.
290.
290.
290.
290.
300.
300.
300.
300.
300.
300.
300.
300.
300.
300.
315.
315.
315.
315.

315.	220.
315.	230.
315.	240.
315.	250.
315.	260.
315.	270.
315.	280.
330.	180.
330.	190.
330.	200.
330.	210.
330.	220.
330.	230.
330.	240.
330.	250.
330.	260.
330.	270.
330.	280.
350.	180.
350.	190.
350.	200.
350.	210.
350.	220.
350.	230.
350.	240.
350.	250.
350.	260.
350.	270.
350.	280.
370.	180.
370.	190.
370.	200.
370.	210.
370.	220.
370.	230.
370.	240.
370.	250.
370.	260.
370.	270.
370.	280.

1	12	1	2	0
2	12	2	3	0
3	2	3	13	C
4	13	3	14	0
5	3	4	14	0
6	14	4	15	0
7	4	5	15	0
8	15	5	16	C

57	42	35	36	0
58	42	36	43	0
59	43	36	37	0
60	43	37	44	0
61	44	37	38	0
62	44	38	50	0
63	50	38	51	0
64	51	38	29	0
65	51	29	52	0
66	52	29	30	0
67	52	30	59	0
68	59	30	60	0
69	31	60	30	0
70	45	39	40	0
71	45	40	46	0
72	46	40	41	0
73	46	41	47	0
74	47	41	42	0
75	47	42	48	0
76	48	42	43	0
77	48	43	49	0
78	49	43	44	0
79	49	44	57	0
80	57	44	50	0
81	53	45	46	0
82	53	46	54	0
83	54	46	47	0
84	54	47	55	0
85	55	47	48	0
86	55	48	56	0
87	56	48	49	0
88	56	49	65	0
89	65	49	57	0
90	57	50	72	0
91	72	50	73	0
92	73	50	51	0
93	73	51	74	0
94	74	51	58	0
95	58	51	52	0
96	58	52	59	0
97	58	59	75	0
98	75	59	76	0
99	59	60	76	0
100	61	53	54	0
101	61	54	62	0
102	62	54	55	0
103	62	55	63	0
104	63	55	56	0

105	63	56	64	0
106	64	56	65	0
107	64	65	70	0
108	70	65	82	0
109	82	65	71	0
110	71	65	57	0
111	71	57	72	0
112	74	58	88	0
113	88	58	75	0
114	66	61	62	0
115	66	62	67	0
116	67	62	63	0
117	67	63	68	0
118	68	63	64	0
119	68	64	69	0
120	69	64	70	0
121	77	66	67	0
122	77	67	78	0
123	78	67	68	0
124	78	68	79	0
125	79	68	69	0
126	79	69	80	0
127	80	69	97	0
128	97	69	81	0
129	69	70	81	0
130	81	70	82	0
131	83	82	71	0
132	83	71	84	0
133	84	71	72	0
134	84	72	85	0
135	85	72	73	0
136	85	73	86	0
137	86	73	74	0
138	86	74	87	0
139	87	74	88	0
140	89	88	75	0
141	89	75	90	0
142	90	75	76	0
143	92	77	78	0
144	93	92	78	0
145	93	78	79	0
146	94	93	79	0
147	94	79	80	0
148	95	94	80	0
149	96	95	80	0
150	96	80	97	0
151	104	97	81	0
152	104	81	98	0

153	98	81	82	0
154	98	82	83	0
155	87	88	99	0
156	98	88	89	0
157	103	96	97	0
158	103	97	104	0
159	106	103	104	0
160	106	104	107	0
161	107	104	98	0
162	107	98	108	0
163	108	98	83	0
164	108	83	109	0
165	109	83	84	0
166	109	84	110	0
167	110	84	85	0
168	110	85	111	0
169	111	85	86	0
170	111	86	112	0
171	112	86	87	0
172	112	87	113	0
173	113	87	99	0
174	113	99	114	0
175	114	99	100	0
176	99	89	100	0
177	114	100	115	0
178	115	100	105	0
179	100	89	101	0
180	101	105	100	0
181	115	105	116	0
182	101	89	90	0
183	102	101	90	0
184	91	102	90	0
185	76	91	90	0
186	117	106	107	0
187	117	107	118	0
188	118	107	108	0
189	118	108	119	0
190	119	108	109	0
191	119	109	120	0
192	120	109	110	0
193	120	110	121	0
194	121	110	111	0
195	121	111	122	0
196	122	111	112	0
197	122	112	123	0
198	123	112	113	0
199	123	113	124	0
200	124	113	114	0

249	151	141	152	0
250	152	141	142	0
251	152	142	153	0
252	153	142	143	0
253	153	143	154	0
254	154	143	144	0
255	154	144	155	0
256	155	144	145	0
257	155	145	156	0
258	156	145	146	0
259	156	146	157	0
260	157	146	147	0
261	157	147	158	0
262	158	147	148	0
263	158	148	159	0
264	159	148	149	0
265	159	149	160	0
266	161	150	151	0
267	161	151	162	0
268	162	151	152	0
269	162	152	163	0
270	163	152	153	0
271	163	153	164	0
272	164	153	154	0
273	164	154	165	0
274	165	154	155	0
275	165	155	166	0
276	166	155	156	0
277	166	156	167	0
278	167	156	157	0
279	167	157	168	0
280	168	157	158	0
281	168	158	169	0
282	169	158	159	0
283	169	159	170	0
284	170	159	160	0
285	160	171	170	0
286	172	161	162	0
287	172	162	173	0
288	173	162	163	0
289	173	163	174	0
290	174	163	164	0
291	174	164	175	0
292	175	164	165	0
293	175	165	176	0
294	176	165	166	0
295	176	166	177	0
296	177	166	167	0

297	177	167	178	0
298	178	167	168	0
299	178	168	179	0
300	179	168	169	0
301	179	169	180	0
302	180	169	170	0
303	180	170	181	0
304	181	170	171	0
305	181	171	182	0
306	183	172	173	0
307	183	173	184	0
308	184	173	174	0
309	184	174	185	0
310	185	174	175	0
311	185	175	186	0
312	186	175	176	0
313	186	176	187	0
314	187	176	177	0
315	187	177	188	0
316	188	177	178	0
317	188	178	189	0
318	189	178	179	0
319	189	179	190	0
320	190	179	180	0
321	190	180	191	0
322	191	180	181	0
323	191	181	192	0
324	192	181	182	0
325	182	193	192	0
326	194	183	184	0
327	195	194	184	0
328	195	184	185	0
329	196	195	185	0
330	196	185	186	0
331	197	196	186	0
332	197	186	187	0
333	198	197	187	0
334	198	187	188	0
335	199	198	188	0
336	199	188	189	0
337	200	199	189	0
338	200	189	190	0
339	201	200	190	0
340	201	190	191	0
341	202	201	191	0
342	202	191	192	0
343	203	202	192	0
344	203	192	193	0

345	193	204	203	0
346	205	194	195	0
347	206	205	195	0
348	206	195	196	0
349	207	206	196	0
350	207	196	197	0
351	208	207	197	0
352	208	197	198	0
353	209	208	198	0
354	209	198	199	0
355	210	209	199	0
356	210	199	200	0
357	211	210	200	0
358	211	200	201	0
359	212	211	201	0
360	212	201	202	0
361	213	212	202	0
362	213	202	203	0
363	214	213	203	0
364	214	203	204	0
365	204	215	214	0

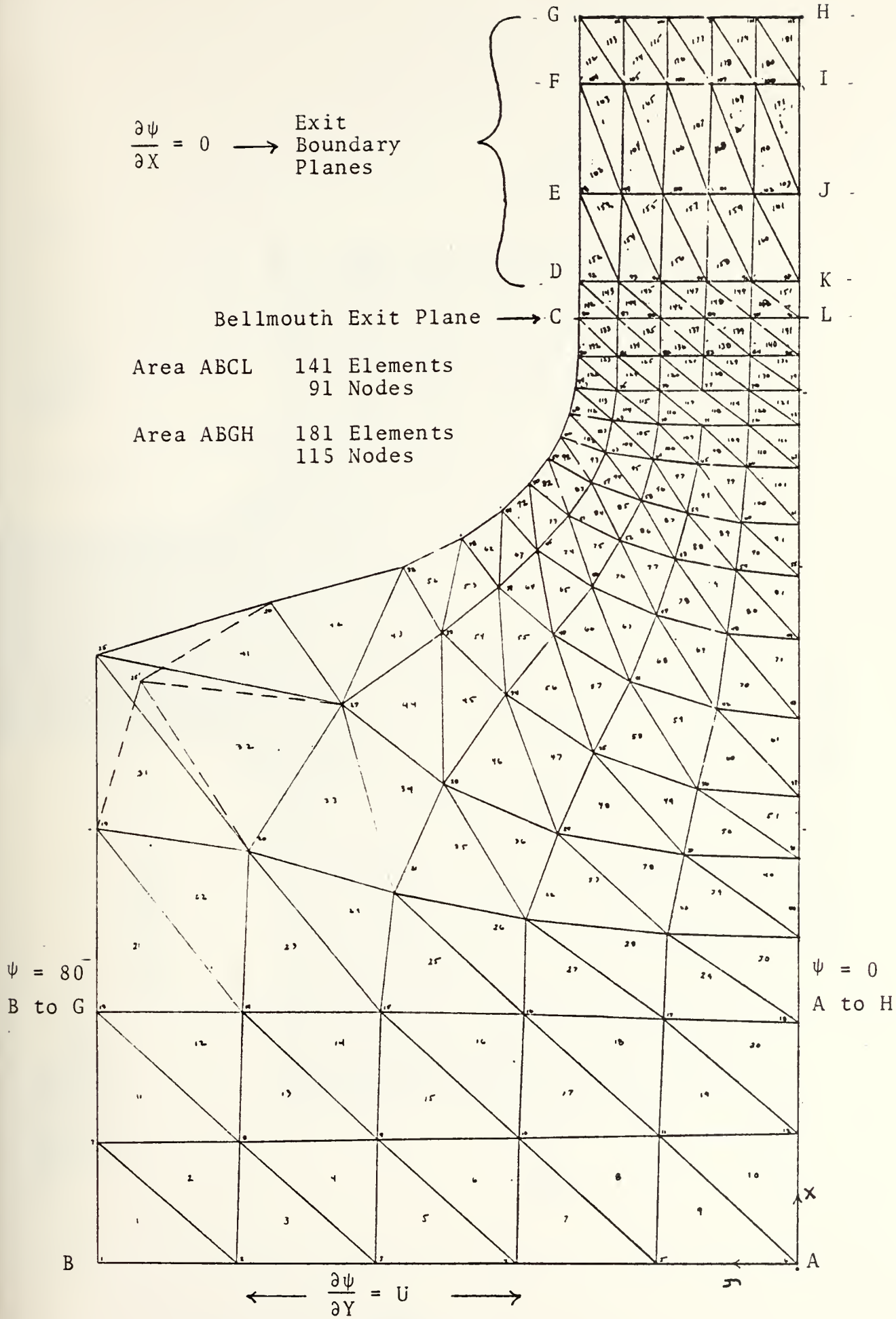

Figure A-1. FEM Model 1

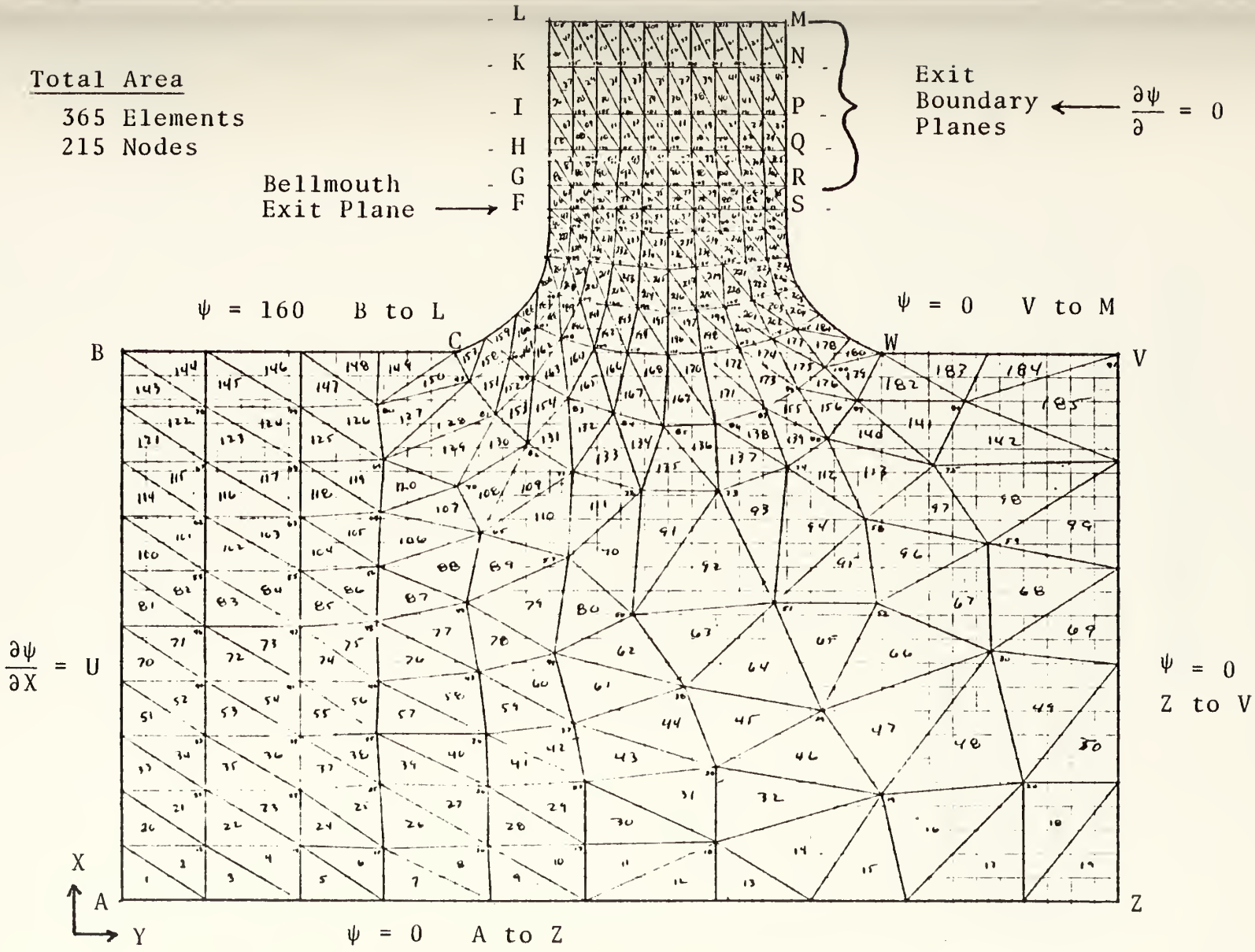

Figure A-2. FEM Model 2

APPENDIX B

PRELIMINARY TEST PROBE DATA

The following figures are data from tests of Configuration #Ø and Configuration #1. The results showed unacceptable variations in total and dynamic pressure in both the blade-to-blade and spanwise directions. The yaw angles were also outside the required bounds.

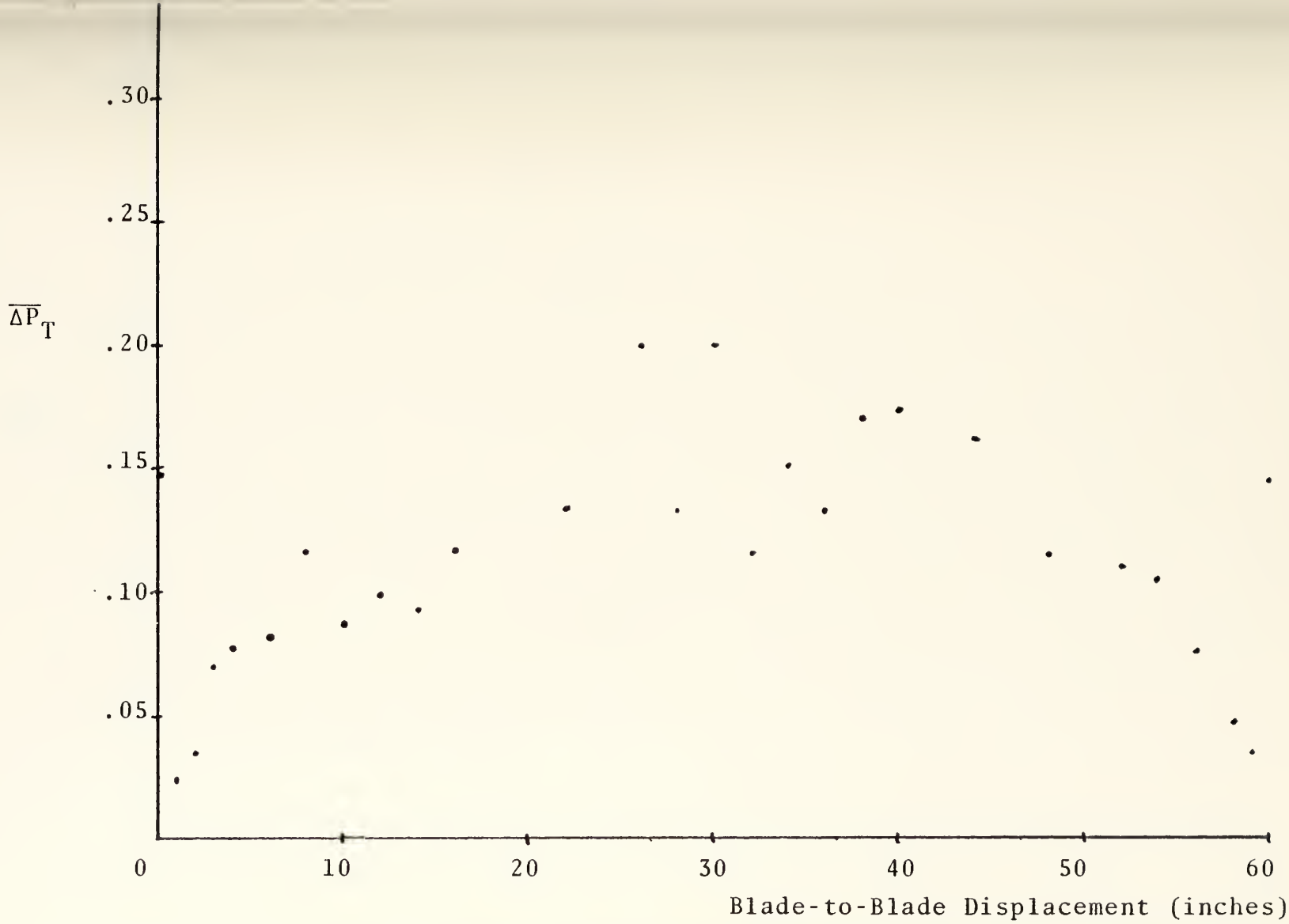

Figure B-1a. Blade-to-Blade Total Pressure Distribution at the Test Plane (at 10% Span, Velocity = 230 ft/sec) - Configuration #Ø

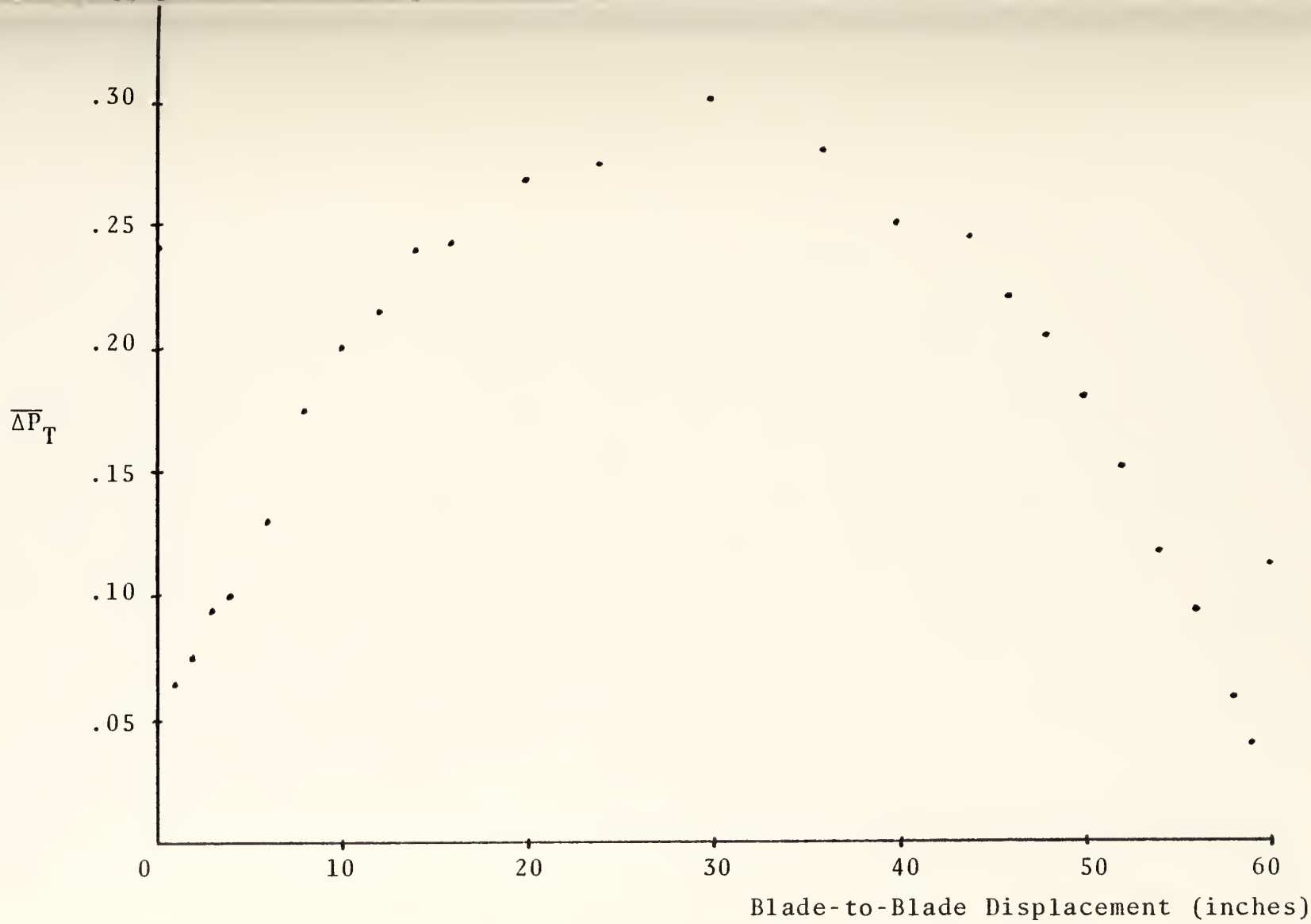

Figure B-1b. Blade-to-Blade Total Pressure Distribution at the Test Plane (at 30% Span, Velocity = 230 ft/sec) - Configuration #Ø

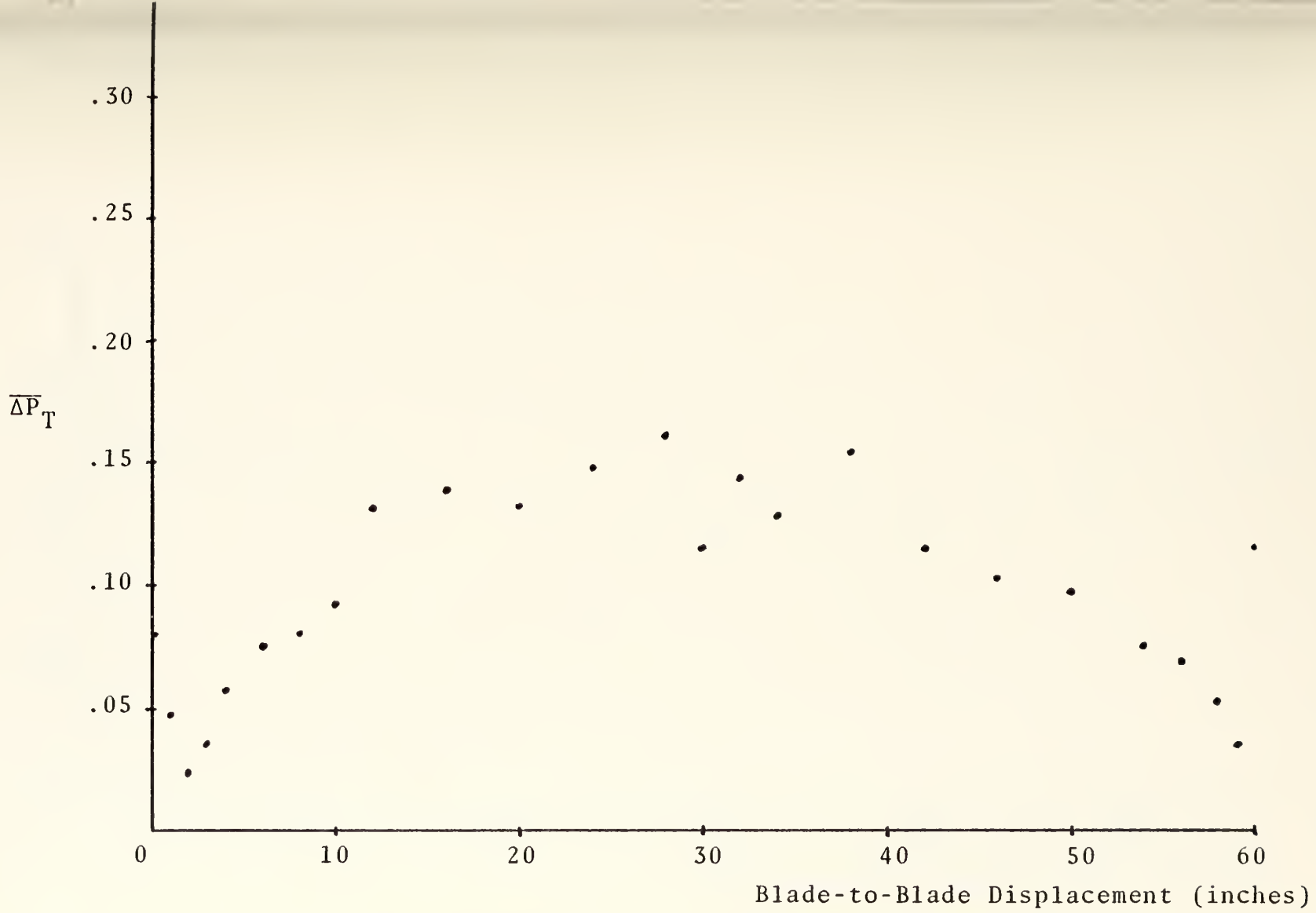

Figure B-1c. Blade-to-Blade Total Pressure Distribution at the Test Plane (at 90% Span, Velocity = 230 ft/sec) - Configuration #Ø

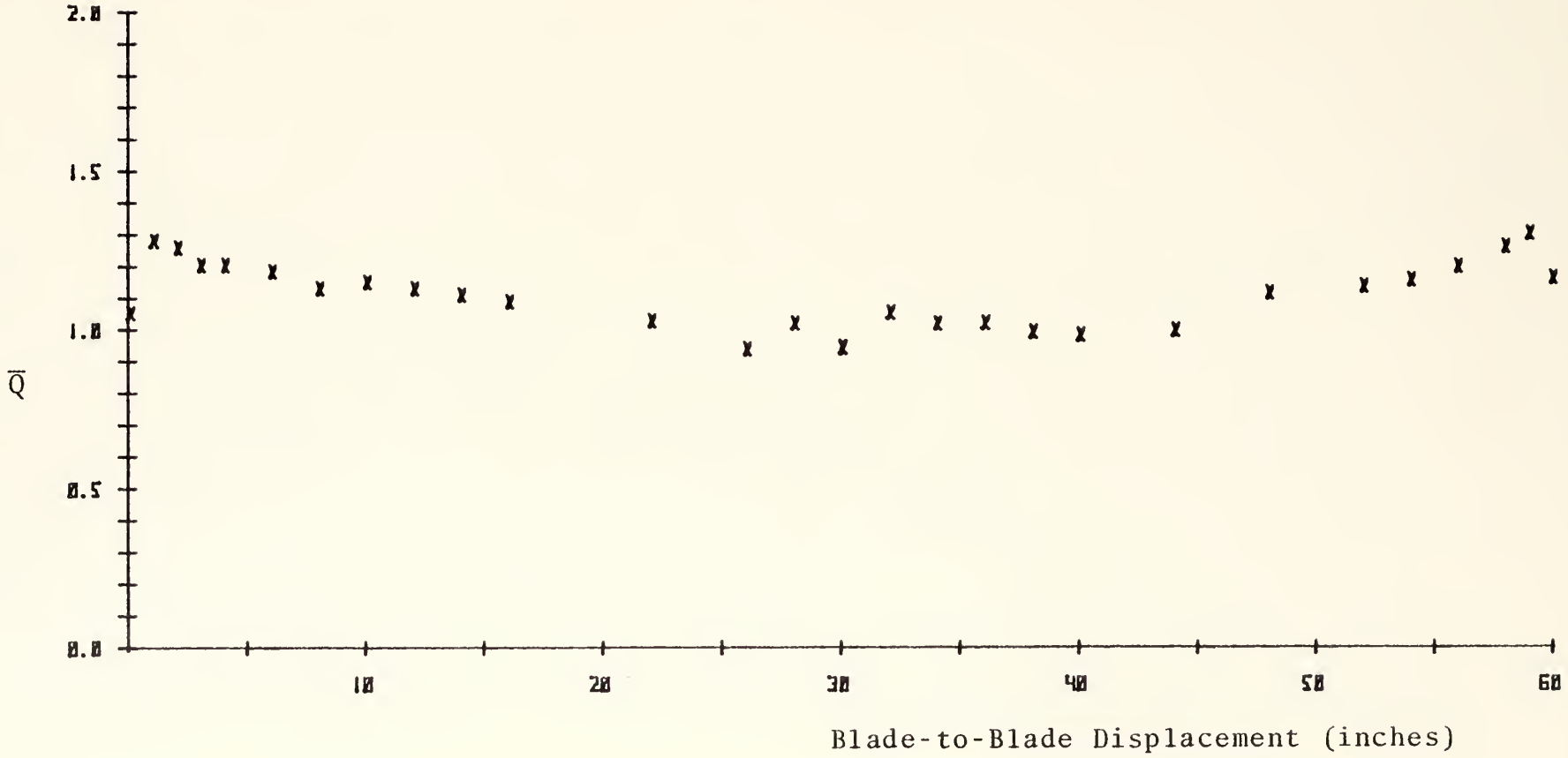

Figure B-2a. Blade-to-Blade Dynamic Pressure Distribution at the Test Plane (at 10% Span, Velocity = 230 ft/sec) - Configuration #Ø

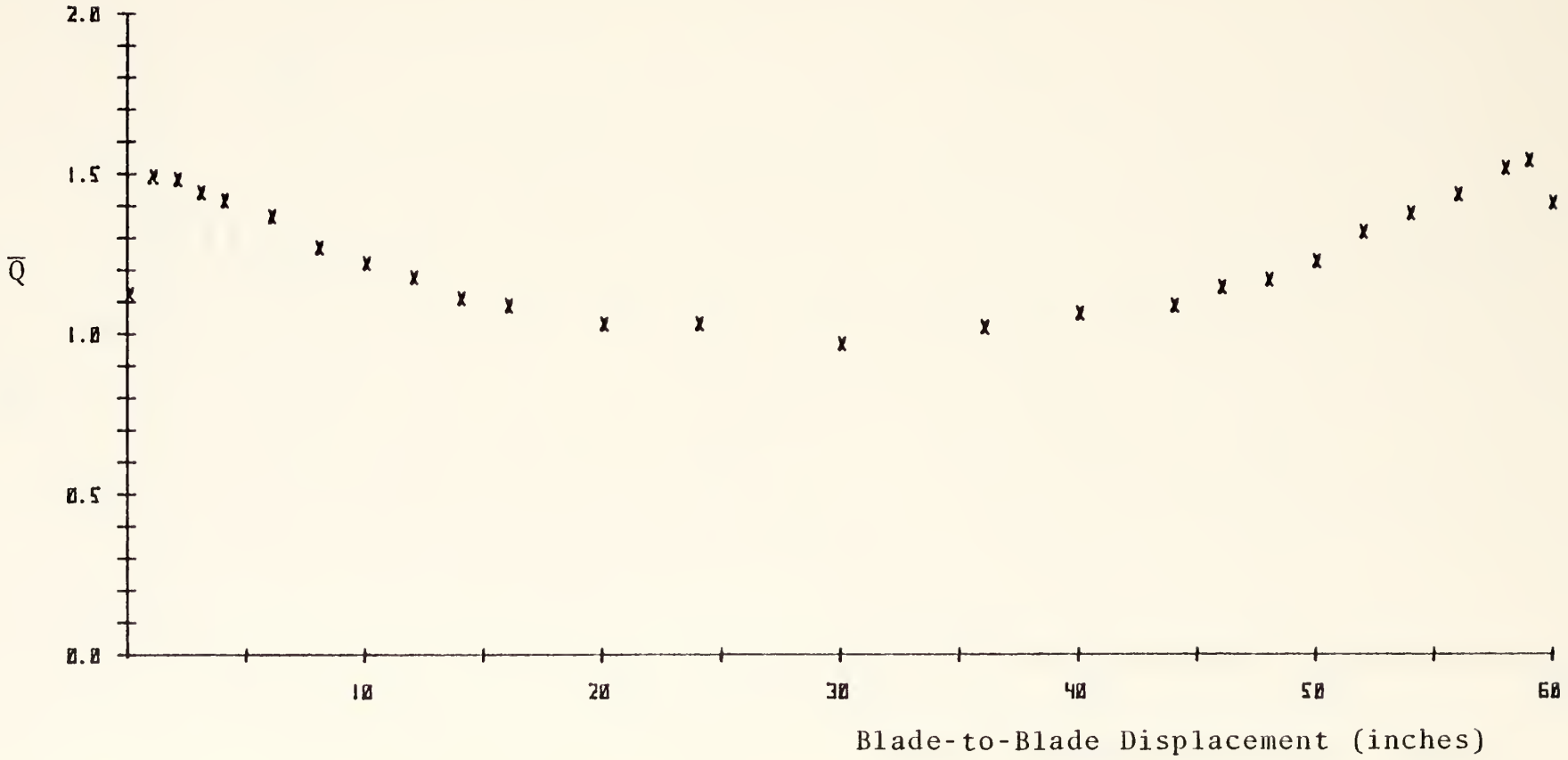

Figure B-2b. Blade-to-Blade Dynamic Pressure Distribution at the Test Plane (at 30% Span, Velocity = 230 ft/sec) - Configuration #Ø

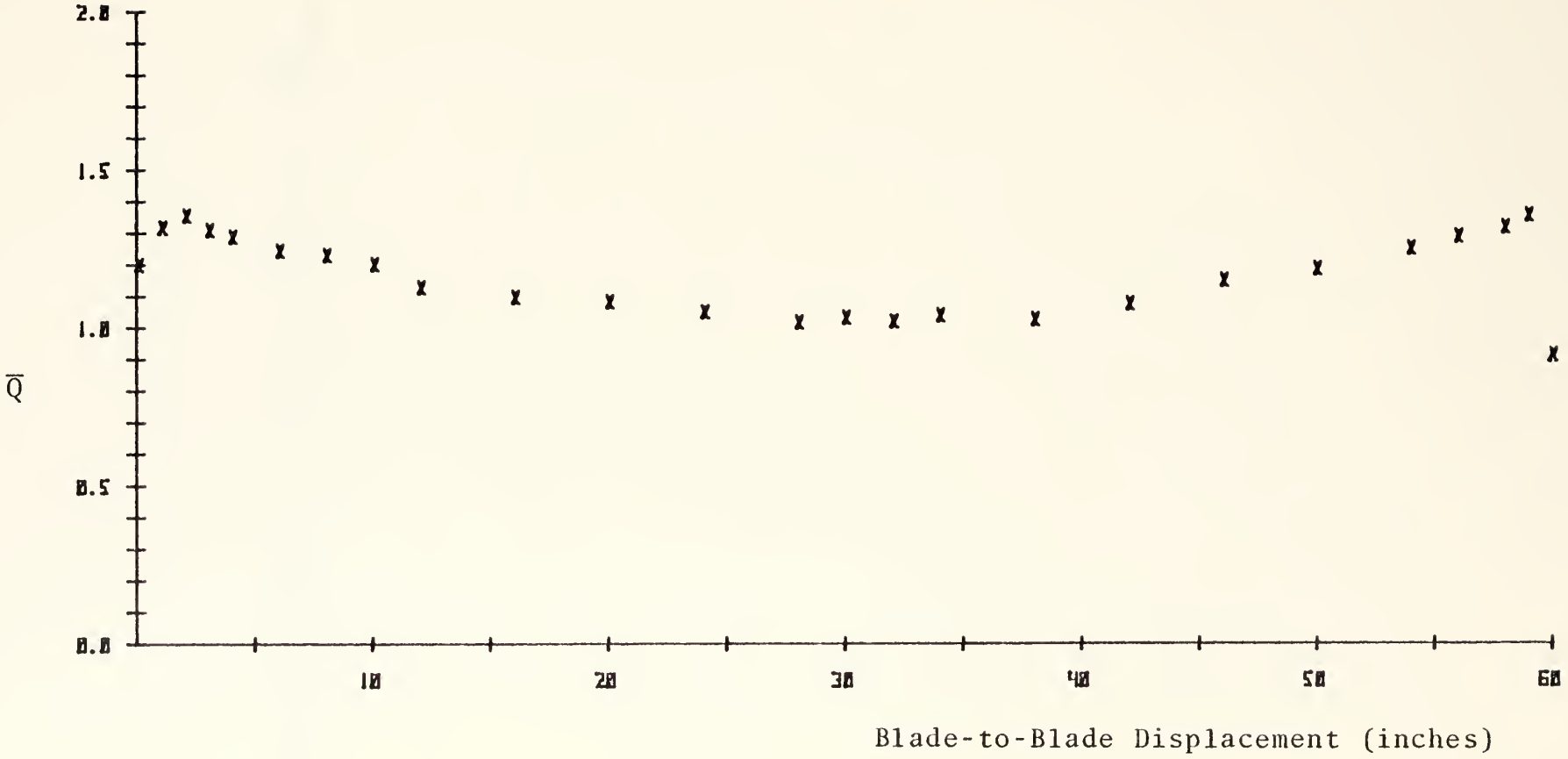

Figure B-2c. Blade-to-Blade Dynamic Pressure Distribution at the Test Plane (at 90% Span, Velocity = 230 ft/sec) - Configuration #Ø

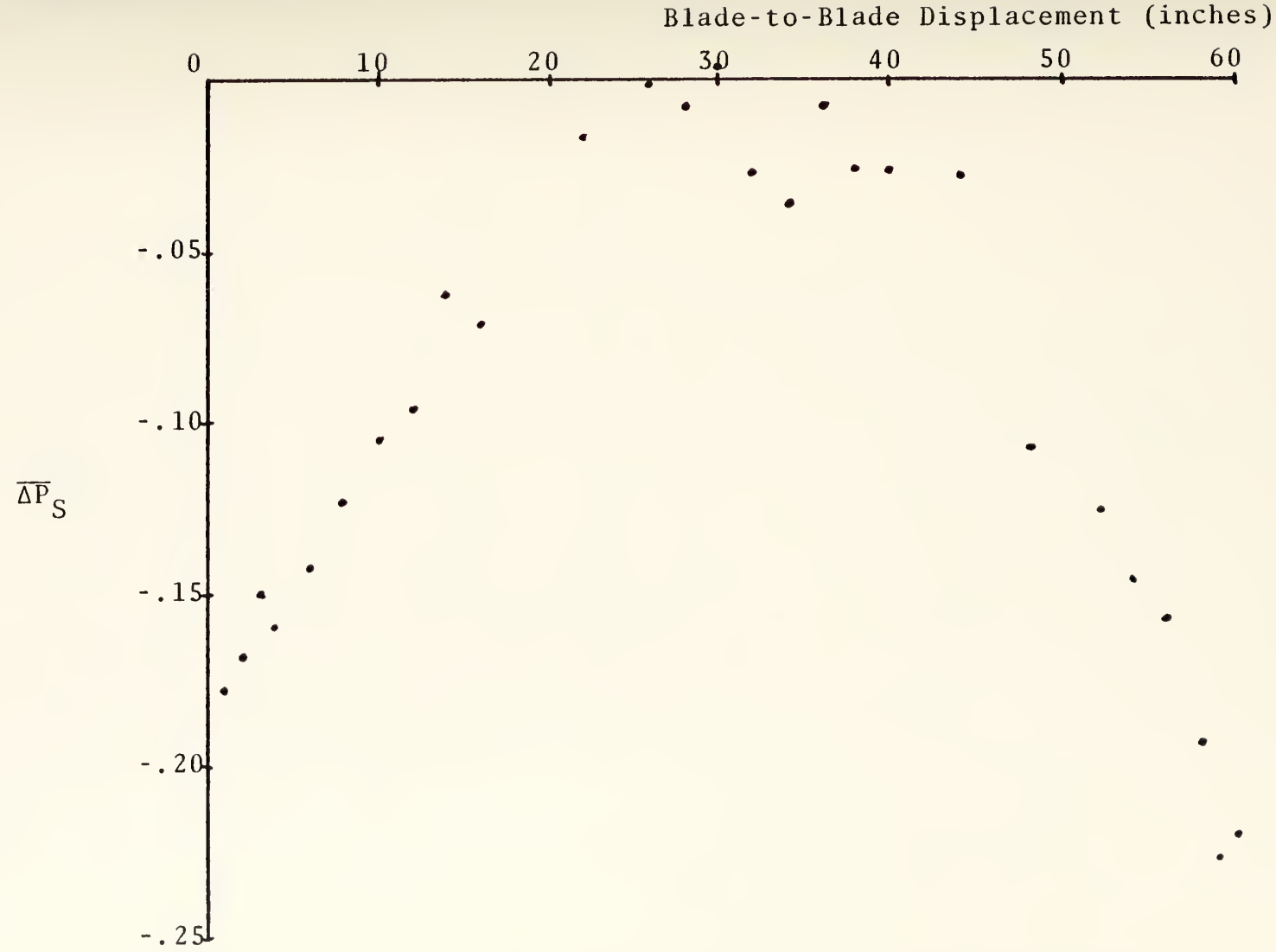

Figure B-3a. Blade-to-Blade Static Pressure Distribution at the Test Plane (at 10% Span, Velocity = 230 ft/sec) - Configuration #Ø

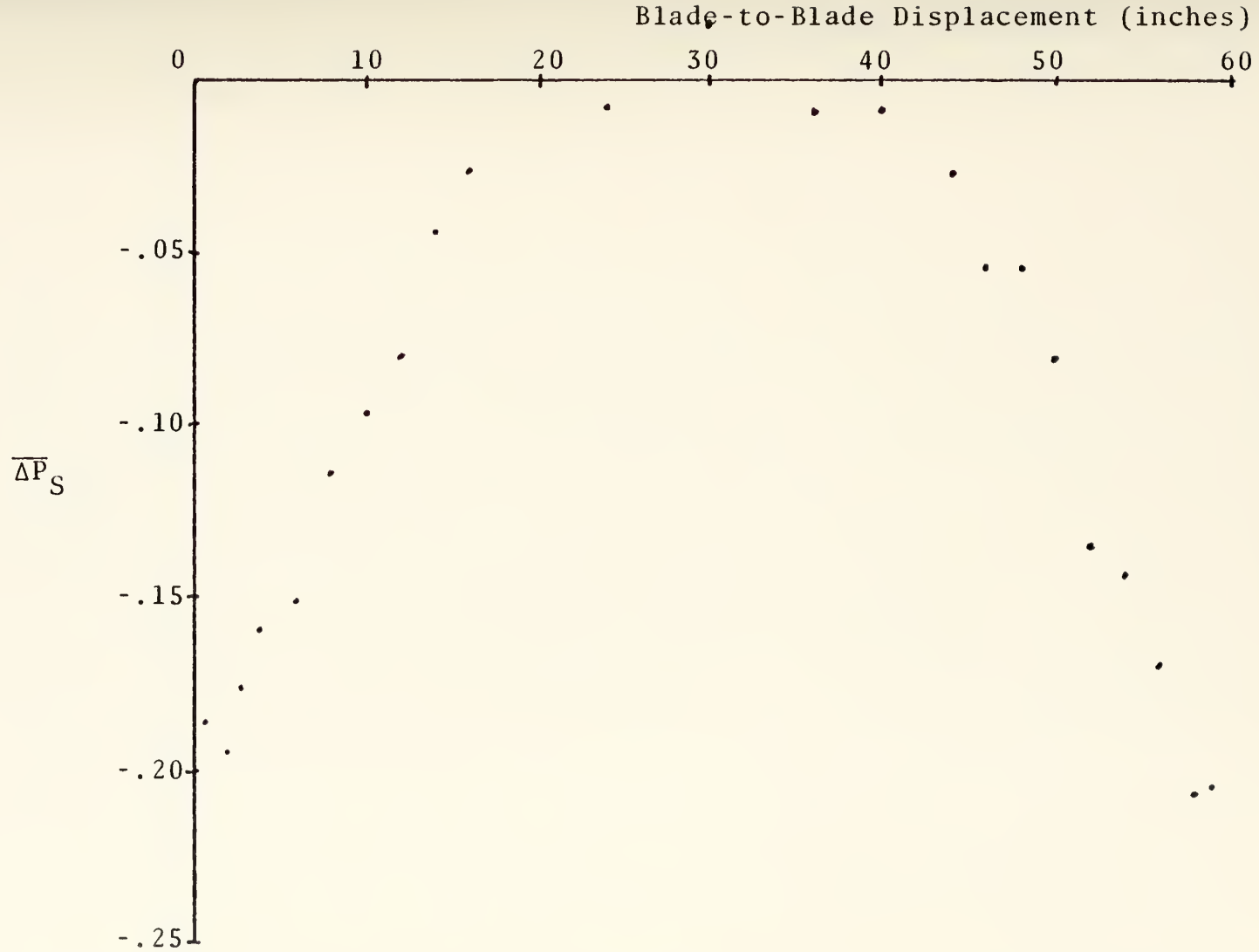

Figure B-3b. Blade-to-Blade Static Pressure Distribution at the Test Plane (at 30% Span, Velocity = 230 ft/sec) - Configuration #Ø

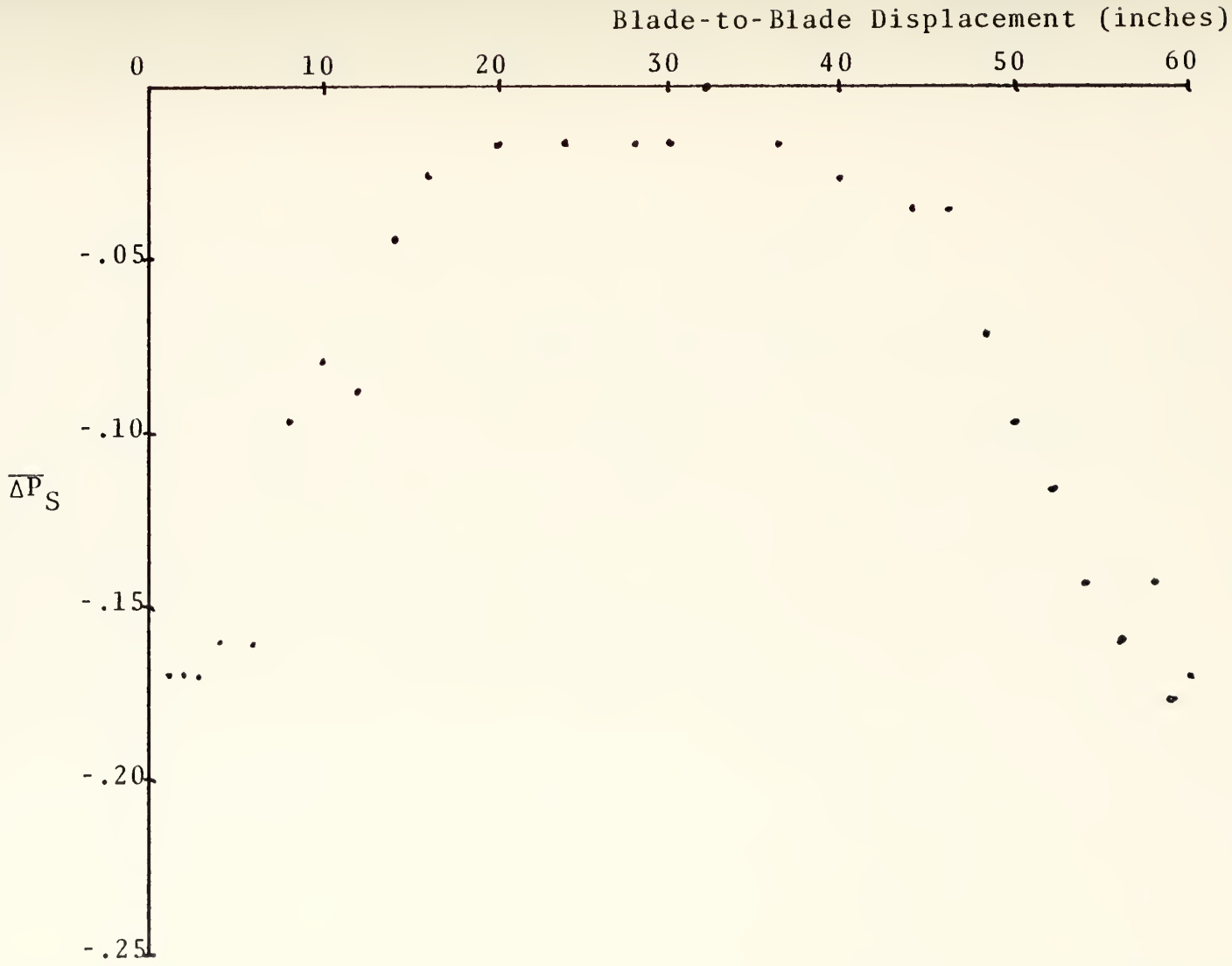

Figure B-3c. Blade-to-Blade Static Pressure Distribution at the Test Plane (at 50% Span, Velocity = 230 ft/sec) - Configuration #Ø

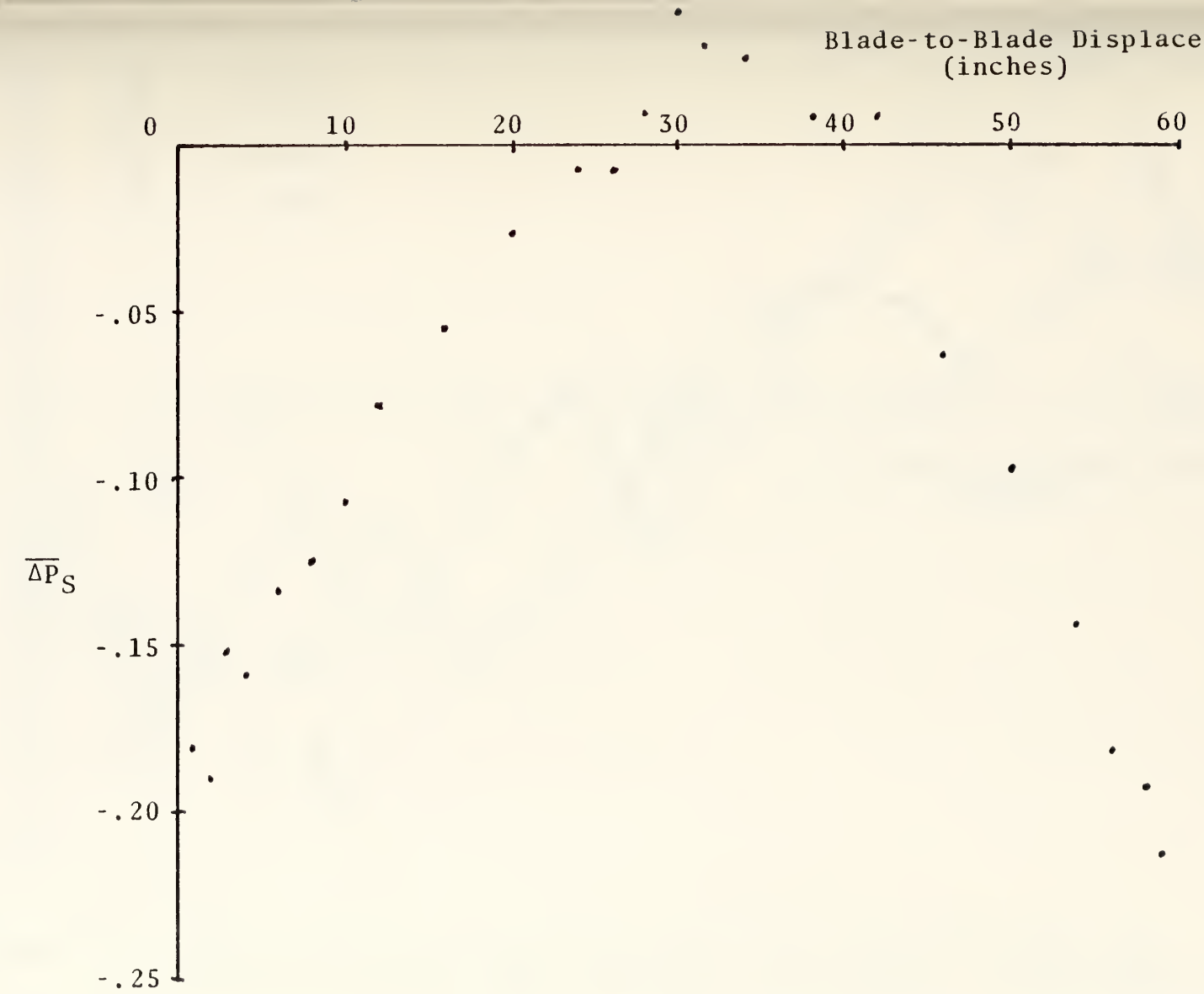

Figure B-3d. Blade-to-Blade Static Pressure Distribution at the Test Plane (at 90% Span, Velocity = 230 ft/sec) - Configuration #Ø

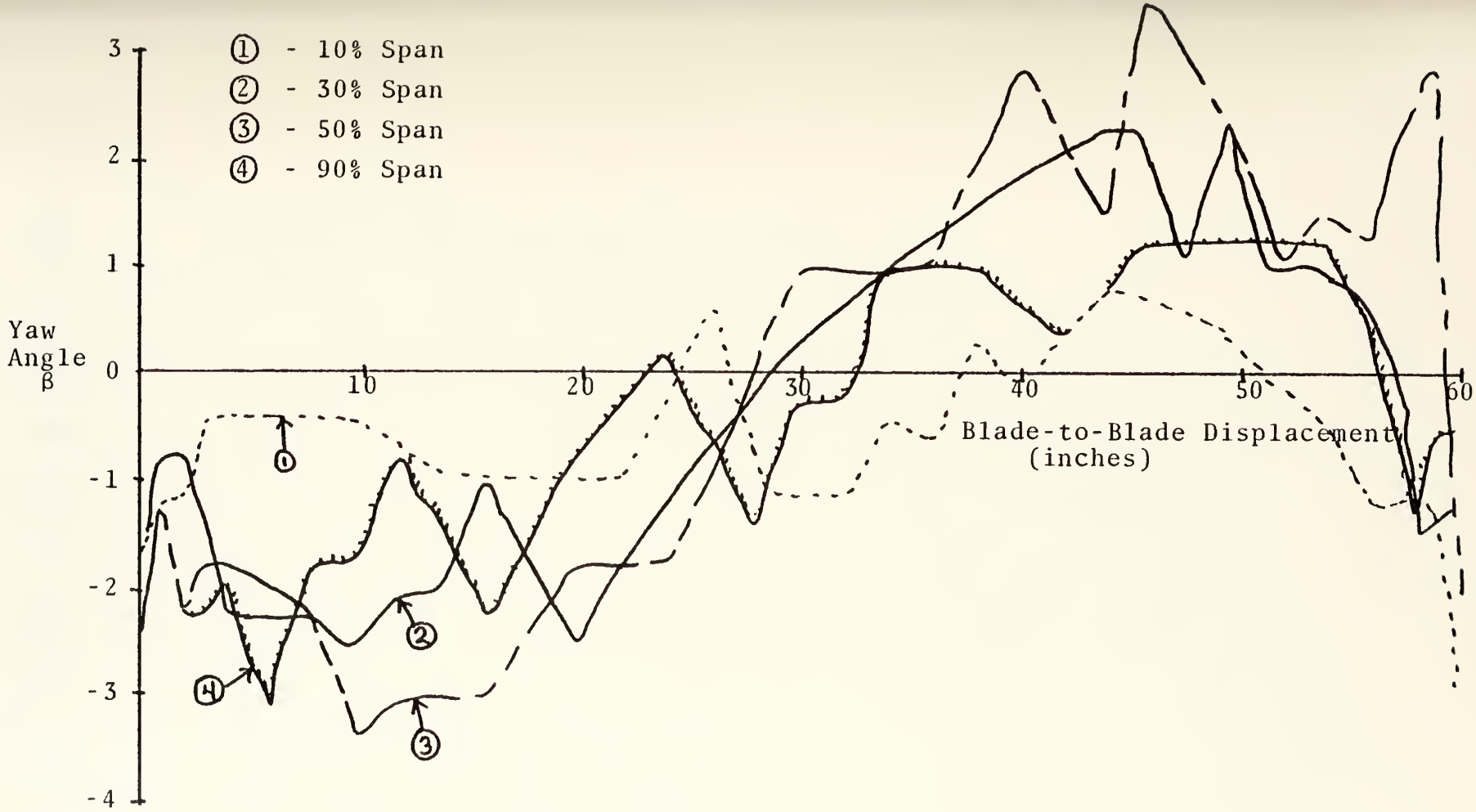

Figure B-4. Blade-to-Blade Yaw Angle Distribution at the Test Plane (at 10, 30, 50 and 90% Span, Velocity = 230 ft/sec) - Configuration #Ø

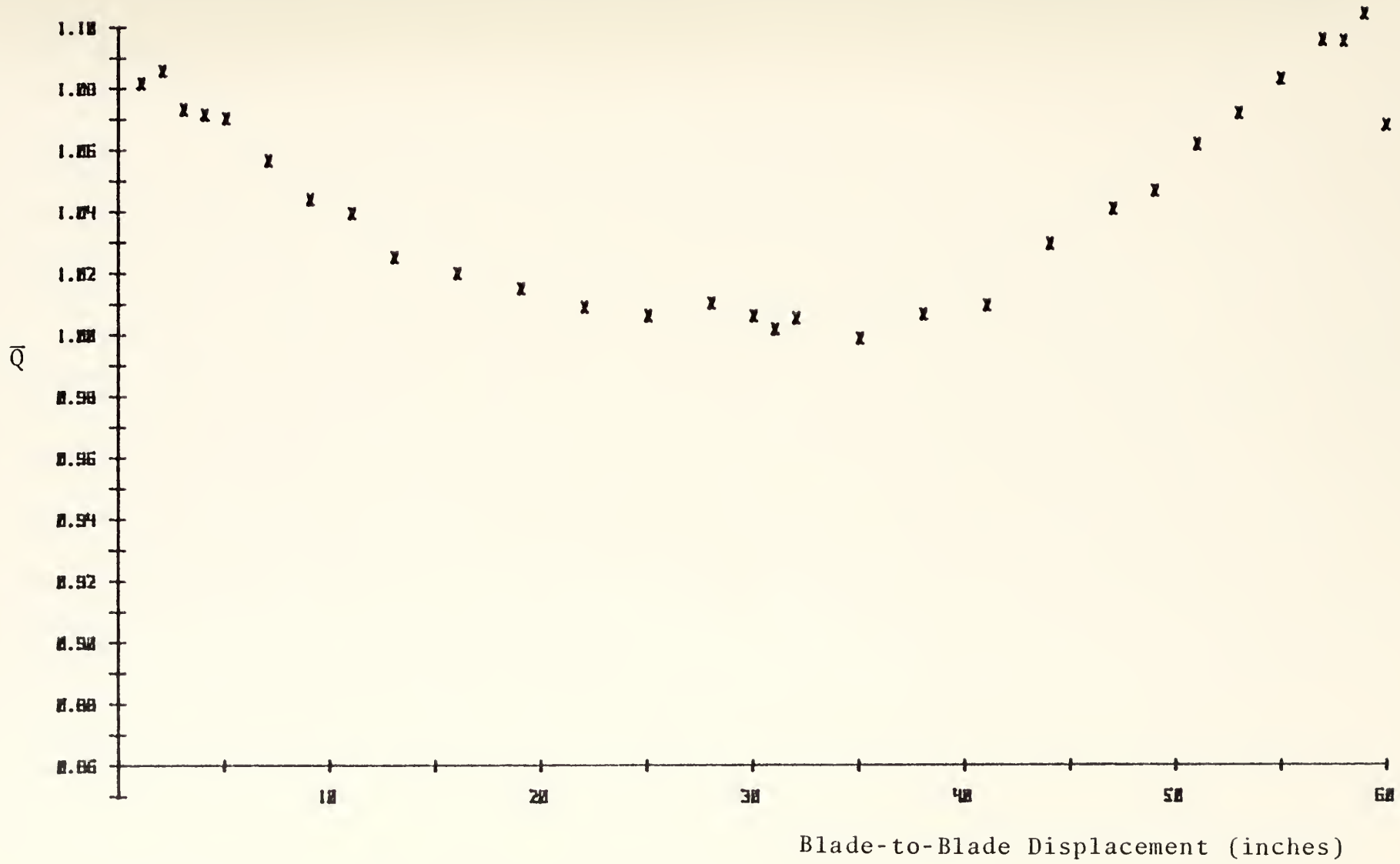

Figure B-5a. Blade-to-Blade Dynamic Pressure Distribution at the Test Plane (at 10% Span, Velocity = 270 ft/sec) - Configuration #1

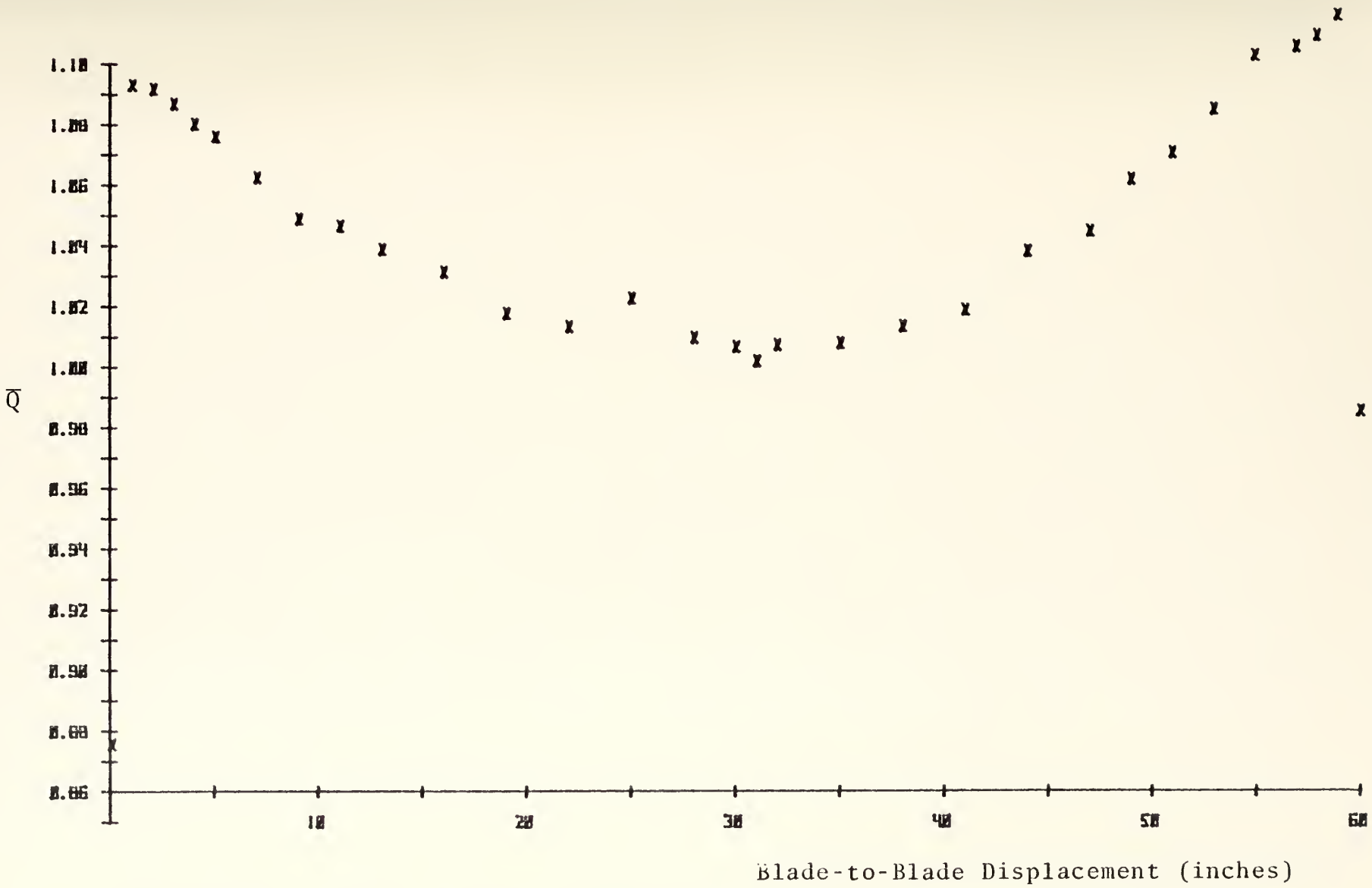

Figure B-5b. Blade-to-Blade Dynamic Pressure Distribution at the Test Plane (at 30% Span, Velocity = 270 ft/sec) - Configuration #1

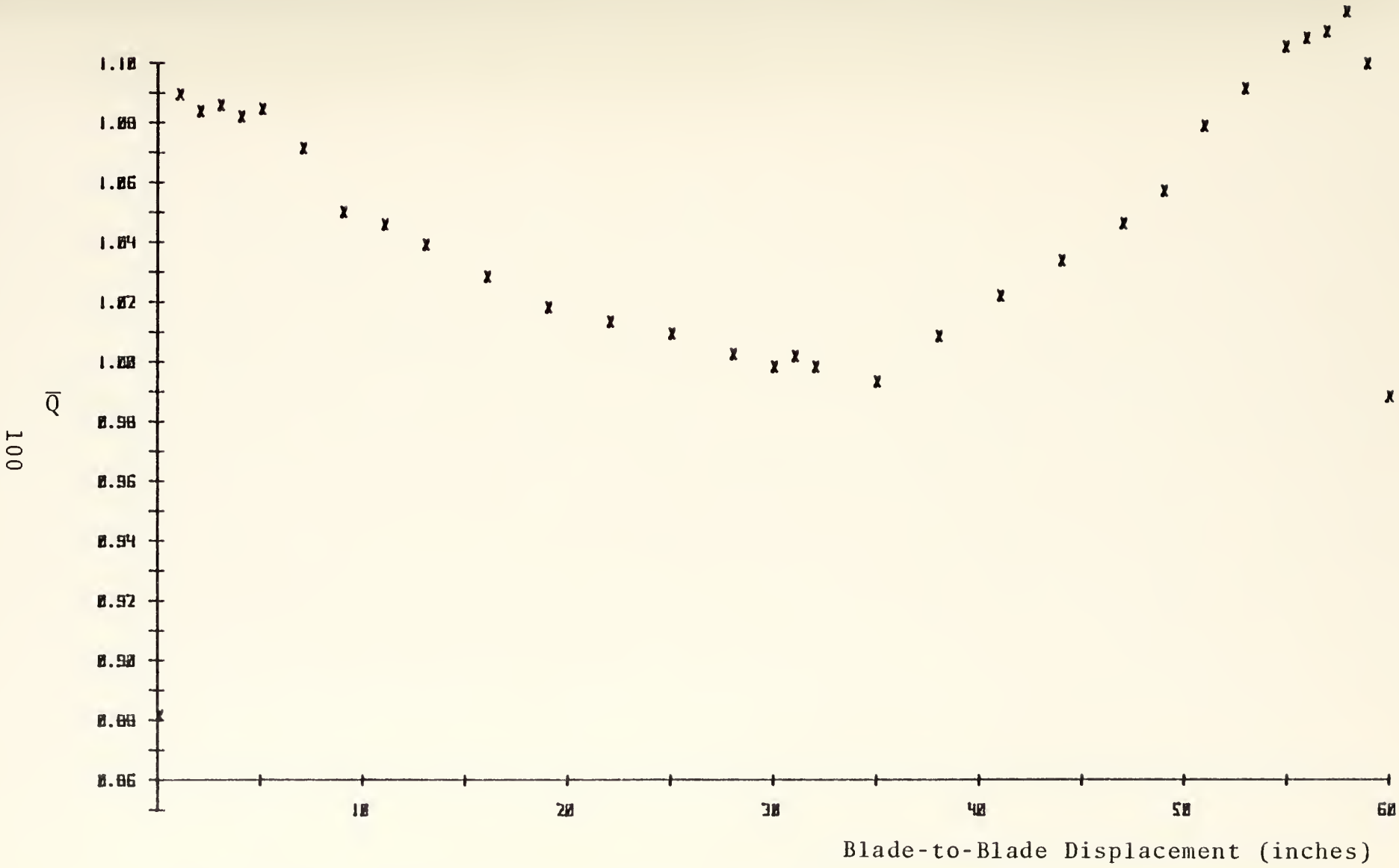

Figure B-5c. Blade-to-Blade Dynamic Pressure Distribution at the Test Plane (at 70% Span, Velocity = 270 ft/sec) - Configuration #1

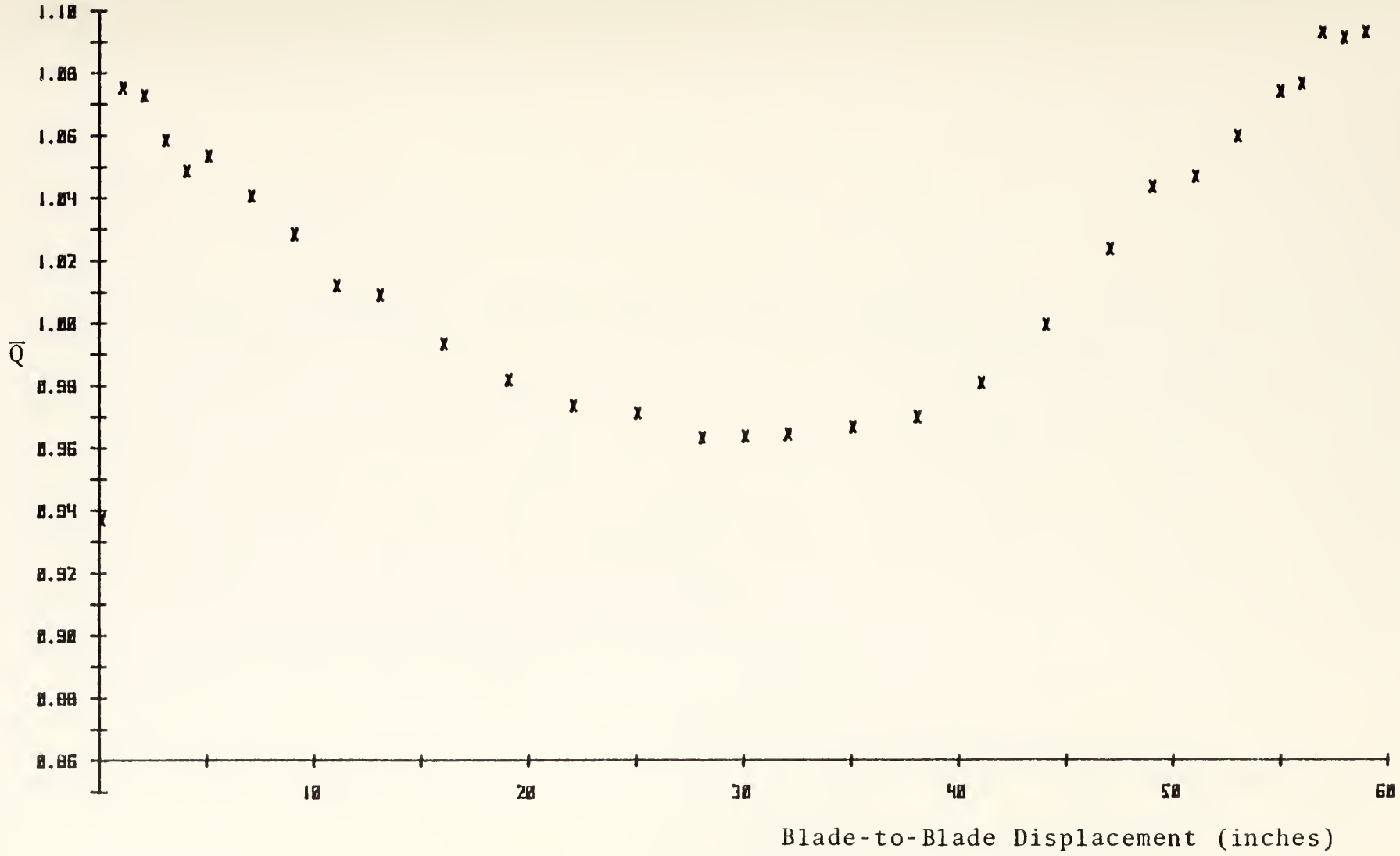

Figure B-5d. Blade-to-Blade Dynamic Pressure Distribution at the Test Plane (at 90% Span, Velocity = 270 ft/sec) - Configuration #1

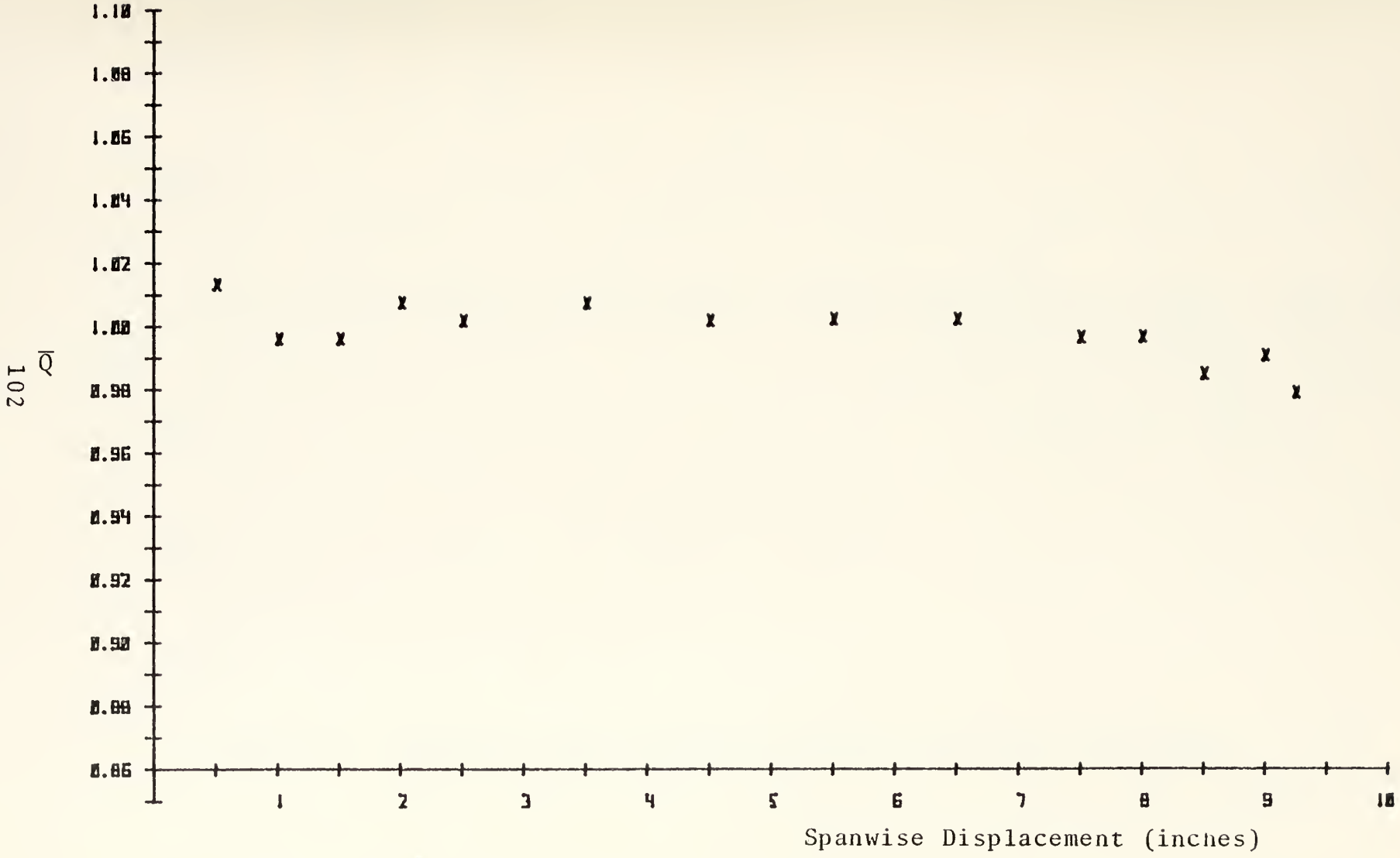

Figure B-6. Spanwise Dynamic Pressure Distribution at the Test Plane (at X = 15 in., Velocity = 280 ft/sec) - Configuration #1

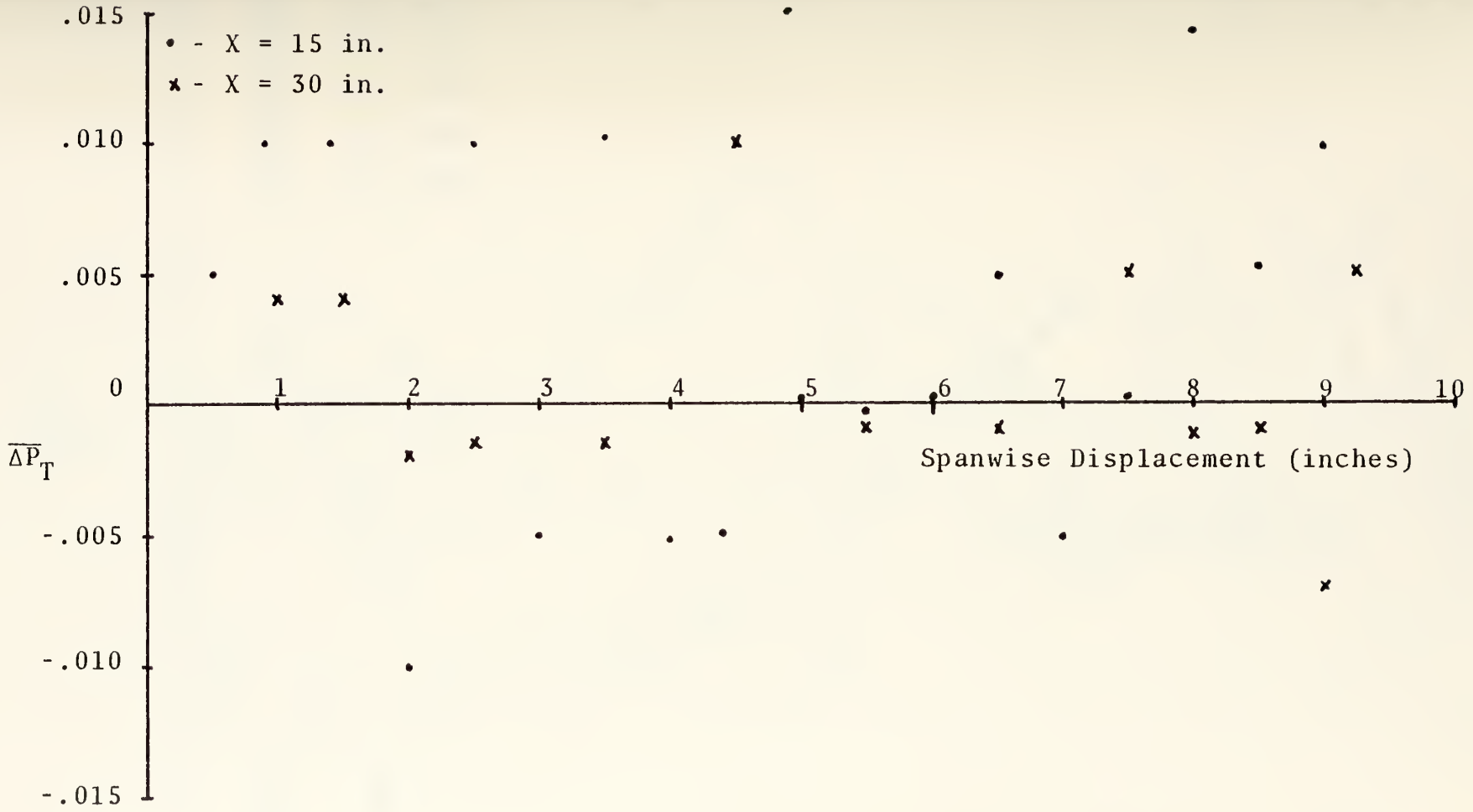

Figure B-7. Spanwise Total Pressure Distribution at the Test Plane (at X = 15 and 30 in., Velocity = 280 ft/sec) - Configuration #1

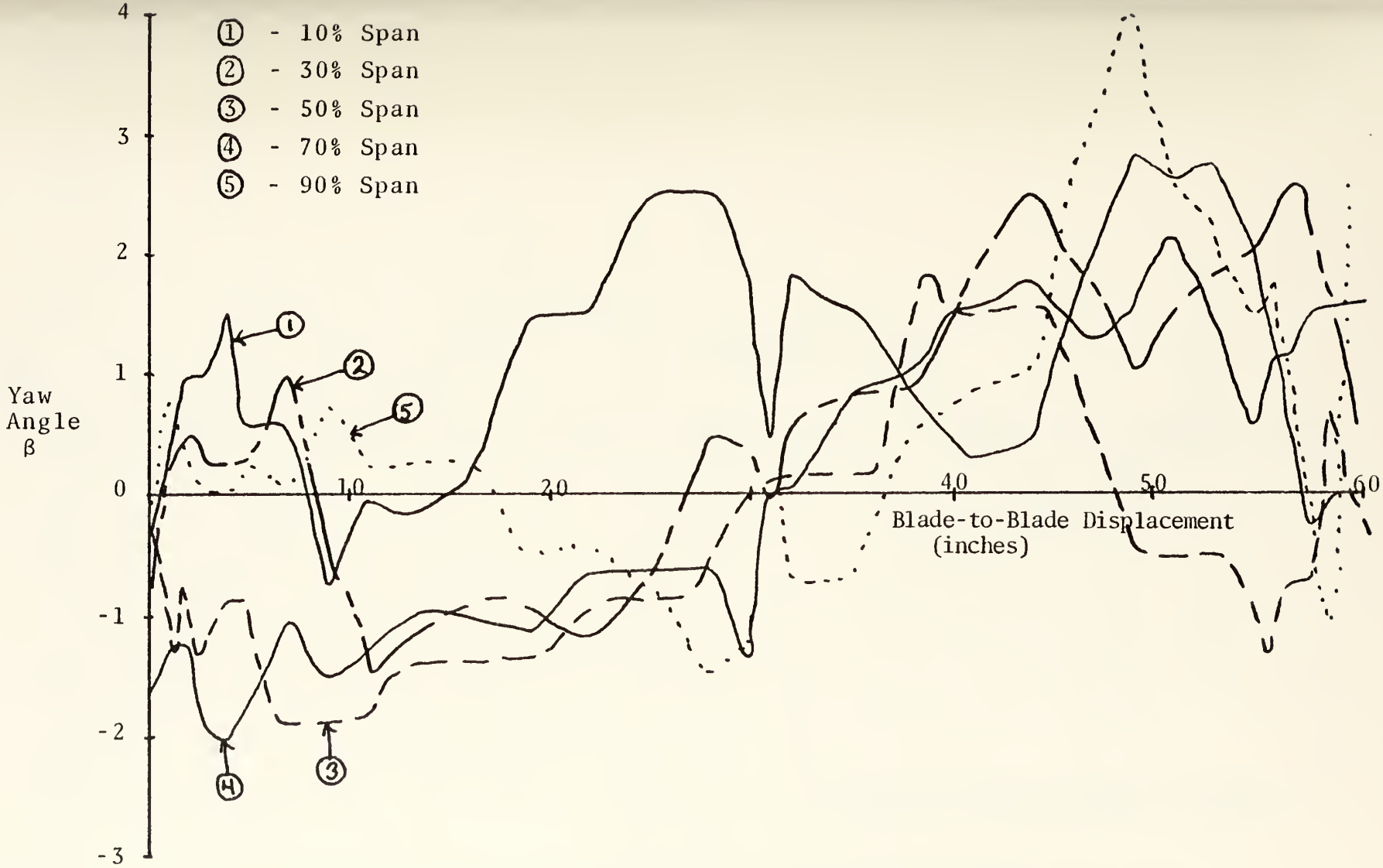

Figure B-8. Blade-to-Blade Yaw Angle Distribution at the Test Plane (at 10, 30, 50, 70 and 90% Span, Velocity = 270 ft/sec) - Configuration #1

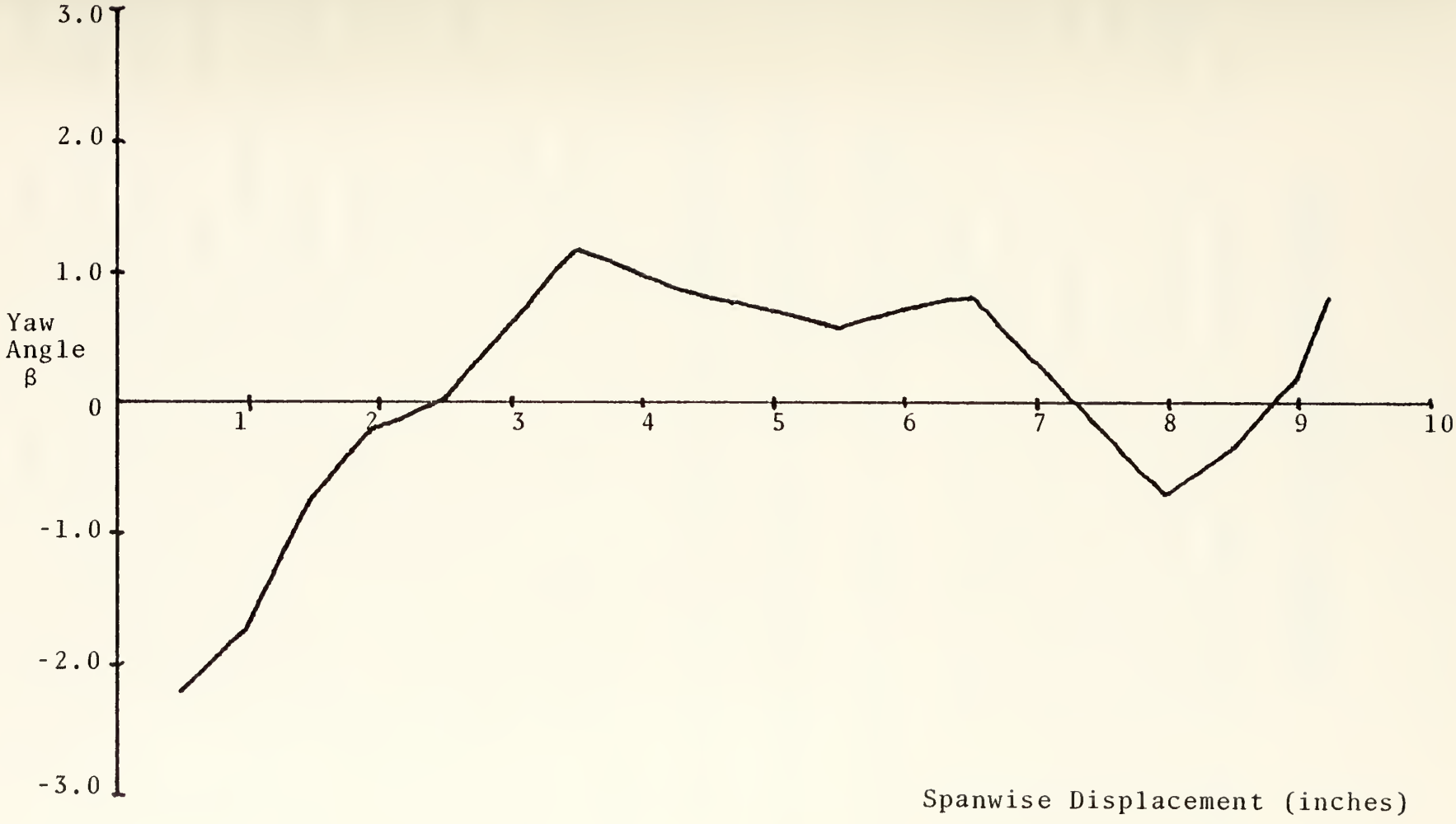

Figure B-9. Spanwise Yaw Angle Distribution at the Test Plane (at X = 15 in., Velocity = 280 ft/sec) - Configuration #1

APPENDIX C

PLENUM DEVELOPMENT TEST PROGRAM

Several alternative designs were proposed to obtain a uniform, steady flow at the exit plane of the original bell-mouth contraction, which was the location for the inlet guide vanes for the cascade test section. Some considerations governing the selection of the approach to be followed were:

1) It was desirable to maintain the benefits of a large settling volume.

2) A simple construction was needed, one which was easy to alter if necessary.

3) Minimum boundary layer buildup was required prior to and within the cascade test section.

4) Equal boundary layer growth on opposite sides of the proposed design was required.

A modification of the plenum and bellmouth was carried out which satisfied all of the above requirements.

As shown by the FEM analysis in Appendix A, the velocity distribution created by an East-West contraction required an additional length of non-converging duct in order to relax (to a uniform condition). Configuration 2, Fig. C-1, was tested as a rough simulation of the "relaxation" concept. The arrangement was generated by using the existing plenum turning vanes and a sheet of 3/4 inch plywood. The measured distribution of $\overline{Q}$ shown in Fig. C-2 showed a 2% variation through most of the tunnel width except in the deadwater regions (evidenced by P_T readings) at either end. The yaw

angles in Fig. C-3 were similar to Configuration 1 except as expected at the ends of the test plane. A major modification was made to the plenum to obtain two separate contractions in series with adequate lengths for relaxation. In Configuration 3, the east and west contours of the bellmouth were covered by vertical walls dropping down to a newly constructed set of East-West contraction contours. The construction sketched in Fig. C-4 (and detailed in Appendix D) allowed some relaxation of the velocity distribution created by the new East-West contours before the flow entered the original North-South bellmouth contours. The cardboard fillets shown in Fig. C-4 were not installed in Configuration 3. Measurements of $\overline{Q}$ and yaw angles were made and the results are shown in Fig. C-5. The non-uniformities were acceptable through the center 40 inches of the test section. The velocity distributions, however, peaked rapidly at both ends and the sudden increase in yaw angles indicated a strong influx of fluid from the East and West walls toward the tunnel center. The close confinement of the deviant yaw angles to the tunnel ends, at X = 10 inches and X = 50 inches, was thought to be partially caused by the proximity of the plenum turning vanes to the lower contraction.

In Configuration 4, the vanes were moved three feet towards the east end of the plenum and the measurements were repeated. The results shown in Figures C-7 and C-8 were similar to those from Configuration 3; however, the peak

velocities at the ends were decreased slightly and the yaw angles varied across the entire 40 inch channel width.

At this point the west end lower contraction surface and vertical wall was tufted with three-inch strips of light string in order to examine the surface flow. A tufted rod was used to probe the flow outside the wall boundary layer. Figure C-9 shows a sketch of the tuft positions with air flow through the test plane at a dynamic pressure of 15 inches of water. The positions were traced from a Polaroid photograph taken from within the lighted plenum. The view was taken from the east end of the plenum looking west at a 45 degree upwards angle. The following observations were made.

1) Flow on the vertical wall in the vicinity of the upper contraction converged more rapidly than the contraction walls.

2) Large regions of deadwater existed in the upper corners.

3) Strong corner vortices (verified by the hand held probe) were present at the junction of the ceiling, upper contraction walls, and vertical walls.

These observations pointed to the presence of substantial secondary flow of the boundary layer fluid. Cardboard fillets were installed in Fig. C-4 to eliminate the deadwater areas. Pneumatic measurements taken with this configuration are shown in Figures C-10 and C-11. The results indicated little change in the $\overline{Q}$ distribution; however, the peak yaw angles were notably increased.

The effect of the position of the turning vanes was questioned. When the plenum turning vanes were displaced three

feet to the east, it was apparent that very little flow was passing through any but the top turning vane passage. The vanes were therefore removed altogether as their functional benefit was questionable. The results of probe measurements for this Configuration 6 are shown in Figures C-12 and C-13. The distribution of $\overline{Q}$ was seen to be similar to the previous one but an increase was noted in the peak values of the yaw angles. The yaw angles measured at 20% and 70% span were consistant with the proposed existance of strong contra-rotating vortices centered at about X = 10 and 45 inches.

An audible low frequency pressure pulsation was noted and the static pressures in the cascade test section gave an unsteady measurement of $\pm$ 0.75 inches of water on the manometer columns. These observations suggested that the plenum turning vanes had served as a damping structure and perhaps as a spoiler which deterred the formation of large scale vortex motions.

The Datametrics Air Velocity Meter was used to probe the plenum chamber. Flow velocities through the sound baffles were quite uniform. However, at a distance of eight feet downstream of the sound baffles approximately 75% of the flow was seen to have passed through the upper one-half of the plenum at this location. It was also noted that little flow was actually moving around the east end lower contraction contour.

It was clear at this point that in order for the lower contraction to work properly, it was necessary to prevent

the flow from forming a smoothly accelerating jet from the distributed source represented by the sound baffles, to the line sink represented by the bellmouth exit plane.

Consequently, the plenum was reconfigured as shown in Section VI, Figures 14 and 15. Baffles were positioned to behave as spoilers and to better distribute the flow below the contraction. A 4-by-12 foot construction of 1/8 inch masonite was installed on the west end ceiling to divert the high velocity fluid from the ceiling down through the baffles. The measurements of $\overline{Q}$ and flow angles for this final Configuration 7 are presented in Section VI.

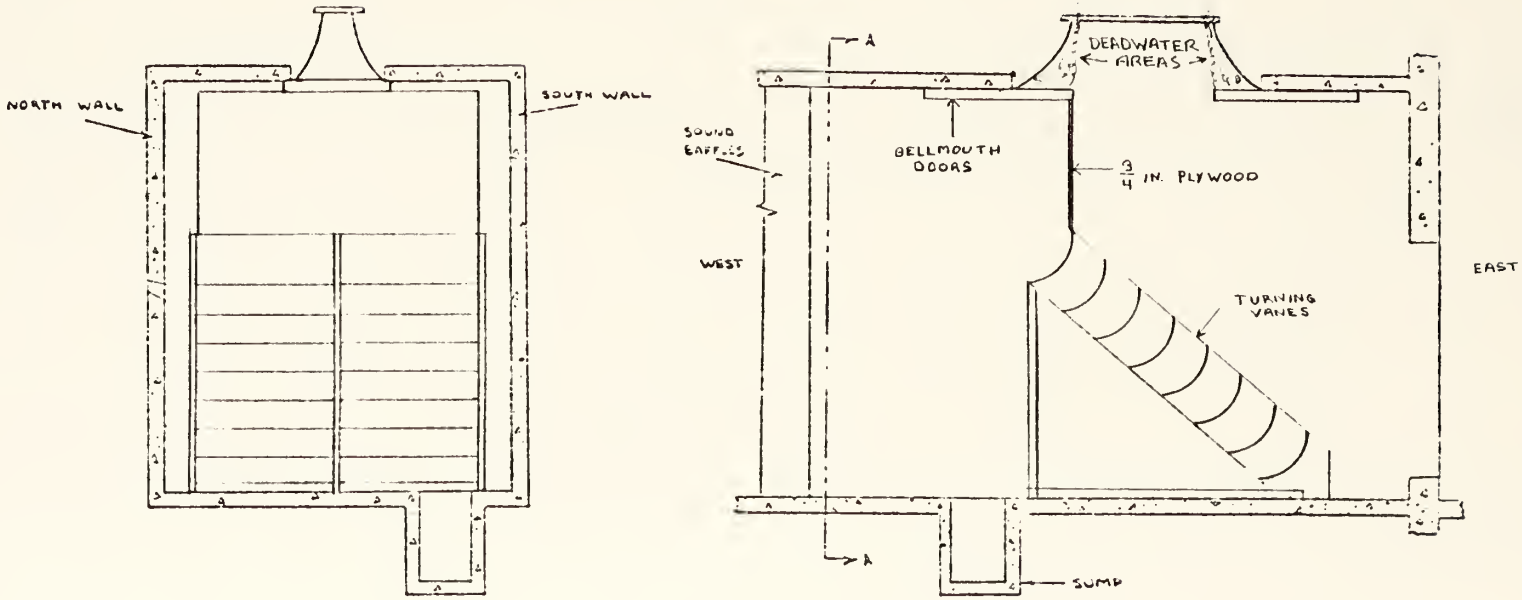

Figure C-1. Plenum - Configuration #2

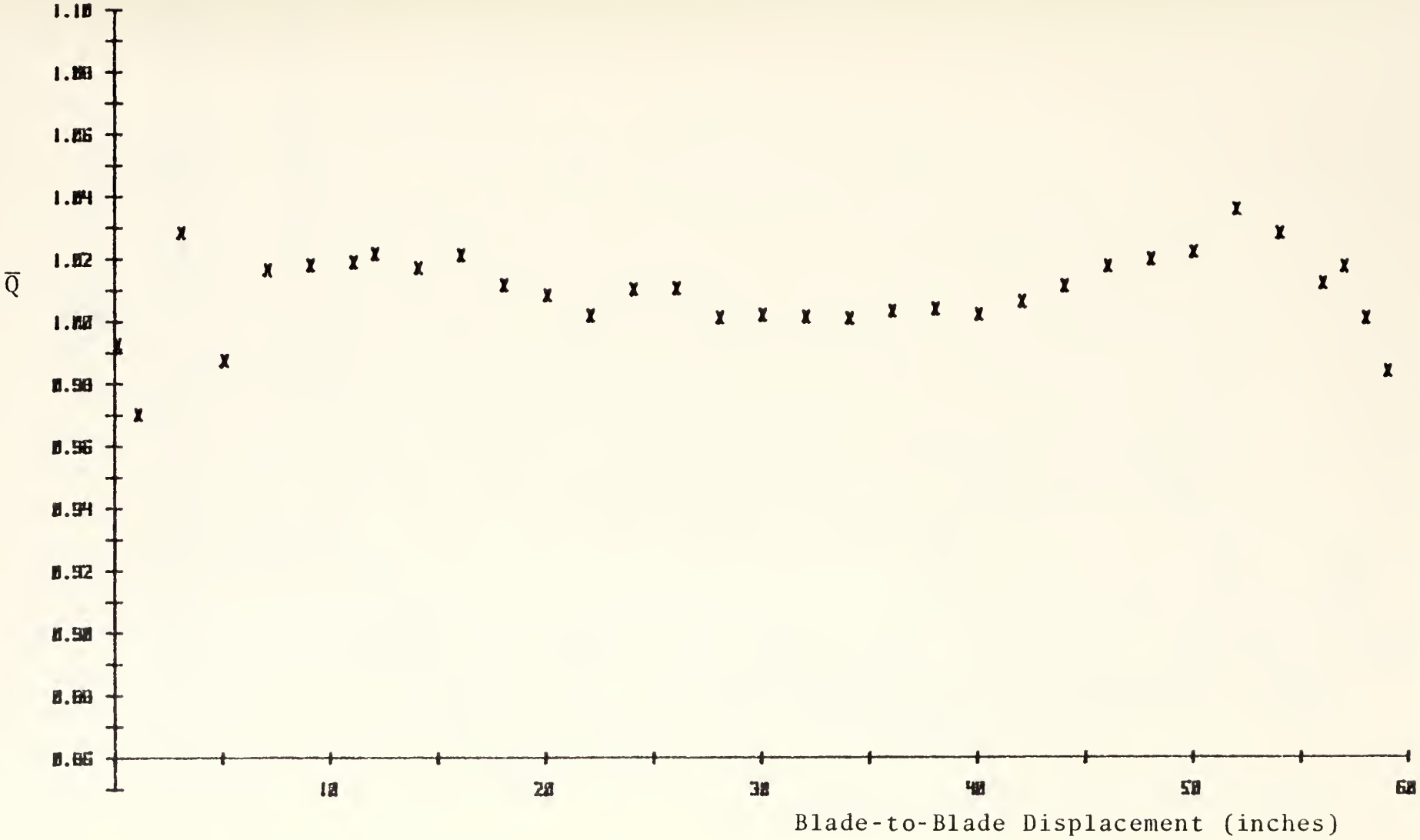

Figure C-2. Blade-to-Blade Dynamic Pressure Distribution at the Test Plane (at 50% Span, Velocity = 260 ft/sec) - Configuration #2

Figure C-3. Blade-to-Blade Yaw Angle Distribution at the Test Plane (at 50% Span, Velocity = 260 ft/sec) - Configuration #2.

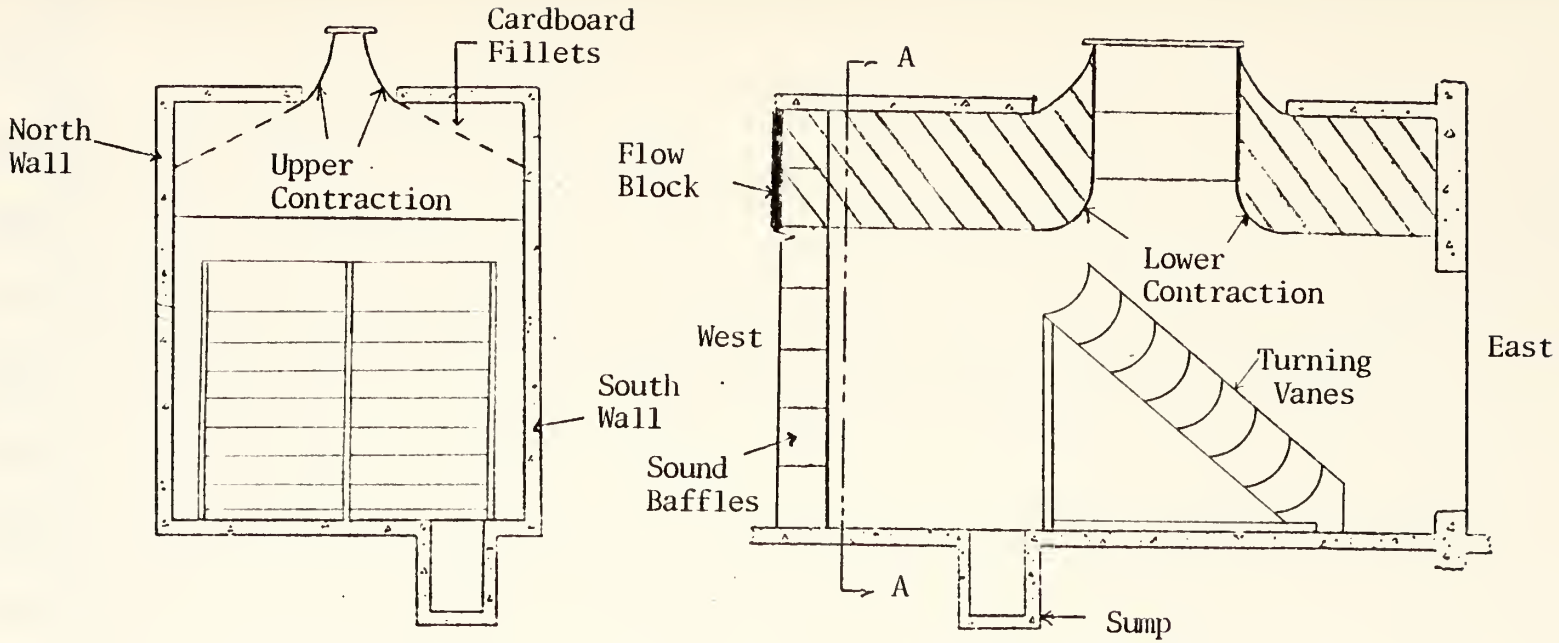

Figure C-4. Plenum - Configuration #3

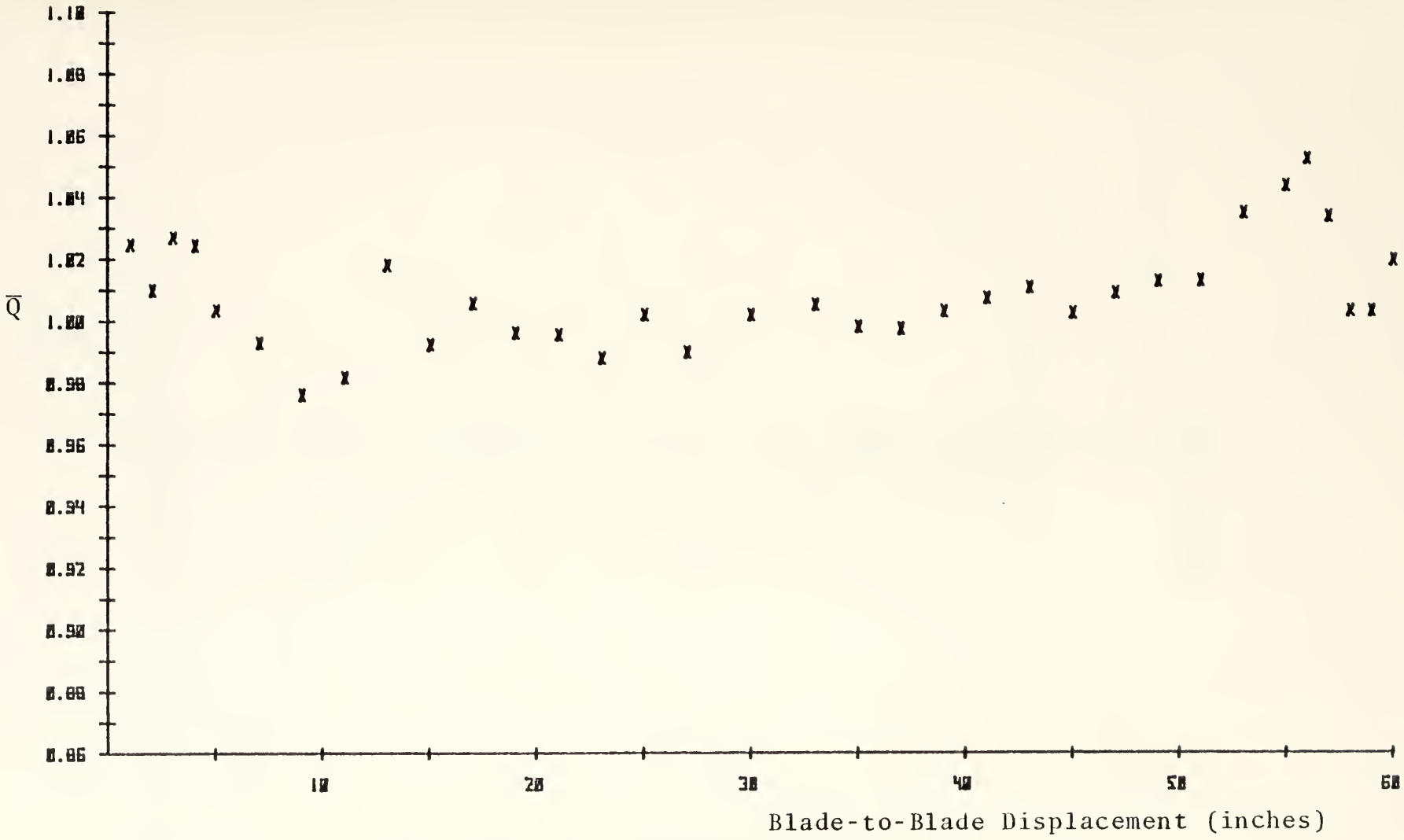

Figure C-5. Blade-to-Blade Dynamic Pressure Distribution at the Test Plane (at 50% Span, Velocity = 250 ft/sec) - Configuration #3

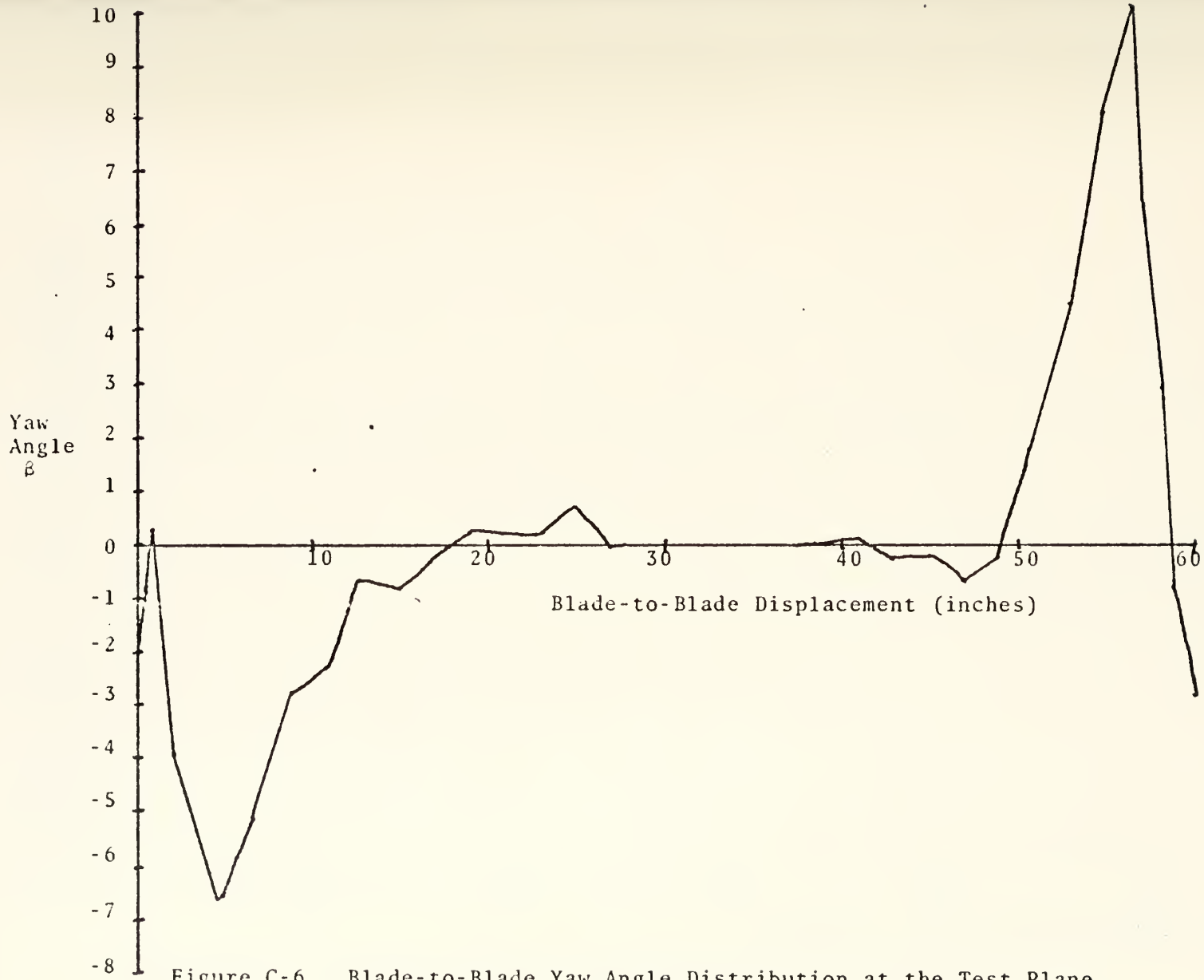

Figure C-6. Blade-to-Blade Yaw Angle Distribution at the Test Plane (at 50% Span, Velocity = 250 ft/sec) - Configuration #3

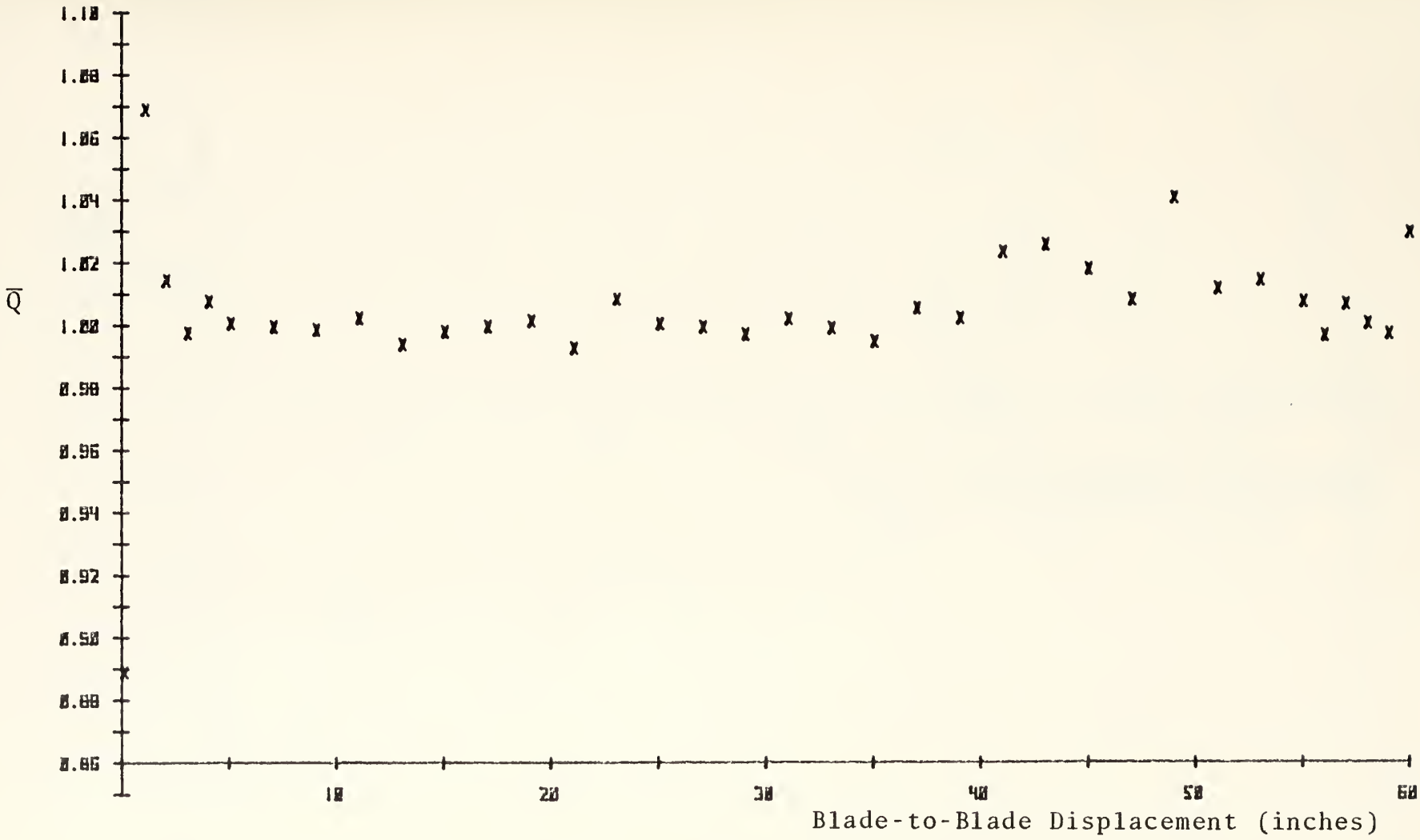

Figure C-7. Blade-to-Blade Dynamic Pressure Distribution at the Test Plane (at 50% Span, Velocity = 250 ft/sec) - Configuration #4

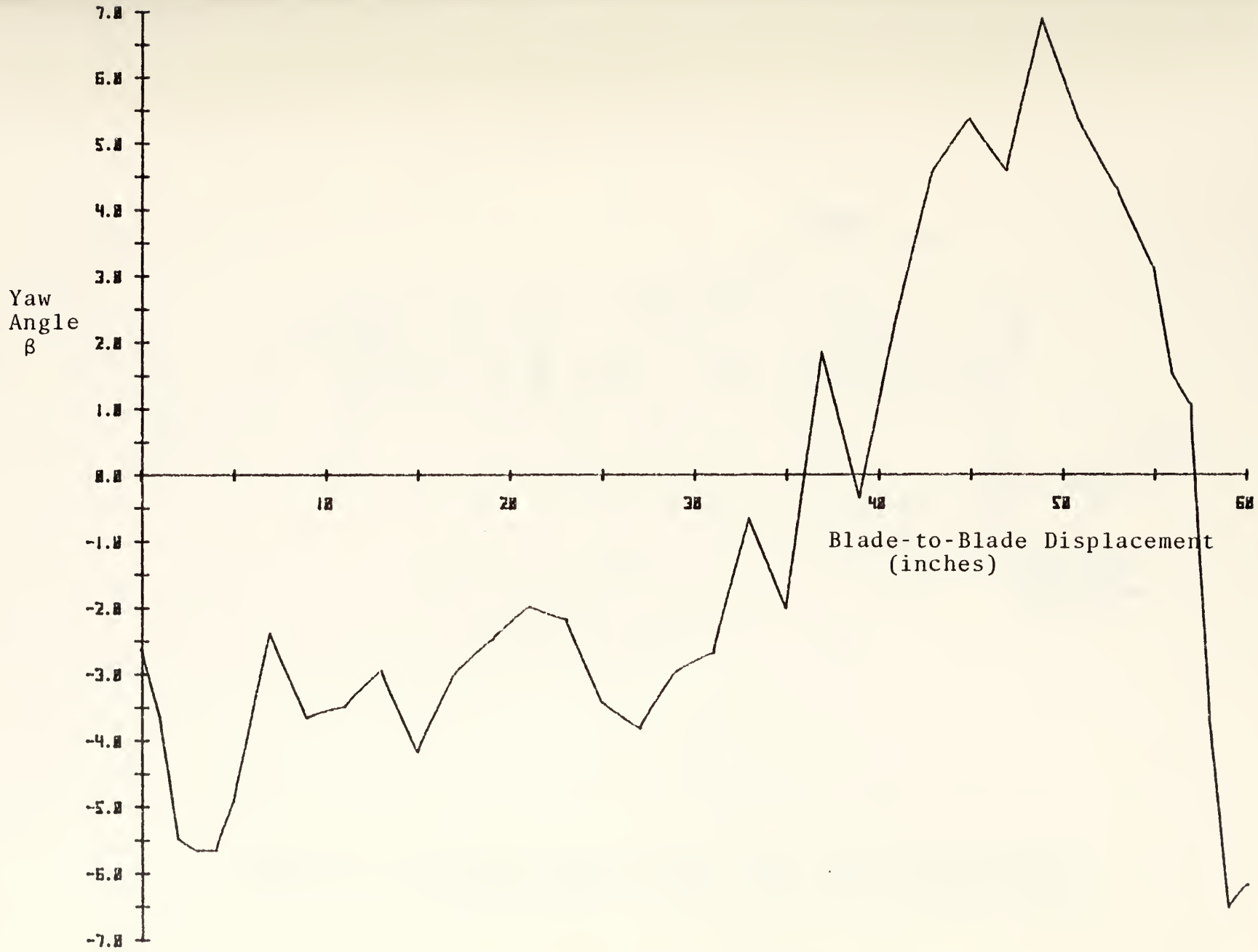

Figure C-8. Blade-to-Blade Yaw Angle Distribution at the Test Plane (at 50% Span, Velocity = 250 ft/sec) - Configuration #4

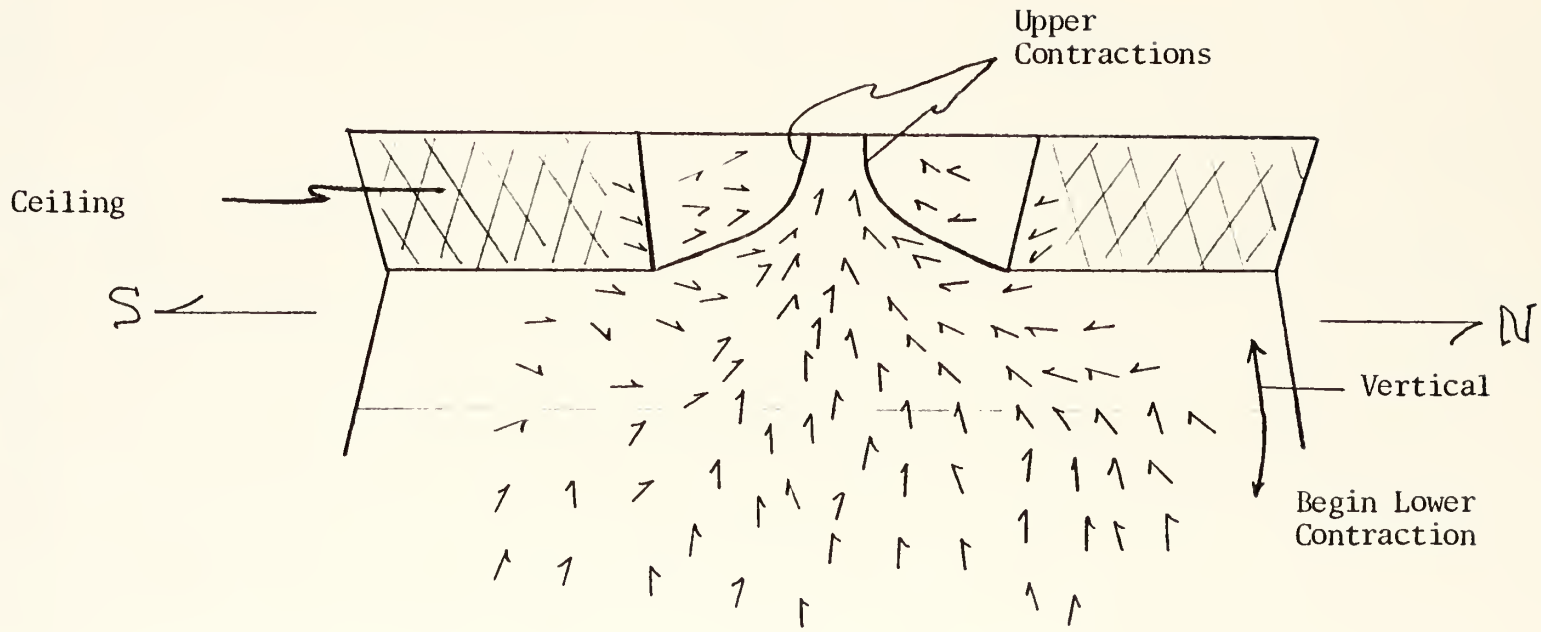

Figure C-9. Tuft Positions on West End Lower Contraction
(Viewing East to West, 45 Degrees Upward Angle)

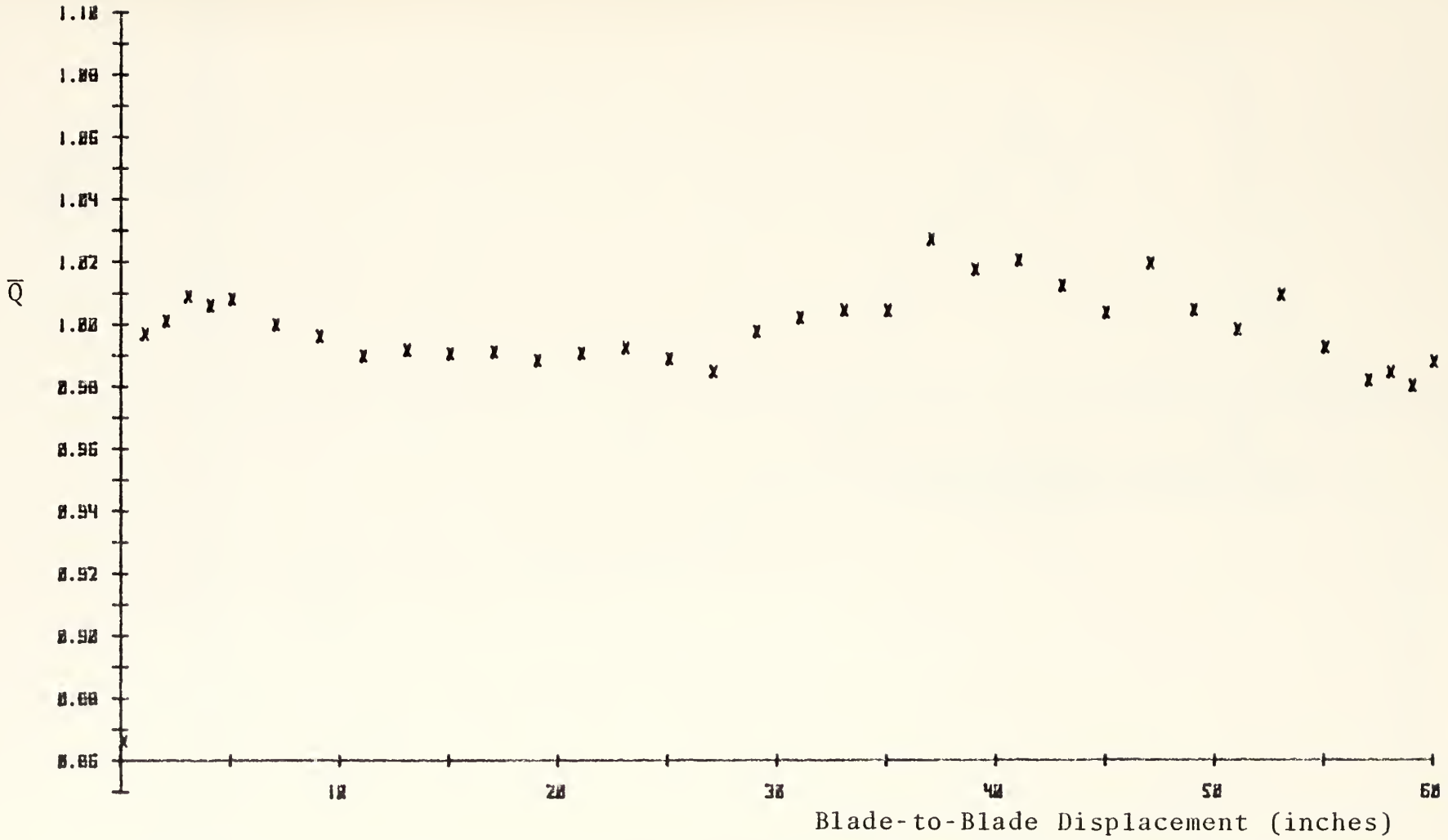

Figure C-10. Blade-to-Blade Dynamic Pressure Distribution at the Test Plane (at 50% Span, Velocity = 270 ft/sec) - Configuration #5

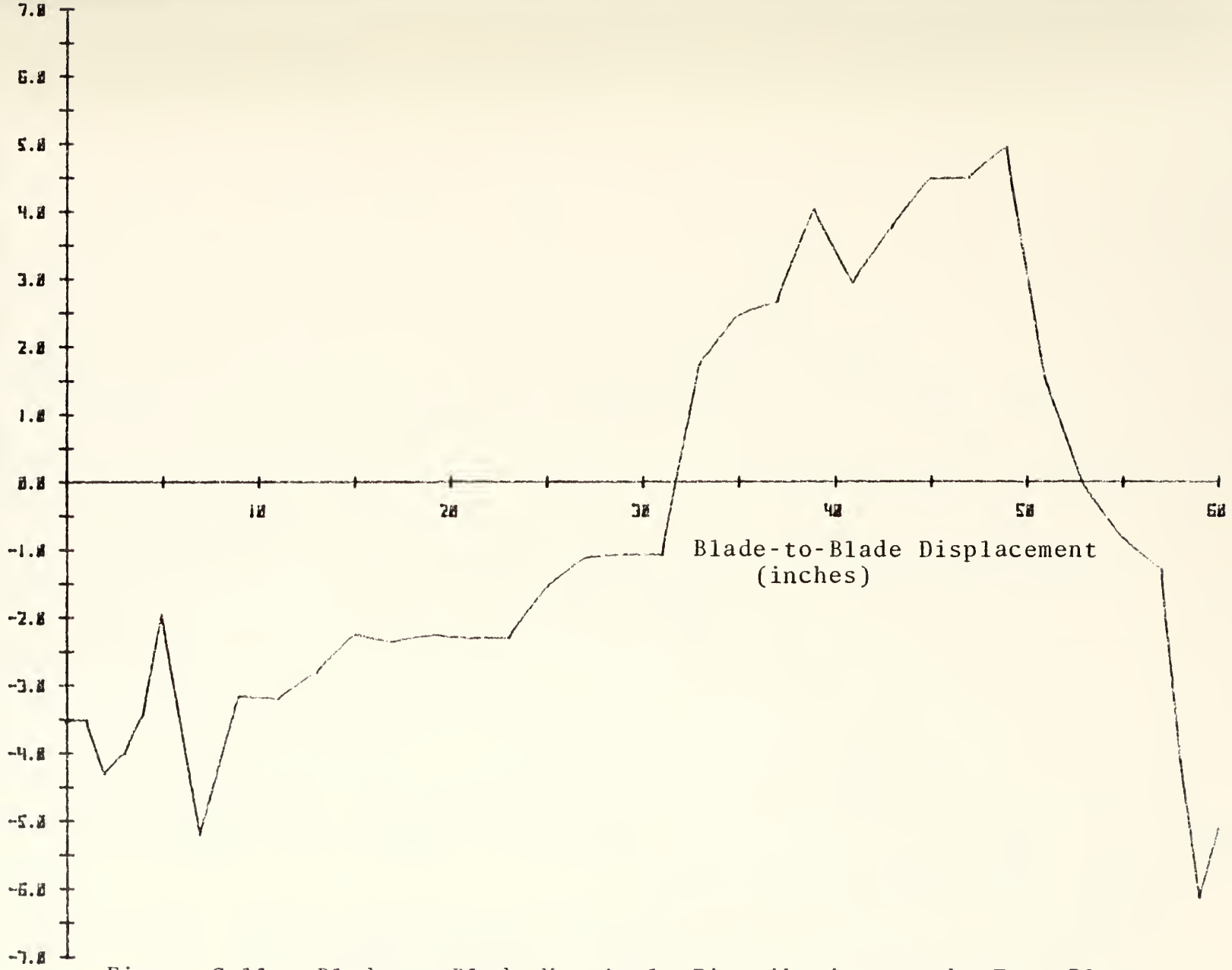

Figure C-11. Blade-to-Blade Yaw Angle Distribution at the Test Plane (at 50% Span, Velocity = 270 ft/sec) - Configuration #5

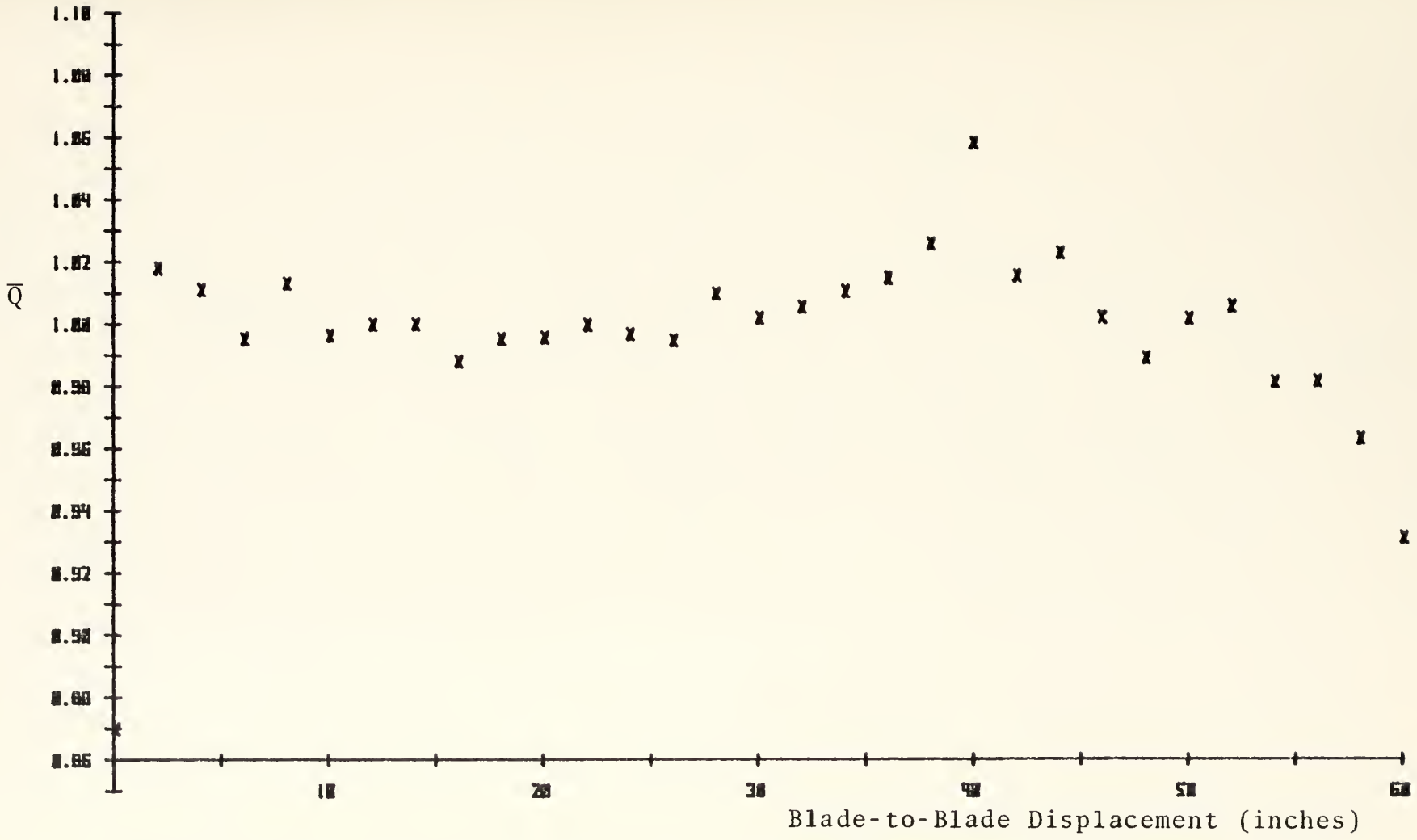

Figure C-12a. Blade-to-Blade Dynamic Pressure Distribution at the Test Plane (at 20% Span, Velocity = 250 ft/sec) - Configuration #6

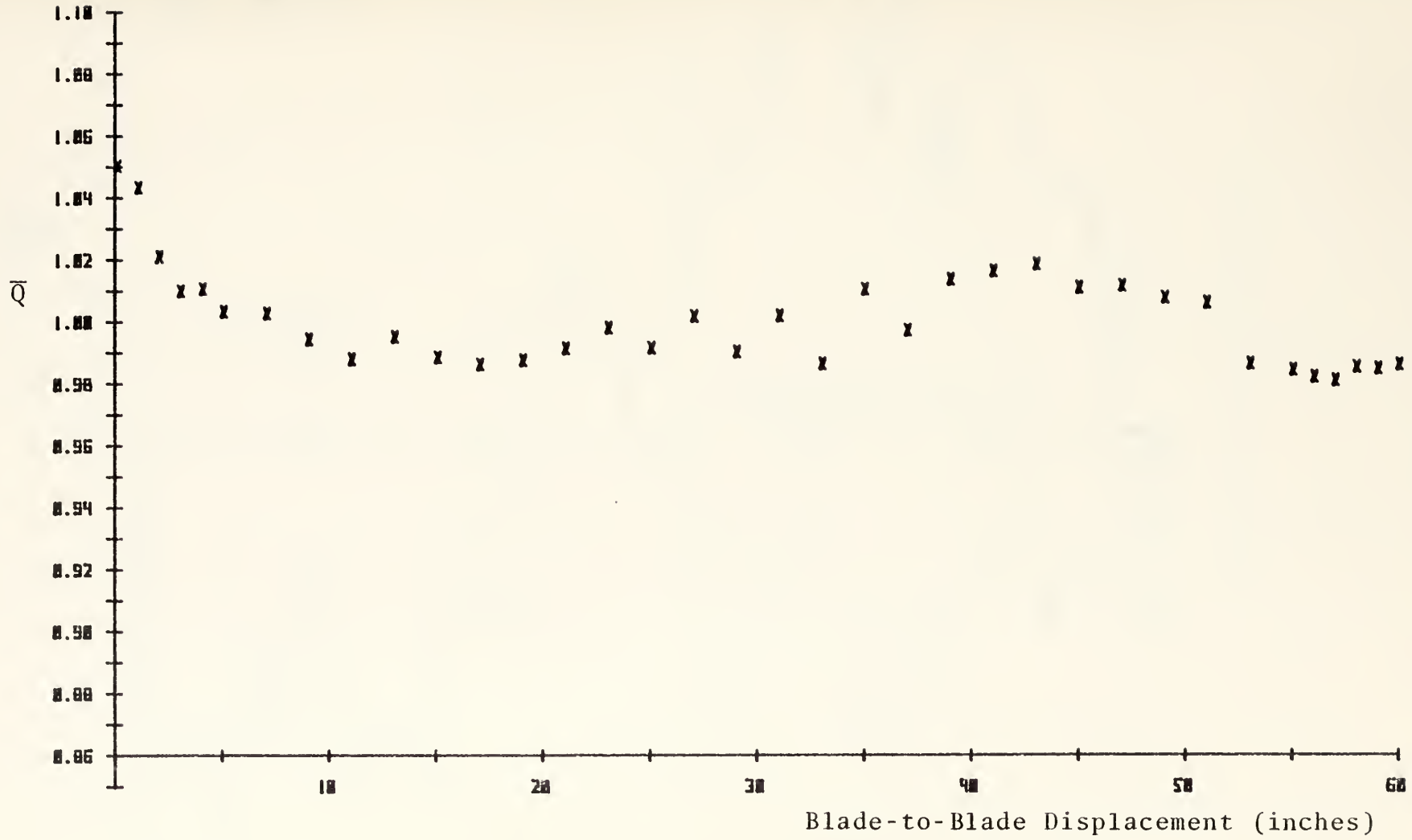

Figure C-12b. Blade-to-Blade Dynamic Pressure Distribution at the Test Plane (at 50% Span, Velocity = 250 ft/sec) - Configuration #6

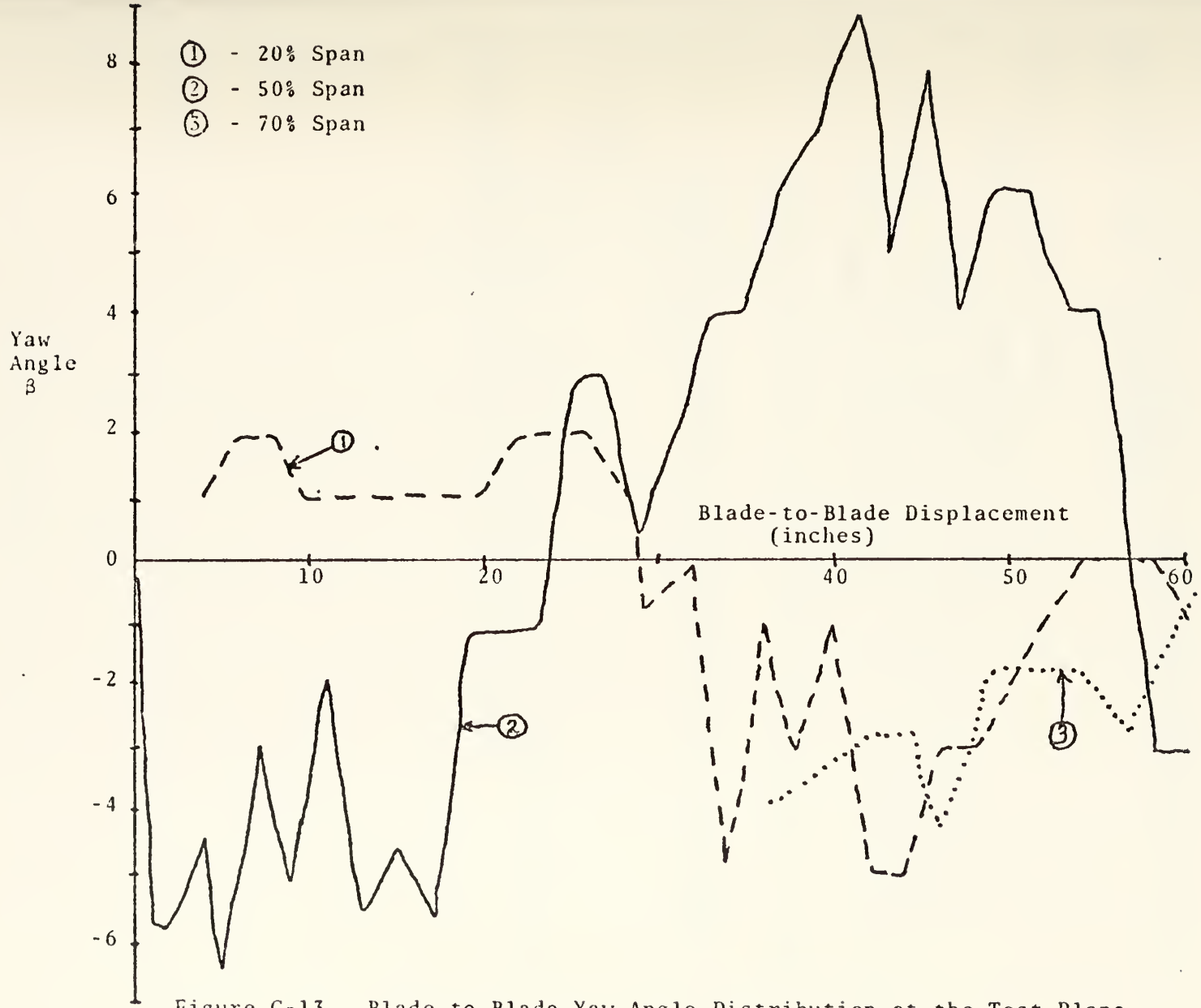

Figure C-13. Blade-to-Blade Yaw Angle Distribution at the Test Plane (at 20, 50 and 70% Span, Velocity = 250 ft/sec) - Configuration #6

APPENDIX D

PLENUM MODIFICATION DRAWINGS

The following drawings show the construction of the east and west lower contractions.

Construction Materials:

Figures D-1 through D-4

1. All framing material is construction grade pine.
2. The surface covering is 1/8 inch untempered masonite paneling in 4 x 8 ft sheets.
3. Countersunk wood screws secure the masonite to the framing.
4. Framing is secured to the cement wall with power-driven nails.

Figure D-5

The upper contour is part of the original bellmouth constructed from welded 1/8 inch steel plate.

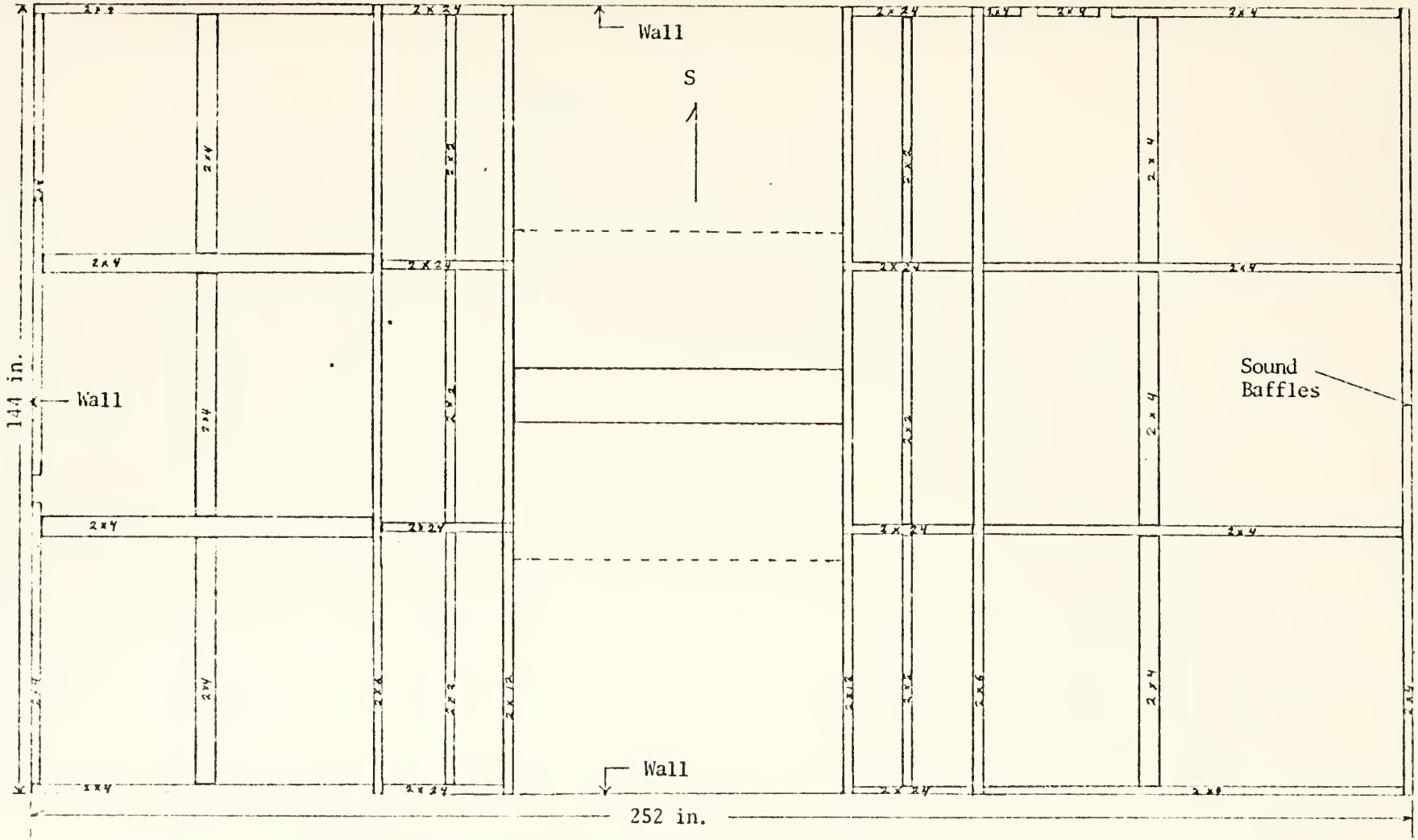

Figure D-1. Eastern and Western Lower Contraction Framework. Top View. Scale 1:25

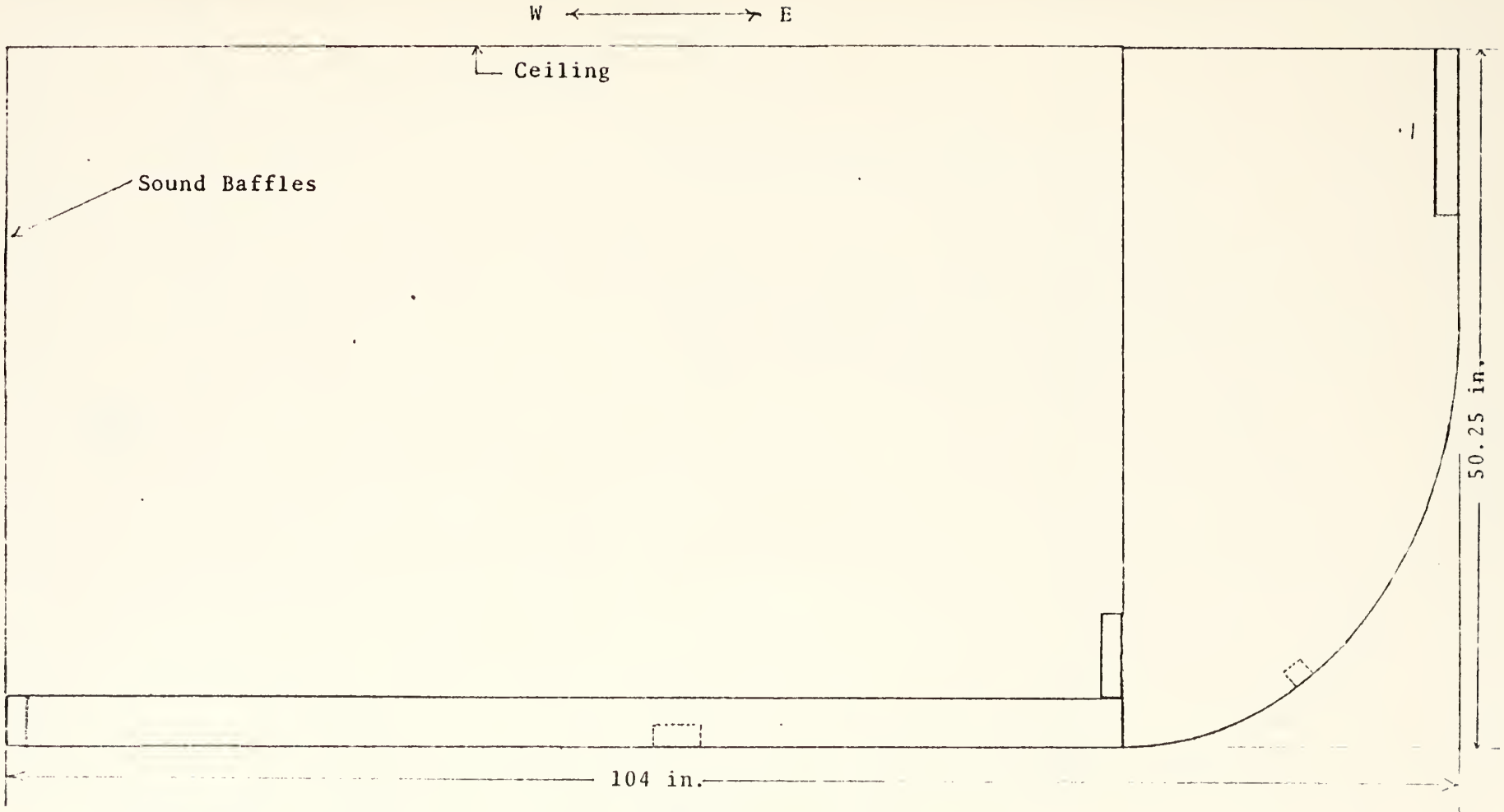

Figure D-2. W-E Elevation, Western Lower Contraction Framework
Side View from South

Scale 1:10

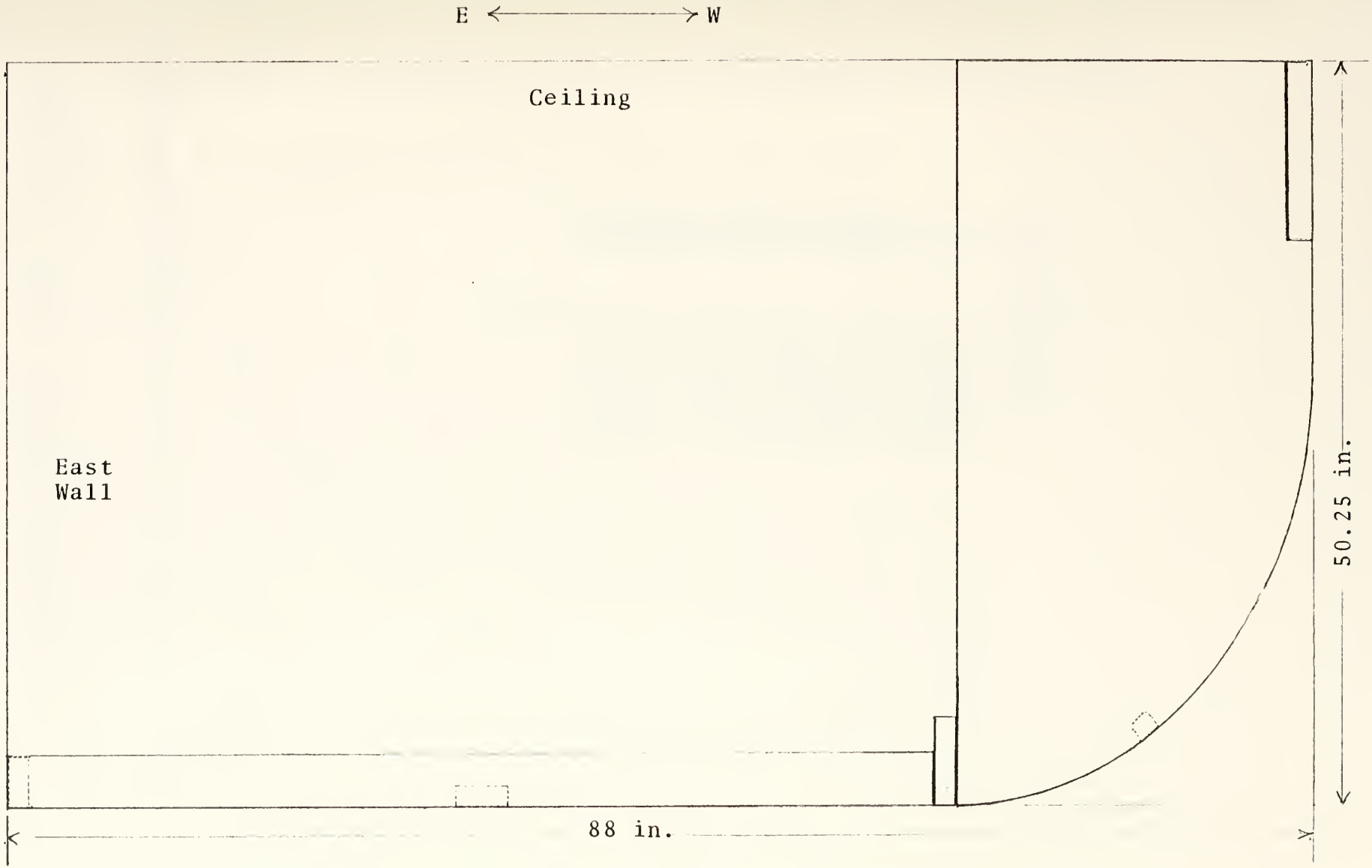

Figure D-3. E-W Elevation, Eastern Lower Contraction Framework
Side View from North Scale 1:10

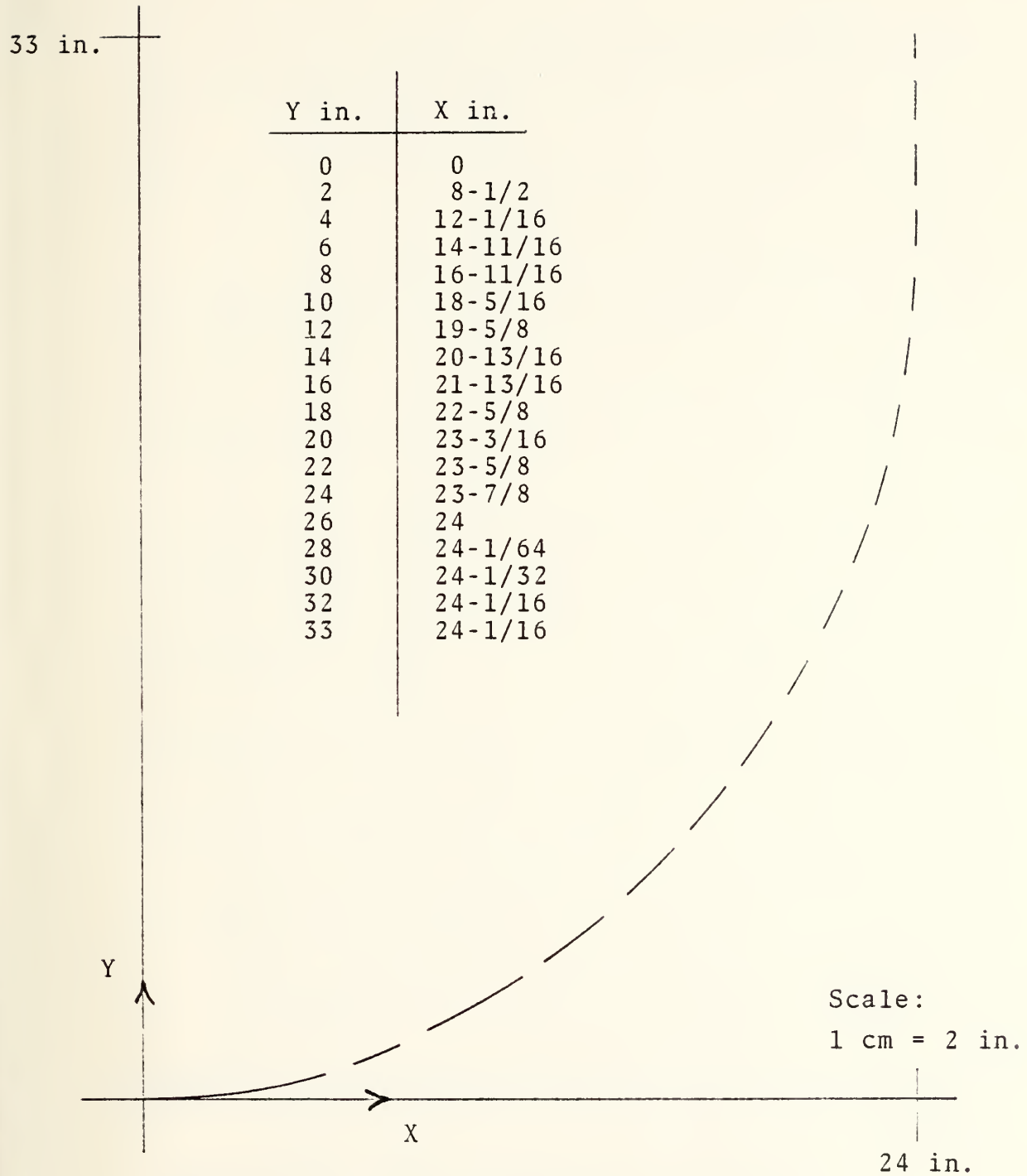

Figure D-4. Lower Contraction Contour

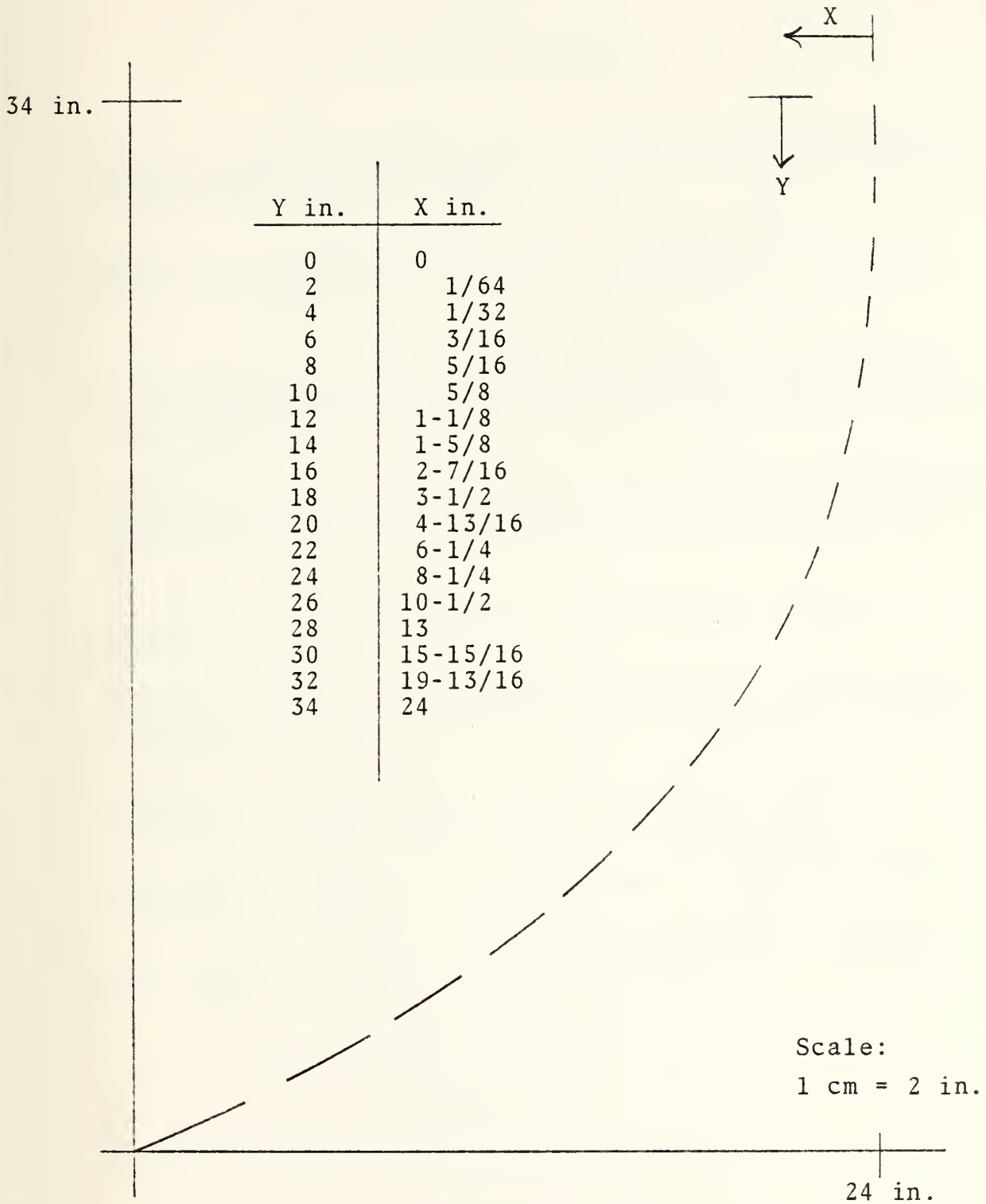

Y in.	X in.
0	0
2	1/64
4	1/32
6	3/16
8	5/16
10	5/8
12	1-1/8
14	1-5/8
16	2-7/16
18	3-1/2
20	4-13/16
22	6-1/4
24	8-1/4
26	10-1/2
28	13
30	15-15/16
32	19-13/16
34	24

Figure D-5. Upper Contraction Contour

LIST OF REFERENCES

1. Rose, C. and Guttormson, D.L., Installation and Test of a Rectilinear Cascade, Master's Thesis, Naval Postgraduate School, Monterey, California, 1964.

2. Johnsen, I.A. and Bullock, R.O., Aerodynamic Design of Axial-Flow Compressors, NASA SP-36, Chap. VI, National Aeronautics and Space Administration, 1965.

3. Bartocci, J.E., An Investigation of the Flow Conditions at the Lower Measuring Plane, and in the Plenum Chamber of the Rectilinear Cascade Test Facility, Master's Thesis, Naval Postgraduate School, Monterey, California, 1966.

4. Wheeler, W.R., Experimental Determination of Turning Angle and Losses of Axial Compressor Inlet Guide Vanes, Master's Thesis, Naval Postgraduate School, Monterey, California, 1972.

5. Streeter, V.L., Handbook of Fluid Dynamics, Chap. 10, McGraw-Hill, 1961.

6. Prandl, L., On Fully Developed Turbulence, Proceedings of the International Congress of Applied Mechanics, Zurich, Switzerland, 1926.

7. Bansod, P. and Bradshaw, P., "The Flow in S-Shaped Ducts," Aeronautical Quarterly, pp. 131-140, June 1971.

8. Chung, T.J., Finite Element Analysis in Fluid Dynamics, McGraw-Hill, 1978.

9. Huebner, K.H., The Finite Element Method for Engineers, Wiley and Sons, 1975.

INITIAL DISTRIBUTION LIST

		No. Copies
1.	Defense Technical Information Center Cameron Station Alexandria, Virginia 22314	2
2.	Library, Code 0142 Naval Postgraduate School Monterey, California 93940	2
3.	Department Chairman, Code 67 Department of Aeronautics Naval Postgraduate School Monterey, California 93940	1
4.	Assoc. Prof. R. P. Shreeve, Code 67 Sf Department of Aeronautics Naval Postgraduate School Monterey, California 93940	1
5.	LT Richard Carl Moebius, USN 2271 St. Marshall Dr. VA. Beach, VA 23454	1
6.	Turbopropulsion Laboratory Code 67 Naval Postgraduate School Monterey, California 93940	10